PLGA depots for controlled release of bevacizumab

by

Rae Sung Chang

A dissertation submitted in partial fulfillment
of the requirements for the degree of
Doctor of Philosophy
(Pharmaceutical Sciences)
in the University of Michigan
2016

Doctoral Committee:

Professor Steven P. Schwendeman, Chair
Associate Professor Wei Cheng
Associate Professor Naír Rodríguez-Hornedo
Professor David N. Zacks

Dedication

To my father Young Jin Chang, my mother Jung Ok Kim,

my wife Jungmi Yu, and my precious daughter Alice Chang

Acknowledgements

I would like to thank my advisors, Prof. Steven Schwendeman and Prof. Anna Schwendeman for not only their guidance throughout my graduate studies but also motivation on being an independent scientist. Whenever I met difficulties in my academic work, they supported me in direct and indirect ways. Also, I would like to thank all my dissertation committee members, Prof. Nair Rodriguez-Hornedo, Prof. Wei Cheng, and Prof. David Zacks for serving as my dissertation committees and their academic advice on my work.

I would like to thank Prof. Yu-Kyoung Oh who was my advisor for my bachelor's and master's degrees for guiding me to the exciting world of science. I could not be what I am here without her guidance and supports. My colleague, Dr. Karthik Pisupati deserves a special mention for all the delightful scientific discussions and reviewing this dissertation. I would like to express my gratitude to Karl Olsen and Rose Ackermann for managing all the lab issues smoothly and safely. In addition, I would like to thank all my previous and current lab fellows: Desai, Vesna, Hiren, Keiji, Greg, Wenmin, Jie, Xuwei, Yajun, Ronak, Brittany, Amy, Max, Kelly, Morgan, Kari, Emily, Dan, Jia, Maria, Alex, Jay, and Sang for creating a warm atmosphere in our lab. I would also like to thank Jenna for her help and collaboration on applying the work of this dissertation to other antibody drugs.

My graduate school life in Ann Arbor would not have been complete without all my friends, tennis fellows, and members of KUAA (Korea University Alumni Association). I really enjoyed all the times with them in Ann Arbor.

Finally, I would love to thank my family for their supports throughout all my life. Now I more respect my father with his role in the family after I became a father. My mother deserves a special mention for being very supportive of all my decisions. And at last but not least, I would like to thank my lovely wife, Jungmi for all the infinite supports, and my adorable girl, Alice for being my daughter. They have been my motivation and happiness throughout all my daily life.

Table of Contents

List of Figures

List of Tables

Abstract

The advent of monoclonal antibody (mAb)-based anti-vascular endothelial growth factor (VEGF) therapy for treatment of wet age-related macular degeneration (AMD) has significantly improved the clinical outcomes in patients. However, monthly intravitreal injection of the anti-VEGF agents is inconvenient for patients and introduce the risks of infection, inflammation, and hemorrhage. Therefore, the development of intravitreal sustained release formulations of anti-VEGF agents would be beneficial to patients. The work in this dissertation investigated poly(lactic-co-glycolic acid) (PLGA) depot formulations to address this unmet need.

Active self-encapsulating PLGA microspheres with high molecular weight dextran sulfate (HDS) as a trapping agent and $ZnCO_3$ as an antacid demonstrated continuous 8-week *in vitro* release of the immunoreactive bevacizumab Fab fragments, however, loading and encapsulation efficiency were low. Adjusting loading parameters (e.g., $ZnCO_3$ and HDS content, loading buffer pH, and protein concentration in loading solution) did not significantly improve those values.

PLGA millicylindrical implants suitable for intravitreal injection were next employed as sustained release formulations of the anti-VEGF full-length mAb, bevacizumab. To stabilize the encapsulated mAb against the acidic microenvironment inside the PLGA implants during release period, $MgCO_3$ was co-encapsulated. To prevent aggregation of bevacizumab during powder preparation, trehalose was co-lyophilized with the mAb above a critical level. The presence of osmotically active

excipients necessary to stabilize the mAb also caused a rapid uncontrolled release due to polymer swelling. To offset this effect, the lateral surface of implants was coated with pure PLGA. The optimized coated implants demonstrated continuous release kinetics *in vitro* over six weeks with high (>80%) total cumulative release. The released bevacizumab over this entire period retained > 90 % monomer content as well as excellent preservation of immunoreactivity and secondary structure.

Although there have been several attempts to develop sustained release formulations of the anti-VEGF mAbs, one or more desirable but unmet characteristics (biocompatibility of formulations, high loading (w/w) and loading efficiency, near zero-order release kinetics with near complete release, and well-preserved stability of the released drugs) have hindered their clinical development. The data presented in this work provide a new paradigm for controlled release of stable bevacizumab from PLGA with the desired characteristics in various aspects, which both supports further development of this approach for wet AMD treatment and a generalizable application to site-specific controlled release of therapeutic mAbs.

Chapter 1: Introduction

1.1 Therapeutic Monoclonal Antibody

Since the end of the twentieth century, macromolecules such as nucleic acids and proteins have been emerging categories of therapeutics. In particular, therapeutic monoclonal antibodies have been developed and approved to the market since the hybridoma technique of Köhler and Milstein was introduced in 1975 [1]. Natural immune systems utilize antibodies to withstand the attacks of microorganism or foreign substances. Antibodies specifically bind to their antigens either on the cell surface or soluble substances and neutralize them. Natural antibodies against the same target molecules are 'polyclonal' antibodies which mean that they are a combination of antibody molecules produced against the same antigen, but typically target different epitopes on the antigen because different B cells produce different antibody molecules. Contrary to this, 'monoclonal' antibodies are produced from the same cell clones and are basically identical molecules which target the same antigen and the same epitope. The hybridoma technique enabled monoclonal antibodies to be produced synthetically *in vitro* by fusing myeloma cells with B cells. Since monoclonal antibodies bind to the target antigens quantitatively and they are homogeneous in terms of molecular identity, they can be developed as therapeutics [2] and monoclonal antibody therapy is defined as the use of monoclonal antibodies to neutralize specific target cells or proteins causing diseases. The indications of therapeutic monoclonal antibodies include several types of

cancer, immune disorders and viral infections. By 2014, more than forty antibody-based therapeutics including Fab fragments, and antibody-drug conjugates have been approved around the world and hundreds of monoclonal antibodies are undergoing clinical trials [3]. Most of them are concerned with immunological and oncological targets [4]. Table 1.1 shows a recent list of antibody-based therapeutics approved in the US and Europe.

Table 1.1: Marketed therapeutic monoclonal antibody-based products. *Adapted from ref* [3].

Brand name (INN)	Original BLA/MAA Applicant	Company Reporting US Sales	Company Reporting EU Sales	Year of First Approval	2013 Global Sales ($M)[a]
Abthrax (raxibacumab)	Human Genome Sciences	GlaxoSmithKline	N/A[b]	2012	23
Actemra (tocilizumab)	Roche	Roche	Roche	2009	1,119
Adcetris[c] (brentuximab vedotin)	Seattle Genetics	Seattle Genetics	Takeda Pharmaceutical Co.	2011	253
AlprolIX[d] (Factor IX Fc fusion protein)	Biogen Idec	Biogen Idec	N/A	2014	NoM[e]
Arcalyst[f] (rilonacept)	Regeneron Pharmaceuticals	Regeneron Pharmaceuticals	N/A	2008	17
Arzerra (ofatumumab)	GlaxoSmithKline	GlaxoSmithKline	GlaxoSmithKline	2009	117
Avastin (bevacizumab)	Genentech	Roche	Roche	2004	6,748
Benlysta (belimumab)	Human Genome Sciences	GlaxoSmithKline	GlaxoSmithKline	2011	228
Cimzia[g] (certolizumab pegol)	UCB	UCB	UCB	2008	789
Cyramza (ramucirumab)	Eli Lilly and Co.	Eli Lilly and Co.	N/A	2014	NoM[e]
Eloctate[h] (Factor VIII Fc fusion protein)	Biogen Idec	Biogen Idec	N/A	2014	NoM[e]
Enbrel[i] (etanercept)	Immunex	Amgen	Pfizer	1998	8,325
Entyvio (vedolizumab)	Takeda Pharmaceuticals U.S.A., Inc	Takeda Pharmaceutical Co.	Takeda Pharmaceutical Co.	2014	NoM[e]
Erbitux (cetuximab)	ImClone Systems	Bristol-Myers Squibb	Merck KGaA	2004	1,926
Eylea[j] (aflibercept)	Regeneron Pharmaceuticals	Regeneron Pharmaceuticals	Bayer Healthcare Pharmaceuticals	2011	1,851
Gazyva (obinutuzumab)	Genentech	Roche	Roche	2013	3

Herceptin (trastuzumab)	**Genentech**	**Roche**	**Roche**	**1998**	**6,559**
Humira (adalimumab)	**Abbott Laboratories**	**AbbVie**	**AbbVie**	**2002**	**10,659**
Ilaris (canakinumab)	**Novartis Pharmaceuticals**	**Novartis Pharmaceuticals**	**Novartis Pharmaceuticals**	**2009**	**119**
Kadcyla[k] (ado-trastuzumab emtansine)	**Genentech**	**Roche**	**Roche**	**2013**	**252**
Keytruda (pembrolizumab)	**Merck & Co.**	**Merck & Co.**	**N/A**	**2014**	**NoM[e]**
Lemtrada (alemtuzumab)	**Genzyme Therapeutics**	**N/A**	**Sanofi**	**2013**	**3**
Lucentis[l] (ranibizumab)	**Genentech**	**Roche**	**Novartis Pharmaceuticals**	**2006**	**4,205**
Nplate[m] (romiplostim)	**Amgen**	**Amgen**	**Amgen**	**2008**	**427**
Nulojix[n] (belatacept)	**Bristol-Myers Squibb**	**Bristol-Myers Squibb**	**Bristol-Myers Squibb**	**2011**	**26**
Orencia[o] (abatacept)	**Bristol-Myers Squibb**	**Bristol-Myers Squibb**	**Bristol-Myers Squibb**	**2005**	**1,444**
Perjeta(pertuzumab)	**Genentech**	**Roche**	**Roche**	**2012**	**352**
Prolia[p] (denosumab)	**Amgen**	**Amgen**	**GlaxoSmithKline**	**2011**	**824**
Remicade (infliximab)	**Centocor**	**Johnson & Johnson**	**Merck & Co.**	**1998**	**8,944**
Removab[q] (catumaxomab)	**Fresenius Biotech**	**N/A**	**NeoPharm Group**	**2009**	**5**
ReoPro[r] (abciximab)	**Centocor**	**Lilly**	**N/A**	**1994**	**127**
Rituxan (rituximab)	**Genentech**	**Roche**	**Roche**	**1997**	**7,500**
Simponi/ Simponi Aria (golimumab)	**Centocor Ortho Biotech**	**Johnson & Johnson**	**Merck & Co.**	**2009**	**1,432**
Simulect (basiliximab)	**Novartis Pharmaceuticals**	**Novartis Pharmaceuticals**	**Novartis Pharmaceuticals**	**1998**	**30[s]**
Soliris (eculizumab)	**Alexion Pharmaceuticals**	**Alexion Pharmaceuticals**	**Alexion Pharmaceuticals**	**2007**	**1,551**
Stelara (ustekinumab)	**Janssen-Cilag International**	**Johnson & Johnson**	**Johnson & Johnson**	**2009**	**1,504**
Sylvant (siltuximab)	**Janssen Biotech**	**Johnson & Johnson**	**Johnson & Johnson**	**2014**	**NoM[e]**
Synagis (palivizumab)	**Abbott Laboratories**	**AstraZeneca**	**Abbvie**	**1998**	**1,887**
Tysabri (natalizumab)	**Biogen Idec**	**Biogen Idec**	**Biogen Idec**	**2004**	**1,527**
Vectibix (panitumumab)	**Amgen**	**Amgen**	**Amgen**	**2006**	**389**
Xgeva[p] (denosumab)	**Amgen**	**Amgen**	**Amgen**	**2010**	**1,030**
Xolair (omalizumab)	**Genentech**	**Roche**	**Novartis**	**2003**	**1,465**
Yervoy (ipilimumab)	**Bristol-Myers Squibb**	**Bristol-Myers Squibb**	**Bristol-Myers Squibb**	**2011**	**960**
Zaltrap[t] (ziv-aflibercept)	**Sanofi Aventis**	**Sanofi**	**Sanofi**	**2012**	**70**

Zevalin[u] (ibritumomab tiuxetan)	**IDEC Pharmaceuticals**	**Spectrum Pharmaceuticals**	**Spectrum Pharmaceuticals**	**2002**	**29**

[a] Sales information obtained from company annual reports and other publically available sources.
[b] N/A denote product not available in this region.
[c] Antibody-Drug Conjugate, MMAE.
[d] Fc Fusion Protein, Fc-Factor IX.
[e] Product approval in 2014; no sales in 2013.
[f] Fc Fusion Protein, Fc-IL1R.
[g] Fab Conjugate, PEG (produced by microbial fermentation).
[h] Fc Fusion Protein, Fc-Factor VIII.
[i] Fc Fusion Protein, Fc-TNFR.
[j] Fc Fusion Protein, Fc-VEGFR.
[k] Antibody-Drug Conjugate, DM1.
[l] Fab (produced by microbial fermentation).
[m] Fc Fusion Protein, Fc-TPO-R binding peptide (produced by microbial fermentation).
[n] Fc Fusion Protein, Fc-CTLA-4 with amino acid substitutions.
[o] Fc Fusion Protein, Fc-CTLA-4.
[p] Prolia and Xgeva are considered as two individual products even though they contain the same bulk monoclonal antibody.
[q] Bispecific, Tri-functional Antibody.
[r] Sales data not disclosed, small patient market, bioTRAK® estimate of global sales.
[s] Fab, produced by papain digestion of full length monoclonal antibody.
[t] Fc Fusion Protein, Fc-VEGFR.
[u] Antibody Conjugate, Y-90.

Since the beginning of the twenty-first century, the market for therapeutic monoclonal antibodies has grown exponentially. In 2015, therapeutic monoclonal antibody-based products occupied six spots among the ten best-selling drugs worldwide (Table 1.2) [5]. As a new era of personalized therapy emerges in modern medicine, the use of therapeutic monoclonal antibodies lies at the forefront, and much research in the broad therapeutic antibody field is still necessary.

Table 1.2: Top ten drugs by sales. *Adapted from ref* [5].

Ranking	Product	Active Ingredient	Main Therapeutic Indication	Company	2015 Revenue[a]
1	**Humira[b]**	**Adalimumab**	**Immunology (Organ Transplant, Arthritis etc.)**	**AbbVie**	**14,012**
2	**Harvoni**	**Ledipasvir and Sofosbuvir**	**Infectious Diseases (HIV, Hepatitis etc.)**	**Gilead Sciences**	**13,864**
3	**Enbrel[b]**	**Etanercept**	**Immunology (Organ Transplant, Arthritis etc.)**	**Amgen/ Pfizer**	**8,697**
4	**Remicade[b]**	**Infliximab**	**Immunology (Organ Transplant, Arthritis etc.)**	**Johnson & Johnson/ Merck**	**8,355**
5	**MabThera /Rituxan[b]**	**Rituximab**	**Oncology**	**Roche**	**7,115**

6	**Lantus**	**Insulin Glargine**	**Diabetes**	**Sanofi**	**7,029**
7	**Avastin[b]**	**Bevacizumab**	**Oncology**	**Roche**	**6,751**
8	**Herceptin[b]**	**Trastuzumab**	**Oncology**	**Roche**	**6,603**
9	**Revlimid**	**Lenalidomide**	**Blood Related Disorders**	**Celgene Corporation**	**5,801**
10	**Sovaldi**	**Sofosbuvir**	**Infectious Diseases (HIV, Hepatitis etc.)**	**Gilead Sciences**	**5,276**

[a] US$ in millions.
[b] Therapeutic monoclonal antibody-based product.

1.1.1 Production and characteristics of monoclonal antibodies

In the late nineteenth century, Kitasato and Behring showed that the serum from human or horses recovered from an infectious disease can treat the same disease in another human patients or animals, which is called, ‘serum therapy’ [4]. Behring was awarded the Nobel Prize in Medicine and Physiology for discovery of the serum therapy in 1901. Early serum therapy utilized crude serum, thus it had a lot of side effects. Later, improved serum therapy using isolated natural antibodies from the immunized serum reduced some of the side effects. However, using isolated polyclonal antibodies from the serum of human or animals still had some drawbacks, which are inefficient manufacturing processes and inconsistent efficacy due to the undefined nature of polyclonal antibodies.

After the hybridoma technique was introduced in 1975, most of the antibody therapies have utilized monoclonal antibodies. Hybridoma cells can produce monoclonal antibodies either in cell culture medium or in animal ascites after injection of the hybridoma cells into the peritoneal cavity, but production in cell culture is usually preferred due to ethical concerns [6]. After collecting a media from cell culture or ascites fluid, antibodies should be purified. For purification, several methods can be used,

including filtration, size exclusion chromatography, ion exchange chromatography, protein A/G affinity chromatography, and antigen affinity purification [7].

Early therapeutic monoclonal antibodies were murine antibodies because natural murine spleen B cells were used to make hydridoma cells. But the difference between murine and human immune systems resulted in immunogenic issues of murine antibodies injected into human body. Murine antibodies have shorter half-lives than human antibodies in human plasma and elicit immunogenic response, thus potentially endangering patients. To overcome these problems, chimeric and humanized monoclonal antibodies were later developed using recombinant DNA technology (Figure 1.1). Chimeric antibodies consist of murine variable regions and human constant regions, thus making them less immunogenic in human and increasing serum half-life. Humanized antibodies were also developed by grafting 'complementarity-determining regions (CDRs)' into the human antibody framework, thus making them even less immunogenic. Initially, the binding affinity of humanized antibodies was weaker than the original murine antibodies. Therefore, mutation in the CDR using recombinant techniques was introduced to increase the binding affinity of humanized antibodies [4]. Now, human monoclonal antibodies can also be produced using transgenic mice or phage display libraries [8].

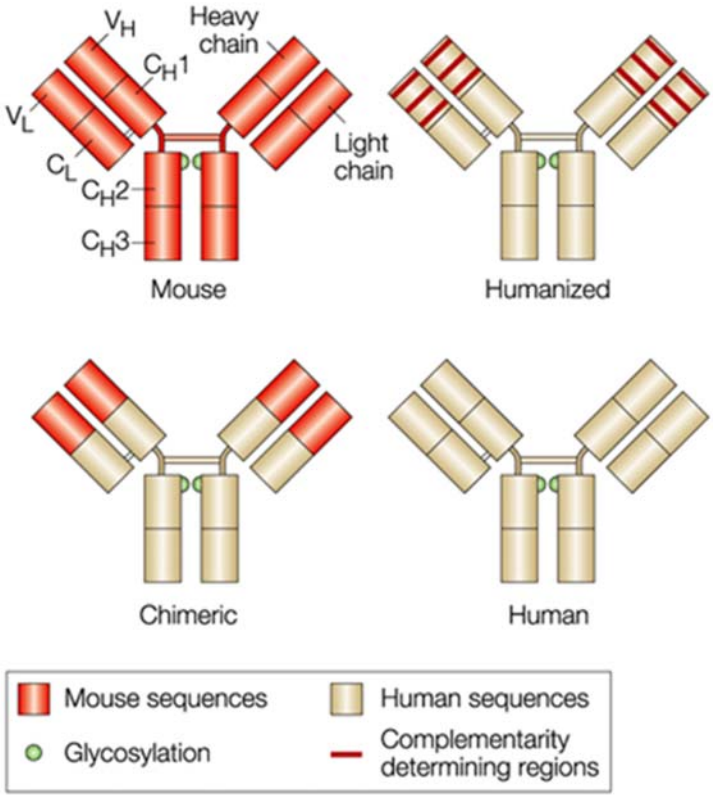

Figure 1.1: Schematic diagrams describing murine, chimeric, humanized and human antibodies. *From ref* [9].

1.1.2 Stability of monoclonal antibodies

Physicochemical and biological stability of monoclonal antibodies has been an important issue for clinical development and overcoming this issue should be an important goal to produce a final product. Physicochemical stability of antibodies can be viewed as a combination of 'conformational' stability and 'colloidal' stability [10]. Conformational stability refers thermodynamic stability of antibodies, which is about how the native antibodies are unfolded and refolded and it can be influenced by pH, ionic strength, and temperature. Colloidal stability of antibodies reflects how stable antibody molecules are when interacting with each other. Conformational and colloidal

instabilities of antibodies cause aggregation which is one of the most critical concerns in developing therapeutic monoclonal antibody products since antibody molecules have a propensity to aggregate easily [11]. Conformational and colloidal stabilities cannot be considered separately and should influence each other.

The instabilities during manufacturing and storage can be enhanced by antibody engineering and controlling pH, temperature, physical stress, concentration and excipients [10]. Temperature and pH during manufacturing and storage can be easily controlled. However, physical stress such as agitation cannot be completely avoided during manufacturing and storage and is one of the major factors inducing aggregation of antibodies, so it is a major hurdle for the development of therapeutic monoclonal antibody products. There has been some research to prevent agitation-induced aggregation of antibodies using protein A or G, peptides [12] or cyclodextrin [13]. High concentrations of antibodies in formulations are also needed since some methods of administration can accommodate limited volume of injection, but high concentration often accelerates aggregation of antibodies. To prevent aggregation of antibodies in formulations, surfactants such as polysorbates are commonly used in antibody formulations, but they cannot prevent aggregation completely [14]. Another common excipient to improve stability of antibodies in formulations is sugars or sugar alcohols such as trehalose, sucrose, sorbitol and mannitol [15]. Three theories have been proposed as stabilizing mechanisms of sugars for proteins: vitrification, preferential exclusion and water replacement theories [16–18]. Vitrification theory proposes the physical entrapment of protein in the glassy sugar matrix, thus the entrapped proteins have restricted mobility which inhibits unfolding and denaturation under stress condition. In

preferential exclusion theory, sugar does not interact directly with protein. Instead, they compete for the formation of hydrogen bonds with water molecules. Trehalose is especially known to interact with water molecules strongly, thus reducing available water molecules to interact with the protein. By this, the hydration radius of protein decreases, resulting in compactness and rigidity of the protein and increased stability. On the other hand, water molecules play a key role in maintaining the three-dimensional structure of proteins in aqueous solution through hydrogen bonds with the hydrophilic residues of proteins. Therefore, loss of water molecules during lyophilization can collapse the three-dimensional structure and decrease protein stability. In water replacement theory, abundant hydroxyl groups in sugar molecules are thought to interact with proteins in the solid state through hydrogen bonds and effectively replace water molecules to stabilize the protein structure. Figure 1.2 simply describes the stabilizing mechanism of the three theories.

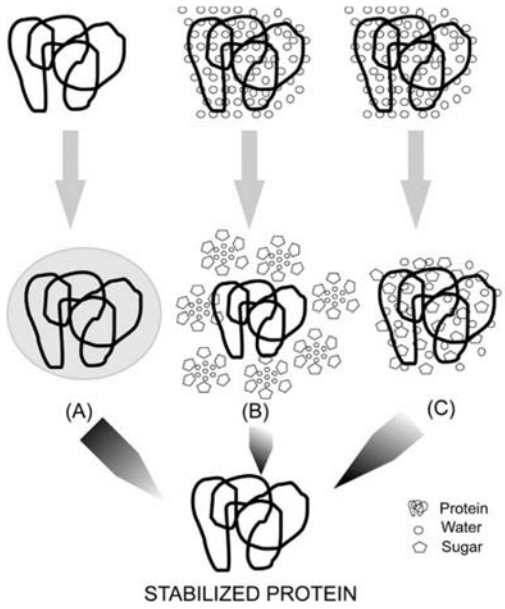

Figure 1.2: Various theories to explain the stabilizing mechanism of sugar for protein. *Modified from ref* [17].

1.2 Wet Age-related Macular Degeneration

Age-related macular degeneration (AMD) is a condition in which the macula (the center of retina) is displaced from its normal position due to drusen, geographic atrophy, choroidal neovascularization, or disciform scar formation, resulting in decreased or blurry vision and finally central vision loss in patients aged 50 years and older [19–21]. The prevalence of AMD in people aged 50 years and older in the United states is 9.2 % and it is the main cause of vision loss [19]. There are two forms of AMD, which are dry and wet. In the dry form of AMD, the degeneration of the retina is associated with the formation of small yellow or white accumulations of extracellular material, known as drusen, under the macula. Currently, there is no effective treatment for this form of AMD [22]. Although dry AMD accounts for 90 % of AMD, the wet form is responsible for 90 % of severe vision loss from AMD [19,20]. In wet AMD, abnormal blood vessels grow under the retina and macula, which is known as choroidal neovascularization (CNV). Then, the new blood vessels may bleed or leak fluid, and cause the macula to bulge or lift up from its normal position, thus resulting in the distortion or loss of central vision. There have been three types of treatments to limit or delay loss of vision in patients: laser photocoagulation, photodynamic therapy, and anti-vascular endothelial growth factor (VEGF) therapy. Laser photocoagulation is a type of laser surgery that uses an intense argon laser to burn small areas of the retina and the abnormal blood vessels under the macula. The burns seal the blood vessels by forming scar tissue, thus preventing them from leaking fluid under the macula. Photodynamic therapy (PDT) utilizes an intravascular photosensitizer, verteporfin, and low energy visible red laser to seal the leaking. This “cold laser” activates verteporfin flowing through the blood vessels

under the macula, creating highly reactive singlet oxygen which directly damages the endothelial cells of the abnormal blood vessels. However, these two treatment options for wet AMD represent only a palliative therapy since they temporarily seal the existing leaky blood vessels, but do not prevent the growth of new abnormal vessels [23]. Since 2004, the advent of anti-VEGF therapies has efficiently slowed vision loss and even improved visual acuity in wet AMD patients [24].

1.2.1 Anti-VEGF therapy

In wet AMD, the overexpression of VEGF stimulates the growth of abnormal blood vessels under the retina. Therefore, anti-VEGF agents have been developed to treat wet AMD by neutralizing VEGF activity. The first FDA-approved anti-VEGF agent in 2004 was Macugen® (pegaptanib, anti-VEGF aptamer) which demonstrated better outcomes than the conventional treatment such as laser coagulation or PDT did, however it did not improve visual acuity in patients [24]. The second FDA-approved anti-VEGF agent for wet AMD was Lucentis® (ranibizumab, anti-VEGF monoclonal antibody Fab fragment), which was, until recently, leading the market for wet AMD treatment since it was able to improve visual acuity significantly in patients [25]. On the other hand, Avastin® (bevacizumab, anti-VEGF whole monoclonal antibody) has been extensively used off-label by physicians although it is only officially FDA-approved for certain types of cancer, since a single dose of it for wet AMD costs only one-fortieth of that of Lucentis® while it demonstrates similar efficacy to Lucentis® [26,27]. The recently FDA-approved Eylea® (aflibercept, a recombinant fusion protein of human VEGF receptors 1 and 2 extracellular domains and a Fc portion of human IgG1) for wet AMD in 2011 is

currently the leading anti-VEGF agent product since it showed better outcomes than the other anti-VEGF agents [28].

1.2.2 Need for sustained release formulations

The anti-VEGF antibodies are administered monthly by intravitreal injection, but the dosing regimen is very inconvenient for patients [29] and repeated injections into the eye may induce infection, inflammation and hemorrhage [30]. Therefore, developing sustained release formulations of the anti-VEGF agents is needed to reduce their administration frequency for improved patient compliance and convenience and minimize the complications. It is important for drugs to maintain the concentration in the therapeutic window in the target sites for high efficacy and low toxicity. Sustained release formulations can help maintain the optimal concentrations of the anti-VEGF antibodies in the therapeutic window for a long period with minimal instability.

1.3 Poly(lactic-co-glycolic acid) Depots for Controlled Release

Poly(lactic-co-glycolic acid) (PLGA) is a copolymer which is synthesized from two different monomers, lactic acid and glycolic acid (Figure 1.3) [31]. PLGA has been used in numerous FDA-approved therapeutic devices since the polymer is biodegradable and biocompatible [32–35]. Therefore, there has been a large body of research utilizing PLGA as a component of drug delivery systems. The shapes of PLGA formulations are diverse, and range from microspheres, nanoparticles, implants, and films [36–39]. Factors such as molecular weight, hydrophilicity, and crystallinity influence the rate of degradation of PLGA and subsequently the release of the drug. Generally, more

hydrophilic PLGA with lower molecular weight degrades faster and since glycolic acid is more hydrophilic than lactic acid, therefore, PLGA with more glycolic acid degrades faster [40]. However, the exception to this rule is that PLGA with 50:50 (lactic acid:glycolic acid) ratio shows the fastest degradation rate because increasing glycolic acid content above 50 % results in crystallinity in the polymer. PLGA with more amorphous nature degrades faster as crystallites limit water penetration and polymer mobility [41].

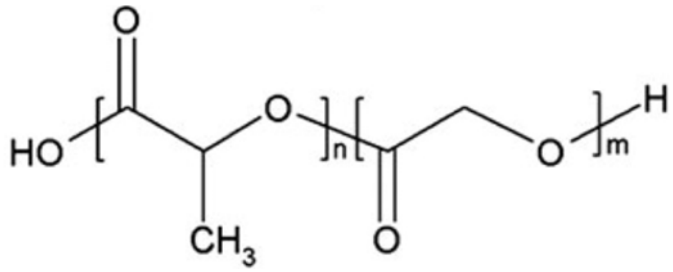

Figure 1.3: Structure of poly(lactic-co-glycolic acid). *n= number of units of lactic acid; m= number of units of glycolic acid. Modified from ref* [31].

1.3.1 Active self-encapsulating PLGA microspheres

Encapsulation of drugs into PLGA microspheres can be achieved by a number of methods, such as spray drying, coacervation, and emulsion-based methods [42]. Among these preparing methods, the emulsion-solvent evaporation method is the most common and suitable for encapsulation of therapeutic monoclonal antibodies because the other two methods have some drawbacks. Spray drying requires high temperature to remove the organic solvent, which is not good for antibody stability and some agglomeration of microspheres can also occur affecting product performance. Microspheres prepared by

coacervation may have residual toxic solvents, coacervating agents, and hardening agents [43].

To encapsulate monoclonal antibodies into PLGA microspheres, double emulsion method, water-in-oil-in-water (W/O/W) is preferred rather than single emulsion methods such as oil-in-water (O/W), oil-in-oil (O/O), and solid-in-oil-in-water (S/O/W) since W/O/W emulsion is the most suitable for encapsulation of hydrophilic antibodies [44]. Briefly describing the procedure, the inner water phase which dissolves antibodies is added to organic solvent, such as methylene chloride, dissolving PLGA and homogenized, to create the first emulsion. Immediately, this first emulsion is added into the bulk outer water phase and vortexed, thus creating double emulsions. This method can encapsulate large amount of antibody inside the microspheres. However, this also has drawbacks, which are instability of antibodies due to the interface of water and organic solvent and micronization force, and difficulty of sterilization of microspheres because they already have antibodies inside themselves and the process of sterilization may harm the activity of antibodies. To overcome these limitations, the “active self-encapsulating” method was developed in the Schwendeman laboratory [44,45]. In this method, the antibodies can be loaded into the already-prepared drug-free PLGA microspheres containing a trapping agent in the interconnected pores, and avoid stresses during the preparation of microspheres. The role of the trapping agent is to entrap the antibody from the outside solution by maintaining a concentration gradient from outside to inside microspheres. The first example of such a trapping agent that was used was $Al(OH)_3$ gel, which binds to protein antigens with high efficiency [45]. By ’self-encapsulating’, there is no chance for antibody molecules to make contact with organic solvent and

sterilization of the particles can be performed before loading of antibodies, thus be less damaging to the proteins overall. Figure 1.4 describes the advantages of this new encapsulation technology over the traditional double emulsion method. PLGA microspheres prepared by W/O/W double emulsion method are porous, thus providing large inner space for active loading of antibodies. However, this large surface created by the pore network also could potentially induce undesired fast release of encapsulated drugs. Pore closing of PLGA microspheres solves this problem. The mechanism of pore closing applied by the Schwendeman laboratory is based on passive polymer healing after incubating the microspheres above the glass transition temperature (T_g) of PLGA. Above the T_g, PLGA polymers become mobile and rearrange, therefore, pores are closed spontaneously to achieve minimal surface energy. After, the pore-closed PLGA microspheres can release the encapsulated drugs in a sustained manner. Hereafter, the phrase, 'active self-encapsulation' will refer to the concept combining 'active loading' and 'pore closing.'

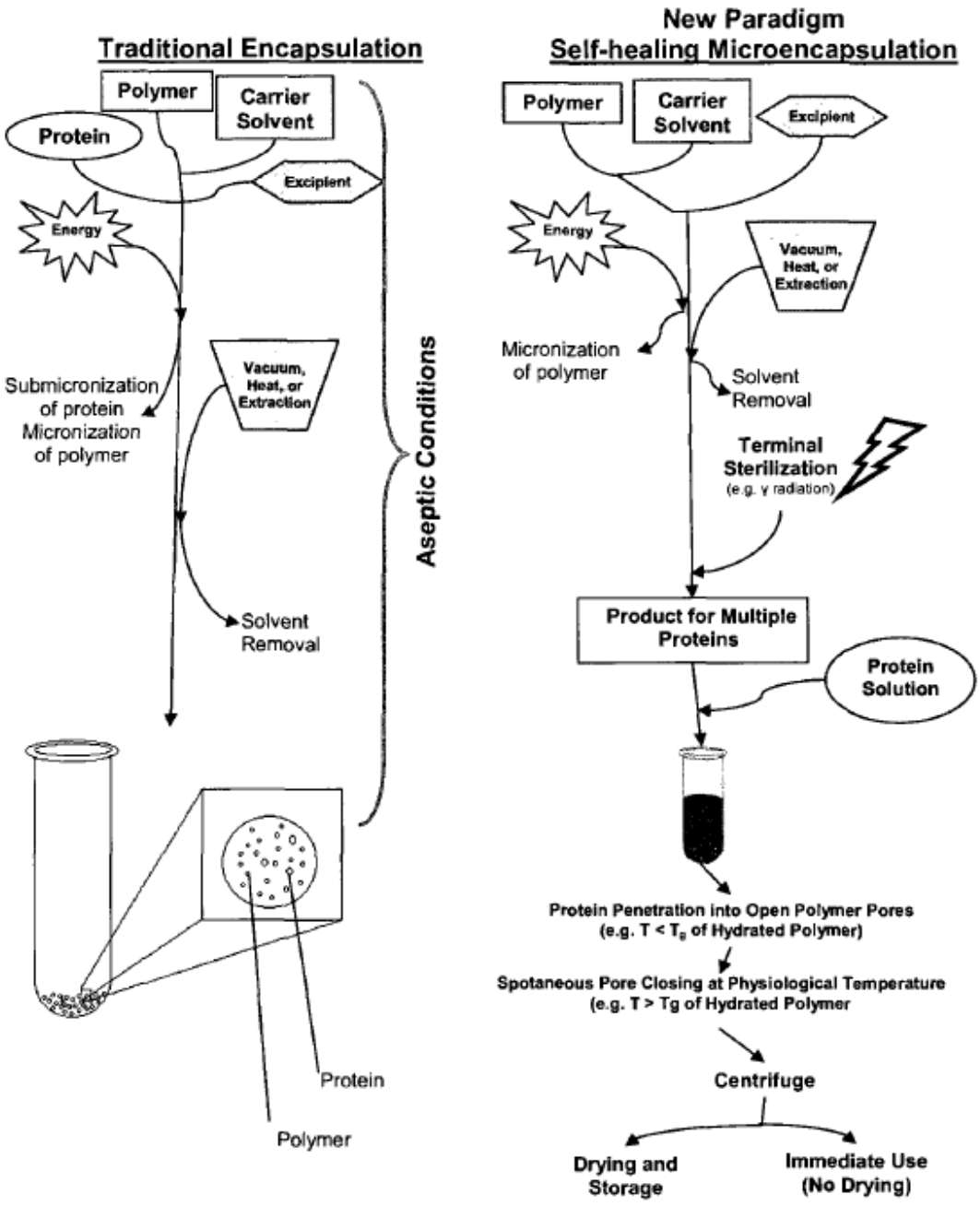

Figure 1.4: Comparison of traditional vs. self-encapsulating PLGA microspheres. *From ref* [44].

1.3.2 PLGA millicylindrical implants

PLGA millicylindrical implant (or simply PLGA implant) is another common form of PLGA depot formulations which can be employed for sustained release of the antibodies. Loading of drugs into PLGA implants is simply achieved by suspending drug powders in the PLGA/acetone solution, therefore the loading efficiency is theoretically 100 %, and it is easy to control loading of drugs [38,46]. There has been an FDA-approved, intravitreally injectable PLGA implant for controlled release of dexamethasone, Ozurdex® [47], providing a clinical precedent for use of PLGA implants in the eye. The administration of this implant is accomplished by intravitreal injection via a special applicator without any surgical procedures. The use of anhydrous microencapsulation when preparing PLGA millicylindrical implants similar to Ozurdex® was additionally developed by the Schwendeman group in order to eliminate the stress from organic solvent/water interface as occurs during common methods of protein encapsulation [38,46,48].

1.4 Current Strategies for Sustained Delivery of Anti-VEGF Agents

In order to reduce administration frequency for improved compliance and convenience of wet AMD patients, multiple strategies for sustained delivery of the anti-VEGF agents have been suggested, ranging from biodegradable polymeric depots to non-degradable reservoir systems.

1.4.1 Biodegradable polymer-based depot formulations

Anti-VEGF antibodies (bevacizumab or ranibizumab) have been encapsulated in PLGA-based depot formulations for sustained delivery. Li *et al*. reported that bevacizumab-encapsulating PLGA spheres of which the size ranged from 0.2 to 3 μm continuously released bevacizumab *in vitro* over 91 days without high initial burst release [49]. However, the loading (w/w) of bevacizumab in the well-formed spheres was only 1.6 % and the total cumulative release was only 47 %. When the loading was increased to 13 %, the particles no longer showed shape uniformity. Yandrapu *et al*. developed bevacizumab-encapsulating polylactic acid (PLA) nanoparticles in porous PLGA microparticles (NPinPMP) prepared by supercritical infusion and pressure quench technology [50]. By the technology, they achieved organic solvent-free encapsulation and continuous release of the antibodies for 4 months *in vitro* which was not achieved when the proteins were encapsulated directly in PLGA microparticles without PLA nanoparticles. The released bevacizumab from the NPinPMP showed high stability in various aspects, which was analyzed by size-exclusion chromatography (SEC), fluorescence spectroscopy, circular dichroism spectroscopy (CD), sodium dodecyl sulfate polyacrylamide gel electrophoresis (SDS-PAGE), and enzyme-linked immunosorbent assay (ELISA). They also demonstrated longer residence times of bevacizumab encapsulated in the NPinPMP compared to free bevacizumab in a rat model. But, the limitation of this formulation was low loading (<1 %). On the other hand, to stabilize the antibodies during emulsification which is a common step to prepare PLGA particulate formulations, albumin was co-encapsulated [51,52]. By co-encapsulating albumin, they replaced the organic solvent/water interfaces which are deleterious for protein stability,

thus stabilizing bevacizumab. However, the aggregated albumin instead of bevacizumab could be problematic because protein aggregates are immunogenic [53].

Biodegradable polymers other than PLGA have also been utilized for sustained delivery of the anti-VEGF agents. Despite the several attempts, only a few of them, e.g. silk hydrogels [54], nanoporous thin film of polycaprolactone [55], poly(ethylene glycol)-poly- (serinol hexamethylene urethane) reverse thermal gel [56,57], and pentablock copolymer nanoparticles [58], have achieved long duration (3-4 months) of release to be advantageous over the current dosing interval of the anti-VEGF agents. Although these previous researches with novel polymers were successful to extend the duration of release, more thorough evaluations of biocompatibility of the polymers and stability of the released proteins are needed for clinical development.

1.4.2 Port delivery system

The port delivery system (PDS), which was initially developed by ForSight Vision4 and licensed by Genentech for delivery of ranibizumab, is a refillable, non-biodegradable implant designed to provide sustained release of ranibizumab into the vitreous for treatment of wet AMD (Figure 1.5) [59]. The ranibizumab-preloaded implant is inserted in the pars plana beneath the conjunctiva via the 3.2-mm scleral incision using standard retinal surgical procedures and sutures are not needed to close. The surgical procedure usually takes less than 15 minutes. After the initial implantation, ranibizumab can be refilled through the subconjunctival refill port in the office as needed. The device provides continuous release of ranibizumab into the vitreous between refill procedures. ForSight Vision4 has successfully completed a phase 1 clinical trial I in which most of the observed adverse effects were mild and transient in nature and the approximate visual

acuity gain was 15 letters at month 12 with the average refills of 4.2 in 18 efficacy-evaluable study subjects. Genentech initiated a phase 2 clinical trial in 2015.

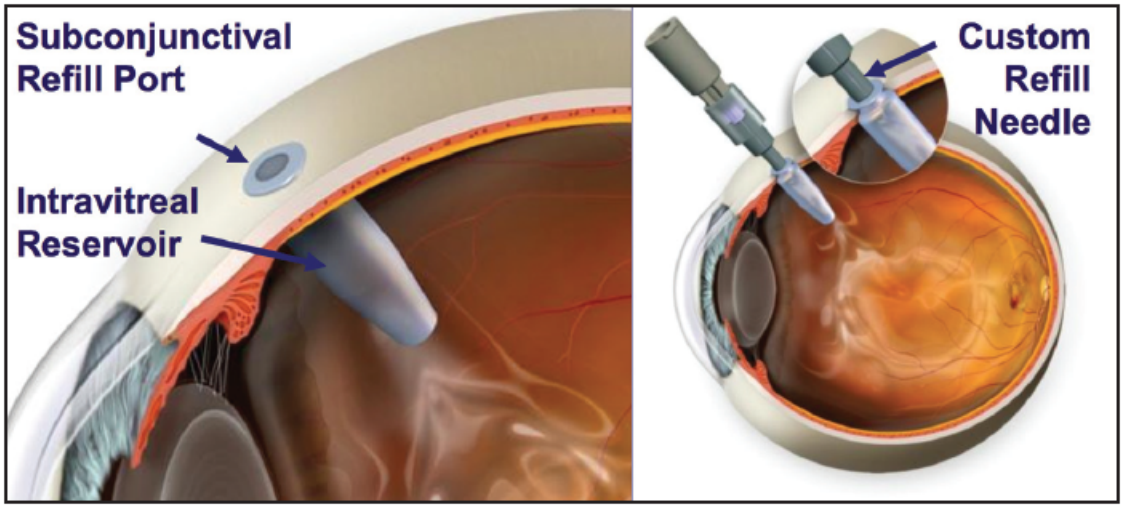

Figure 1.5: The ranibizumab port delivery system. *From ref* [59].

1.4.3 NT-503 ECT implant

Encapsulated cell technology (ECT) which has been licensed by Neurotech is a genetically engineered ocular implant that enables continuous production of therapeutic proteins from the encapsulated therapeutic cells in a non-biodegradable implant to the eye for over 2 years [60]. The ECT platform is based on the customized cell line which is immortalized, non-tumorigenic, and derived from normal human retinal pigment epithelial cells. NT-503, in which cells have been engineered to continuously produce a soluble VEGF receptor (sVEGFR) fusion protein, has been developed for the treatment of wet AMD and other neovascular diseases of the retina. Through a semipermeable membrane of the implant, inward diffusion of oxygen and nutrients for the cell survival and outward diffusion of the sVEGFR fusion protein for treatment of wet AMD are

enabled. Immune cells and host antibodies cannot permeate through the membrane, so the encapsulated cells are protected from the immune system. The NT-503 ECT implant has completed a phase 1 clinical trial, but the phase 2 clinical trial has been discontinued due to a larger than anticipated number of patients requiring rescue medication in the treatment arm.

1.5 Thesis Scope Overview

In this dissertation, PLGA depot formulations of the anti-VEGF antibodies for treatment of wet AMD were evaluated. The overall objective of this work is to achieve high w/w loading and loading efficiency, and near zero-order, and complete release for 1-3 months or longer with minimal instabilities of the antibodies by formulating them as PLGA controlled release depots.

Chapter 2 of this work evaluates the active self-encapsulating PLGA microspheres previously developed in our lab as a depot formulation for the antibodies. High molecular weight dextran sulfate (HDS) and $ZnCO_3$ were investigated as a trapping agent and an antacid, respectively. Various factors including HDS and $ZnCO_3$ contents, loading buffer pH, and protein concentration in loading solution were studied to increase w/w loading and encapsulation efficiency.

Chapter 3 investigates PLGA millicylindrical implants for sustained release of bevacizumab. In this chapter, trehalose was found to stabilize the antibodies against aggregation during powder preparation and an optimal ratio of trehalose and bevacizumab was sought to reduce the release rate of bevacizumab while maintaining its

anti-aggregating ability. This chapter also demonstrates how loading of total drug powder affects release kinetics of the antibodies.

Chapter 4 further improves the PLGA implants from Chapter 3 by coating the lateral side of the implants with pure PLGA. Different PLGA concentrations for coating were tested and the stabilities of the released bevacizumab from the optimized coated implants were analyzed in various aspects. Confocal microscopy observed the release of proteins through the lateral side of coated implants.

Chapter 5 emphasizes the key conclusions of this dissertation and discusses the future work to improve the PLGA depot formulations for clinical development.

There is an appendix briefly describing preliminary work to develop a sustained release PLGA depot formulation of adeno-associated viruses (AAV) for improved gene therapy, which has a potential to improve long-term transduction and reduce the dose of AAV administration for reducing immune response.

1.6 References

[1] G. Köhler, C. Milstein, Continuous cultures of fused cells secreting antibody of predefined specificity., Nature. 256 (1975) 495–7. http://www.ncbi.nlm.nih.gov/pubmed/1172191 (accessed September 2, 2016).

[2] N.S. Lipman, L.R. Jackson, F. Weis-Garcia, L.J. Trudel, Monoclonal versus polyclonal antibodies: distinguishing characteristics, applications, and information resources., ILAR J. 46 (2005) 258–68. doi:10.1093/ilar.46.3.258.

[3] D.M. Ecker, S.D. Jones, H.L. Levine, The therapeutic monoclonal antibody market, MAbs. 7 (2015) 9–14. doi:10.4161/19420862.2015.989042.

[4] T. Yamada, Therapeutic monoclonal antibodies., Keio J. Med. 60 (2011) 37–46. http://www.ncbi.nlm.nih.gov/pubmed/21720199 (accessed September 3, 2016).

[5] Top drugs by sales revenue in 2015: Who sold the biggest blockbuster drugs?, (n.d.). http://www.pharmacompass.com/radio-compass-blog/top-drugs-by-sales-revenue-in-2015-who-sold-the-biggest-blockbuster-drugs (accessed September 2, 2016).

[6] H.E. Chadd, S.M. Chamow, Therapeutic antibody expression technology, Curr. Opin. Biotechnol. 12 (2001) 188–194. doi:10.1016/S0958-1669(00)00198-1.

[7] H.F. Liu, J. Ma, C. Winter, R. Bayer, Recovery and purification process development for monoclonal antibody production, MAbs. 2 (2010) 480–499. doi:10.4161/mabs.2.5.12645.

[8] A.L. Nelson, E. Dhimolea, J.M. Reichert, Development trends for human monoclonal antibody therapeutics., Nat Rev Drug Discov. 9 (2010) 767–74. doi:10.1038/nrd3229.

[9] P. Carter, Improving the efficacy of antibody-based cancer therapies., Nat. Rev. Cancer. 1 (2001) 118–129. doi:10.1038/35101072.

[10] D. Lowe, K. Dudgeon, R. Rouet, P. Schofield, L. Jermutus, D. Christ, Aggregation, stability, and formulation of human antibody therapeutics, 1st ed., Elsevier Inc., 2011. doi:10.1016/B978-0-12-386483-3.00004-5.

[11] D. Arzenšek, D. Kuzman, R. Podgornik, Colloidal interactions between monoclonal antibodies in aqueous solutions, J. Colloid Interface Sci. 384 (2012) 207–216. doi:10.1016/j.jcis.2012.06.055.

[12] J. Zhang, E.M. Topp, Protein G, protein A and protein A-derived peptides inhibit the agitation induced aggregation of IgG, Mol. Pharm. 9 (2012) 622–628. doi:10.1021/mp200548x.

[13] T. Serno, J.F. Carpenter, T.W. Randolph, G. Winter, Inhibition of agitation-induced aggregation of an IgG-antibody by hydroxypropyl-??-cyclodextrin, J. Pharm. Sci. 99 (2010) 1193–1206. doi:10.1002/jps.21931.

[14] M. Vázquez-Rey, D.A. Lang, Aggregates in monoclonal antibody manufacturing

processes, Biotechnol. Bioeng. 108 (2011) 1494–1508. doi:10.1002/bit.23155.

[15] S. Saito, J. Hasegawa, N. Kobayashi, T. Tomitsuka, S. Uchiyama, K. Fukui, Effects of ionic strength and sugars on the aggregation propensity of monoclonal antibodies: Influence of colloidal and conformational stabilities, Pharm. Res. 30 (2013) 1263–1280. doi:10.1007/s11095-012-0965-4.

[16] N.K. Jain, I. Roy, Trehalose and protein stability, Curr. Protoc. Protein Sci. (2010) 1–12. doi:10.1002/0471140864.ps0409s59.

[17] N.K. Jain, I. Roy, Effect of trehalose on protein structure, Protein Sci. 18 (2009) 24–36. doi:10.1002/pro.3.

[18] L. Chang, D. Shepherd, J. Sun, D. Ouellette, K.L. Grant, X. Tang, M.J. Pikal, Mechanism of protein stabilization by sugars during freeze-drying and storage: Native structure preservation, specific interaction, and/or immobilization in a glassy matrix?, J. Pharm. Sci. 94 (2005) 1427–1444. doi:10.1002/jps.20364.

[19] S. Mehta, Age-Related Macular Degeneration, Prim. Care Clin. Off. Pract. 42 (2015) 377–391. doi:10.1016/j.pop.2015.05.009.

[20] A.D. Kulkarni, B.D. Kuppermann, Wet age-related macular degeneration, Adv. Drug Deliv. Rev. 57 (2005) 1994–2009. doi:10.1016/j.addr.2005.09.003.

[21] B.A. Syed, J.B. Evans, L. Bielory, Wet AMD market, Nat. Rev. Drug Discov. (2012) 1–2. doi:10.1038/nrd3790.

[22] H.M. Zaj??c-Pytrus, A. Pilecka, A. Turno-Kr??cicka, J. Adamiec-Mroczek, M. Misiuk-Hoj??o, The Dry Form of Age-Related Macular Degeneration (AMD): The Current Concepts of Pathogenesis and Prospects for Treatment, Adv. Clin. Exp. Med. 24 (2015) 1099–1104. doi:10.17219/acem/27093.

[23] J.Z. Nowak, Age-related macular degeneration (AMD): pathogenesis and therapy., Pharmacol. Rep. 58 (2006) 353–63. doi:papers3://publication/uuid/AF1BF145-C2D4-4A5F-B56A-078F954CCDB5.

[24] M. V Emerson, A.K. Lauer, Emerging therapies for the treatment of neovascular age-related macular degeneration and diabetic macular edema, BioDrugs. 21 (2007) 245–257. doi:2145 [pii].

[25] P. Mitchell, J.-F. Korobelnik, P. Lanzetta, F.G. Holz, C. Prunte, U. Schmidt-Erfurth, Y. Tano, S. Wolf, Ranibizumab (Lucentis) in neovascular age-related macular degeneration: evidence from clinical trials, Br. J. Ophthalmol. 94 (2010) 2–13. doi:10.1136/bjo.2009.159160.

[26] N. Ferrara, A.P. Adamis, Ten years of anti-vascular endothelial growth factor therapy, Nat. Rev. Drug Discov. (2016) 1–19. doi:10.1038/nrd.2015.17.

[27] J.L. Kovach, S.G. Schwartz, H.W. Flynn, I.U. Scott, Anti-VEGF treatment strategies for wet AMD, J. Ophthalmol. 2012 (2012). doi:10.1155/2012/786870.

[28] E. Dhrami-gavazi, Q. Ghadiali, Aflibercept : a review of its use in the treatment of

choroidal neovascularization due to age-related macular degeneration, (2015) 2355–2371. doi:10.2147/OPTH.S80040.

[29] K.M. Droege, P.S. Muether, M.M. Hermann, A. Caramoy, U. Viebahn, B. Kirchhof, S. Fauser, Adherence to ranibizumab treatment for neovascular age-related macular degeneration in real life, Graefe's Arch. Clin. Exp. Ophthalmol. 251 (2013) 1281–1284. doi:10.1007/s00417-012-2177-3.

[30] K.G. Falavarjani, Q.D. Nguyen, Adverse events and complications associated with intravitreal injection of anti-VEGF agents: a review of literature., Eye (Lond). 27 (2013) 787–94. doi:10.1038/eye.2013.107.

[31] P. Gentile, V. Chiono, I. Carmagnola, P. V. Hatton, An overview of poly(lactic-co-glycolic) Acid (PLGA)-based biomaterials for bone tissue engineering, Int. J. Mol. Sci. 15 (2014) 3640–3659. doi:10.3390/ijms15033640.

[32] J.-M. Lü, X. Wang, C. Marin-Muller, H. Wang, P.H. Lin, Q. Yao, C. Chen, Current advances in research and clinical applications of PLGA-based nanotechnology., Expert Rev. Mol. Diagn. 9 (2009) 325–41. doi:10.1586/erm.09.15.

[33] F. Wan, M. Yang, Design of PLGA-based depot delivery systems for biopharmaceuticals prepared by spray drying., Int. J. Pharm. 498 (2016) 82–95. doi:10.1016/j.ijpharm.2015.12.025.

[34] F.Y. Han, K.J. Thurecht, A.K. Whittaker, M.T. Smith, Bioerodable PLGA-Based Microparticles for Producing Sustained-Release Drug Formulations and Strategies for Improving Drug Loading, Front. Pharmacol. 7 (2016) 1–11. doi:10.3389/fphar.2016.00185.

[35] S.P. Schwendeman, R.B. Shah, B.A. Bailey, A.S. Schwendeman, Injectable controlled release depots for large molecules, J. Control. Release. 190 (2014) 240–253. doi:10.1016/j.jconrel.2014.05.057.

[36] R.B. Shah, S.P. Schwendeman, A biomimetic approach to active self-microencapsulation of proteins in PLGA, J. Control. Release. 196 (2014) 60–70. doi:10.1016/j.jconrel.2014.08.029.

[37] M.M. Pakulska, I.E. Donaghue, J.M. Obermeyer, A. Tuladhar, C.K. Mclaughlin, T.N. Shendruk, M.S. Shoichet, Encapsulation-free controlled release : Electrostatic adsorption eliminates the need for protein encapsulation in PLGA nanoparticles, (2016).

[38] V. Milacic, S.P. Schwendeman, Lysozyme Release and Polymer Erosion Behavior of Injectable Implants Prepared from PLGA-PEG Block Copolymers and PLGA/PLGA-PEG Blends., Pharm. Res. 31 (2013) 436–448. doi:10.1007/s11095-013-1173-6.

[39] X. Qu, Y. Cao, C. Chen, X. Die, Q. Kang, A poly(lactide-co-glycolide) film loaded with abundant bone morphogenetic protein-2: A substrate-promoting osteoblast attachment, proliferation, and differentiation in bone tissue engineering,

J. Biomed. Mater. Res. - Part A. 103 (2015) 2786–2796. doi:10.1002/jbm.a.35379.

[40] M.J. Alonso, S. Cohen, T.G. Park, R.K. Gupta, G.R. Siber, R. Langer, Determinants of Release Rate of Tetanus Vaccine from Polyester Microspheres, Pharm. Res. An Off. J. Am. Assoc. Pharm. Sci. 10 (1993) 945–953. doi:10.1023/A:1018942118148.

[41] A. Frank, S.K. Rath, S.S. Venkatraman, Controlled release from bioerodible polymers: Effect of drug type and polymer composition, J. Control. Release. 102 (2005) 333–344. doi:10.1016/j.jconrel.2004.10.019.

[42] R.C. Mundargi, V.R. Babu, V. Rangaswamy, P. Patel, T.M. Aminabhavi, Nano/micro technologies for delivering macromolecular therapeutics using poly(d,l-lactide-co-glycolide) and its derivatives, J. Control. Release. 125 (2008) 193–209. doi:10.1016/j.jconrel.2007.09.013.

[43] C. Thomasin, H. Nam-Tr??n, H.P. Merkle, B. Gander, Drug microencapsulation by PLA/PLGA coacervation in the light of thermodynamics. 1. Overview and theoretical considerations, J. Pharm. Sci. 87 (1998) 259–268. doi:10.1021/js970047r.

[44] S.E. Reinhold, Self -healing polymers microencapsulate biomacromolecules without organic solvents - Dissertations & Theses - ProQuest, (n.d.). http://search.proquest.com/dissertations/docview/304928707/CC3774ABA2FC4F39PQ/1?accountid=14667 (accessed September 4, 2016).

[45] S.E. Reinhold, K.G.H. Desai, L. Zhang, K.F. Olsen, S.P. Schwendeman, Self-healing microencapsulation of biomacromolecules without organic solvents, Angew. Chemie - Int. Ed. 51 (2012) 10800–10803. doi:10.1002/anie.201206387.

[46] Y. Zhong, L. Zhang, A.G. Ding, A. Shenderova, G. Zhu, P. Pei, R.R. Chen, S.R. Mallery, D.J. Mooney, S.P. Schwendeman, Rescue of SCID murine ischemic hindlimbs with pH-modified rhbFGF/Poly(DL-lactic-co-glycolic acid) implants, J. Control. Release. 122 (2007) 331–337. doi:10.1016/j.jconrel.2007.05.016.

[47] H. Mehta, M. Gillies, S. Fraser-Bell, Perspective on the role of Ozurdex (dexamethasone intravitreal implant) in the management of diabetic macular oedema., Ther. Adv. Chronic Dis. 6 (2015) 234–45. doi:10.1177/2040622315590319.

[48] K.G.H. Desai, S.R. Mallery, S.P. Schwendeman, Formulation and characterization of injectable poly(DL-lactide-co- glycolide) implants loaded with N-acetylcysteine, a MMP inhibitor, Pharm. Res. 25 (2008) 586–597. doi:10.1007/s11095-007-9430-1.

[49] F. Li, B. Hurley, Y. Liu, B. Leonard, M. Griffith, Controlled Release of Bevacizumab Through Nanospheres for Extended Treatment of Age-Related Macular Degeneration, (2012) 54–58.

[50] S.K. Yandrapu, A.K. Upadhyay, J.M. Petrash, U.B. Kompella, Nanoparticles in Porous Microparticles Prepared by Supercritical Infusion and Pressure Quench

Technology for Sustained Delivery of Bevacizumab, (2013).

[51] R. Varshochian, M. Riazi-esfahani, M. Jeddi-tehrani, A. Mahmoudi, S. Aghazadeh, M. Mahbod, M. Movassat, F. Atyabi, A. Sabzevari, R. Dinarvand, Albuminated PLGA nanoparticles containing bevacizumab intended for ocular neovascularization treatment, (2015) 1–9. doi:10.1002/jbm.a.35446.

[52] R. Varshochian, M. Jeddi-tehrani, A. Reza, European Journal of Pharmaceutical Sciences The protective effect of albumin on bevacizumab activity and stability in PLGA nanoparticles intended for retinal and choroidal neovascularization treatments, Eur. J. Pharm. Sci. 50 (2013) 341–352. doi:10.1016/j.ejps.2013.07.014.

[53] K.D. Ratanji, J.P. Derrick, R.J. Dearman, I. Kimber, Immunogenicity of therapeutic proteins : Influence of aggregation, 6901 (2014). doi:10.3109/1547691X.2013.821564.

[54] M.L. Lovett, X. Wang, T. Yucel, L. York, M. Keirstead, L. Haggerty, D.L. Kaplan, European Journal of Pharmaceutics and Biopharmaceutics Silk hydrogels for sustained ocular delivery of anti-vascular endothelial growth factor (anti-VEGF) therapeutics, Eur. J. Pharm. Biopharm. (2015). doi:10.1016/j.ejpb.2014.12.029.

[55] K.D. Lance, D.A. Bernards, N.A. Ciaccio, S.D. Good, T.S. Mendes, M. Kudisch, E. Chan, M. Ishikiriyama, R.B. Bhisitkul, T.A. Desai, In vivo and in vitro sustained release of ranibizumab from a nanoporous thin-film device, Drug Deliv. Transl. Res. (2016). doi:10.1007/s13346-016-0298-7.

[56] D. Park, V. Shah, B.M. Rauck, T.R. Friberg, Y. Wang, An Anti-angiogenic Reverse Thermal Gel as a Drug-Delivery System for Age-Related Wet Macular Degeneration a, (2013) 464–469. doi:10.1002/mabi.201200384.

[57] B.M. Rauck, T.R. Friberg, C.A.M. Mendez, D. Park, V. Shah, R.A. Bilonick, Y. Wang, Biocompatible Reverse Thermal Gel Sustains the Release of Intravitreal Bevacizumab In Vivo, (2015) 3–5. doi:10.1167/iovs.13-13120.

[58] S.P. Patel, R. Vaishya, G.P. Mishra, V. Tamboli, D. Pal, A.K. Mitra, Tailor-Made Pentablock Copolymer Based Formulation for Sustained Ocular Delivery of Protein Therapeutics, 2014 (2014).

[59] R.G. Rubio, Long-Acting Anti-VEGF Delivery, Retin. Today. July/Augus (2014) 78–80.

[60] http://www.neurotechusa.com.

Chapter 2: Active self-encapsulating PLGA microspheres of bevacizumab and its Fab fragments

2.1 Abstract

In order to develop active self-encapsulating poly(lactic-co-glycolic acid) (PLGA) microspheres for controlled release of the anti-vascular endothelial growth factor (VEGF) antibodies, several candidates of trapping agents have been investigated. Enzymatically produced Fab fragments from bevacizumab were used as a model to mimic ranibizumab (Lucentis®) and to circumvent agitation-induced aggregation which commonly occurs with whole antibody molecules. The first trapping agent tested was Ca-alginate, a natural biopolymer found in brown algae, and is biocompatible, biodegradable and has negative charges for binding of the positively charged antibodies at loading pH of 5.5. Both loading and encapsulation efficiency were 2.8-4.0 % and 56.6-82.4 %, but the initial burst release on day 1 was ~60 % and the release stopped afterwards. Next, high molecular weight dextran sulfate (HDS), another negatively charged biopolymer, was tested as a trapping agent and has been successfully employed for encapsulating lysozyme and VEGF. In addition, $ZnCO_3$ was encapsulated in the HDS-PLGA microspheres as an antacid to stabilize the encapsulated proteins. The formulation resulted in continuous and complete release of the immunoreactive anti-VEGF Fab fragments, however, loading and encapsulation efficiency would require further optimization. Subsequently, other anionic polymers were screened and poly(acrylic acid) (PAA) was chosen to be encapsulated in

PLGA microspheres as a trapping agent, however both loading and encapsulation efficiency were at undesired levels. Active self-encapsulating PLGA microspheres have served as successful formulations for controlled release of varying drugs, and here we have demonstrated the feasibility to use this strategy to encapsulate and stabilize anti-VEGF antibodies. Further efforts to bolster the loading and improve the release profiles are warranted for clinical viability.

2.2 Introduction

Wet age-related macular degeneration (wet AMD) is a severe form which is responsible for approximately 90 % of cases of severe vision loss due to AMD [1]. Overexpression of VEGF leads to abnormal growth of blood vessels under the macula, thus resulting in central vision loss. Therefore, anti-VEGF therapies were developed to treat wet AMD by neutralizing the overexpressed VEGF [2]. The current dosing schedule of anti-VEGF agents for treatment of wet AMD is monthly intravitreal injection, but this is very inconvenient for patients [3] and may induce infection, inflammation, and hemorrhage [4]. Here is a need for controlled release depots for the drugs which can reduce the administration frequency and improve patient comfort.

PLGA microspheres have been extensively researched and used in several FDA-approved products as depot systems of protein therapeutics for controlled release [5–7]. Although PLGA depots exhibit desirable qualities such as biodegradability and biocompatibility [8], a major drawback of conventional PLGA microspheres for protein drugs is the destabilization of proteins during encapsulation, sterilization, and release [9–

12]. A common method of protein encapsulation in PLGA microspheres is the double emulsion-solvent evaporation method. In this process, proteins necessarily encounter deleterious conditions such as aqueous/organic interfaces, shear stress by micronization, and gamma radiation for sterilization. To bypass these stress factors, self-encapsulation technology has been developed, previously in our lab [10]. By this new method, proteins can be loaded into pre-formed porous PLGA microspheres from an aqueous solution, thus avoiding all the above stressors. Through this method, drugs can be encapsulated by either passive or active loading. Passive loading utilizes a concentration gradient as a driving force to encapsulate the drug, however this method requires large quantities or high concentrations of protein and is inefficient. To overcome this, an active loading method was developed, which employs a trapping agent with binding affinity for the drugs to be encapsulated. This binding results in more partition of drugs inside the microspheres [10,11,13]. Proteins in PLGA matrix can also be destabilized due to the low microenvironmental pH created by acid byproducts from the polymer degradation during release. To neutralize the acidic pH in the microenvironment during the release, poorly soluble basic salts have been incorporated [9,14]. Lastly, in the hope of slowing down the release, surface pores were closed by incubating the microspheres at above the glass transition temperature [10,11]. The schematics of these processes were briefly described in Figure 2.1.

In this chapter, we tested the hypothesis that active self-encapsulating PLGA microspheres can serve as controlled release depots for bevacizumab or its Fab fragments. Enzymatically produced Fab fragments from the whole antibodies of bevacizumab were also used to mimic the officially approved anti-VEGF Fab fragment,

ranibizumab (Lucenits®), the cost of which is significantly more expensive than the corresponding dose of bevacizumab (Avastin®) [15]. Bevacizumab and its Fab fragment are positively charged at neutral pH, so anionic polymers were incorporated in PLGA microspheres as a trapping agent to utilize an electrostatic interaction as a binding force. Poorly soluble basic salts were co-encapsulated in the polymer to provide continuous neutralization of the produced acids from polymer degradation [9]. Due to the limit of injection volume into the target site, both the w/w loading of the drug (>5 %), and encapsulation efficiency needs to be to be high. To develop formulations, the effects of basic salts and trapping agent content in microspheres, loading pH and concentration of the proteins in loading solution were tested.

2.3 Materials and Methods

2.3.1 Materials

Avastin® (bevacizumab) was purchased from the Central Pharmacy of the University of Michigan Hospital. PLGA 50:50 (inherent viscosity = 0.64 dL/g and Mw = 54.3 kDa, ester terminated) was purchased from LACTEL Absorbable Polymers (Birmingham, AL). Recombinant human vascular endothelial growth factor (VEGF) was a generous gift from Genentech. All other reagents and supplies were purchased from commercial suppliers and were of analytical grade.

2.3.2 Production of Fab fragments from bevacizumab

Fab fragments of bevacizumab were produced by papain-digestion using a commercial Pierce™ Fab Preparation Kit (Thermo Fisher Scientific, MA). Briefly, the

whole antibodies were digested into their Fab and Fc fragments by immobilized papain resins for 6 h with an end-over-end mixer at 37°C. The resulting proteins were incubated with immobilized protein A columns. By spinning down the protein A columns, only Fab fragments were eluted as undigested antibodies and Fc fragments were bound to immobilized protein A. The bound proteins were eluted separately using elution buffer.

2.3.3 Sodium dodecyl sulfate polyacrylamide gel electrophoresis (SDS-PAGE)

Papain-digested bevacizumabs were analyzed by SDS-PAGE. The antibodies were digested by papain for 2 and 6 h to observe time dependency. Non-reduced and reduced proteins by boiling for 5 min at 95°C in the presence of 2-mercaptoethanol were mixed with sample loading buffer (Bio-Rad, CA) and run on Invitrogen PowerEase 500 at 200 V for 30 min in polyacrylamide gel. Precision Plus Protein™ Unstained Standards (Bio-Rad) were used as molecular weight standard markers. The gel was stained by Coomassie blue dye.

2.3.4 Protein quantification

Protein quantification was performed using either bicinchoninic acid (BCA) assay, size-exclusion high-performance liquid chromatography (SE-HPLC) or size-exclusion ultra-performance liquid chromatography (SE-UPLC) as described below.

2.3.4.1 BCA assay

Protein was quantified by Pierce™ BCA Protein Assay Kit (Thermo Fisher Scientific) according to manufacturer's instruction. Protein samples and standards of known concentration in triplicate were added in a 96-well plate. The mixture of BCA reagent A and B at the ratio of 50:1 was added into each well. The plates were incubated at 37°C for 30 min and read using a plate reader (BioTek, VT) at 595 nm.

2.3.4.2 SE-HPLC & SE-UPLC

The condition of SE-HPLC to quantify whole antibodies and Fab fragments of bevacizumab was followed as previously described [16] with slight modifications. The mobile phase (0.182 M KH_2PO_4, 0.018 M K_2HPO_4, and 0.25 M KCl, pH 6.2) was run at a flow rate of 0.5 mL/min through a column (TSK-GEL G3000SWxl; Tosoh Bioscience, Japan), and elution was monitored at 280 nm. The volume of injection was 50 µL, and the running time was 30 minutes. To quantify Fab fragments of bevacizumab, SE-UPLC was also performed using a ACQUITY UPLC BEH125 SEC column (Waters, MA) with the same mobile phase as in SE-HPLC at 0.3 mL/min. The volume of injection was 5 µL, and the running time was 11 min. The peaks were analyzed at 280 nm. All samples for SE-HPLC and SE-UPLC were filtered through 0.45 µm protein low binding filter.

2.3.5 Determination of binding ratio of antibodies and trapping agents

Aqueous solutions of trapping agents (high molecular weight (~500 kDa) dextran sulfate (HDS), poly acrylic acid (PAA), poly methacrylic acid (PMAA), poly styrenesulfonic acid (PSSA), pectin and carrageenan) were mixed with bevacizumab or its Fab fragment at different mass ratios in 10 mM histidine buffer, pH 5.5 at room temperature. After 1 h of incubation, the complex was centrifuged and unbound free protein in the supernatant was quantified by SE-HPLC.

2.3.6 Preparation of active self-encapsulating PLGA microspheres

Porous self-encapsulating PLGA microspheres were prepared using a water in-oil-in-water (w/o/w) double emulsion method. Two hundred to five hundred µL of inner water phase with varying amounts of trapping agents and D-trehalose in ddH_2O (w/o/w) was homogenized into the oil phase, 200 or 250 mg/mL of PLGA in methylene chloride with 3 %

$MgCO_3$ w/w (weight by weight of total microspheres) or 3-6 % $ZnCO_3$ for 60 s at 17,000 rpm over an ice bath using the Tempest IQ homogenizer (Virtis, USA). To this first emulsion, 2 mL of 5 % (w/v) PVA solution was immediately added and the mixture was vortexed at 70 % intensity for 60 s to create a double emulsion. The double emulsion was quickly poured into 100 mL of 0.5 % (w/v) PVA solution and stirred for 3h in a fume hood at room temperature to form hardened microspheres. Hardened microspheres were than sieved (20-45, 45-90 μm) for collection and subsequently washed with ddH_2O, lyophilized and stored at -20°C for future use.

2.3.7 Active self-encapsulation of antibodies in PLGA microspheres

Active self-encapsulation in porous PLGA microspheres consists of two subsequent steps: the first step is "loading" of the proteins in porous PLGA microspheres and the second step is "pore closing" of the surface of microspheres by incubating at above the glass transition temperature of the polymer. For loading, the porous PLGA microspheres were incubated in a protein solution of varying concentrations in 10 mM histidine buffer (pH 5.5) at 4°C or 25°C for 24 h on an orbital shaker with 320 rpm. Subsequently, the pore closing was carried out by incubating the microspheres at 43°C for 48 h which is well above the hydrated glass transition temperature of the polymer. The resulting particles were centrifuged and the supernatant was collected to measure loaded proteins by subtracting the remaining mass of proteins in the supernatant from the initial mass of proteins in loading solution. The w/w loading and encapsulation efficiency (EE) were calculated by the following equations:

$$w/w\ loading\ = \frac{Mass\ of\ loaded\ proteins\ in\ microspheres}{Total\ mass\ of\ microspheres} \times 100\ \%$$

$$Encapsulation\ efficiency\ = \frac{Mass\ of\ loaded\ proteins\ in\ microspheres}{Initial\ mass\ of\ proteins\ in\ loading\ solution} \times 100\ \%$$

The mass of proteins was measured as described in the above section, "protein quantification."

2.3.8 *In vitro* release study

In vitro release kinetics was determined by suspending 5 - 20 mg of loaded microspheres in either PBST (phosphate buffered saline containing 0.02 % Tween 80 w/w) pH 7.4 or PBST containing 1 % BSA (bovine serum albumin) used for enzyme linked immunosorbent assay (ELISA) assay. The concentration of particles in the release buffer ranged from 3 to 10 mg/mL. The particles were incubated in a 37°C incubator, at select time points were centrifuged at 8000 rpm for 5 min, and the supernatants were collected and replaced with the same volume of fresh release buffer. The protein content in the release supernatant collected from each time point was assayed to determine the release.

2.3.9 Determination of immunoreactivity by ELISA

ELISA was performed to determine immunoreactive activity of Fab fragments and whole antibodies of bevacizumab as described previously [17] with some modifications. Briefly, 96-well ELISA microplates were pre-coated with 50 µl of VEGF (0.5 µg/mL) solution in PBS (phosphate buffered saline, pH 7.4) at 4°C overnight. After washing with 350 µl of PBS four times, 100 µl of PBS containing 1 % BSA was added for blocking and incubated at room temperature for 2 h. After washing, 50 µl of Fab fragment standards (0 ~ 800 ng/mL) or bevacizumab whole antibody standards (0 ~ 2560

ng/mL) and samples diluted in PBST containing 1 % BSA were added into each well and incubated at room temperature for 1 h. After washing, 50 µl of secondary antibody (alkaline phosphatase conjugated goat anti-human IgG, Fab specific) was added at 1: 1000 dilution in PBST containing 1 % BSA into each well and incubated for another 1 h. Detection was carried out by adding 50 µl of p-nitrophenyl phosphate liquid substrate system (Sigma, MO) after washing. Color development was monitored with a plate reader (Dynex MRX II, Richfield, MN) every 10 min for 30 min at 405 nm. A standard curve was plotted using a sigmoidal fit (Figure S2.1) and concentrations of diluted samples were calculated.

2.3.10 Evaluation of reconstituted bevacizumab from the complexes with trapping agents

Complexes of bevacizumab and trapping agents at the optimal ratios were centrifuged and the supernatants were removed. Then, PBST was added into the centrifuged insoluble complexes. It was observed with the naked eye that all the complexes were dissolved immediately after vortexing for a few seconds. These solutions were analyzed by SE-HPLC and ELISA to determine the amount of soluble reconstituted proteins and their immunoreactivity. Solubility and immunoreactivity of bevacizumab after reconstitution were calculated by the following equations:

$$Solubility = \frac{Concentration\ of\ soluble\ bevaicuzmab}{Initial\ concentration} \times 100\ \%$$

$$Immunoreactivity = \frac{Concentration\ of\ immunoreactive\ bevacizumab}{Concentration\ of\ soluble\ bevaicuzmab} \times 100\ \%$$

where concentration of soluble bevacizumab and concentration of immunoreactive bevacizumab were determined by SE-HPLC and ELISA, respectively after reconstitution in PBST.

2.3.11 Scanning electron microscopy (SEM)

The surface morphology of PLGA microspheres was examined by Hitachi S3200N scanning electron microscope (Hitachi, Japan). The microspheres were first fixed on a brass stub using double sided adhesive carbon tape and then were made electrically conductive by coating with a thin layer of gold (~ 5 nm) for 120 s at 40 W. The images of microspheres were taken at an excitation voltage of 8 - 20 kV.

2.4 Results and Discussion

In order to develop PLGA microspheres of bevacizumab and its Fab fragment for sustained release by active self-encapsulation, several factors governing loading and release kinetics must be considered. As a trapping agent, calcium (CA)-alginate, high molecular weight dextran sulfate (HDS) and other negatively charged polymers were investigated to use electrostatic interaction as a binding force since the antibodies are positively charged at neutral pH.

2.4.1 Bevacizumab Fab fragments

Although Lucentis® is an officially approved drug for wet AMD, its whole antibody version, Avastin® is commonly being used off-label in clinics for wet AMD due to its low cost. For research purpose, likewise, bevacizumab was used in this study owing to its cost-effectiveness. However, it is known that the whole antibody has a propensity to

aggregate induced by agitation [18,19] which is a step of active self-encapsulation to facilitate loading. Thus, Fab fragments enzymatically produced from the whole antibody, bevacizumab, were used in order to avoid agitation-induced aggregation and to mimic ranibizumab.

In order to produce Fab fragments from the whole anti-VEGF antibody, bevacizumab, a commercial Fab fragment preparation kit was used (Figure 2.2A). To confirm the production of Fab fragments, SDS-PAGE was performed (Figure 2.2B). Bevacizumab was incubated for 2 and 6 h with an immobilized papain, which specifically cuts at the hinge region of an antibody, to observe the time dependency on digestion. In a non-reducing condition, a band for Fab fragments which have a molecular weight slightly smaller than 50 kDa was observed in the fraction of "flowthrough" from protein A column which captures only proteins with Fc portion. After eluting Fab fragments from the protein A column, the bound proteins were eluted using a low pH eluting buffer and run in a gel. In this fraction (Protein A elution), Fab fragments which are not eluted previously, Fc fragments which are slightly bigger than 50 kDa, partially digested antibodies (~100 kDa), and undigested whole antibodies (~150 kDa) were observed. Although not all of the antibodies were digested, digestion times greater than 6h were not tested as per the kit instructions. In a reducing condition, all the disulfide bonds between chains are broken, therefore, a half-size band of Fab fragments (~25 kDa) was observed in the fraction of "Protein A flowthrough." In the fraction of "Protein A elution", half-size bands of Fab and Fc fragments (~25 kDa) and undigested heavy chains (~50 kDa) were observed as expected. For the future studies, the digestion time was fixed at 6h in order to ensure enough digestion, and to minimize damages by the enzyme.

2.4.2 Ca-alginate gel as a trapping agent

Isoelectric points (pI) of bevacizumab and ranibizumab (Lucentis®) are 8.3 – 8.4 [20,21] and 8.8 [22], respectively, which means they have a net positive charge at neutral pH or below. Ranibizumab is only different by six amino acids from the corresponding part of bevacizumab and one anionic residue is added in total [23], so the Fab fragment produced from bevacizumab should also be positively charged at neutral pH or below as well. Therefore, negatively charged polymers can serve as trapping agents for active loading of bevacizumab by electrostatic interaction. Alginic acid is an anionic polysaccharide found in the cell walls of brown algae, which can form insoluble gel when divalent cations such as Mg^{2+}, Ca^{2+}, Zn^{2+}, Sr^{2+} and Br^{2+} are added by cross-linking the polymers [24]. Along with its negative charge, alginic acid is biodegradable, biocompatible and easily available [24,25], therefore it could be a good candidate of a trapping agent for bevacizumab. In the preliminary study, water-soluble sodium alginate (Na-alginate) was dissolved in an inner water phase of PLGA microspheres, then the resulting microspheres were pre-incubated with the divalent cation salts, $CaCl_2$ or $ZnCl_2$, for 24 h at 4°C, washed with water, and then actively loaded with Fab fragments in 10 mM histidine buffer, pH 5.5, which is the buffer of Lucentis® and pore-closed. Loadings (w/w) were encapsulation efficiencies were too low (below 0.1 % and ~1 %, respectively). When Fab fragments were mixed with the same mass of Ca-alginate powders, over 80 % of Fab fragments were bound. The initial mass of Na-alginate added in the inner water phase was 10 % (w/w) of PLGA, and the mass of Fab fragments in loading solution was 5 % (w/w) of total microspheres, so the binding ratio of Fab fragments and alginate polymers should be enough assuming all the alginate was

encapsulated. However, the results of very low encapsulation efficiency (~1 %) revealed that most of alginate may have been removed during the solvent evaporation step and/or incubation step in the divalent cation salt solution. Loading and encapsulation efficiency slightly increased, to 0.4 % and 8.4 % respectively, without incubation in the divalent cation salt solution, therefore, it can be supposed that the considerable amount of Na-alginate escaped from the microspheres rather than formed insoluble gel in the microspheres during the pre-incubation step. In order to prevent alginate from leaching out of microspheres, lyophilized Ca-alginate powders were prepared and suspended in an inner water phase of PLGA microspheres. Four different formulations were prepared: (A) 10 % (weight/weight of polymer) Ca-alginate suspended in 50 % (weigh/volume of inner water phase) trehalose solution, (B) 10 % Ca-alginate suspended in 10 % trehalose solution, (D) 10 % Ca-alginate suspended in water, (D) 20 % Ca-alginate suspended in 10 % trehalose solution. Trehalose acts as a porosigen, thus affecting pore structures of microspheres and presumably loading of Fab fragments. By suspending Ca-alginate powders in the inner water phase, high loading (2.8, 3.3, 4.1 and 4.0 %, respectively) and encapsulation efficiency (56.6, 65.7, 82.4 and 79.3 %, respectively in A-D) were obtained after active self-encapsulation steps (Figure 2.3). In the following *in vitro* release study, however, the initial burst release on day1 was ~60 % of the total loaded Fab fragments and the release stopped afterward. Sodium ions which are present in the human body and PBST (release medium) can dissolve insoluble Ca-alginate gel into liquid, therefore, they may be responsible for the high initial burst release.

2.4.3 HDS as a trapping agent

As the second candidate of trapping agents, high molecular weight (~500 kDa) dextran sulfate (HDS) was investigated. Previously in our lab, HDS was employed as a trapping agent for successful active self-encapsulating PLGA microspheres of lysozyme and VEGF [13]. Sulfate groups of HDS have highly negative charges, so HDS can bind to Fab fragments of the opposite charge by electrostatic interaction.

2.4.3.1 Fab fragment-HDS binding

To determine the binding ratio of Fab fragments and HDS, they were complexed at varying ratios and the remaining free proteins in the supernatants were measured after centrifugation. The bound proteins to HDS formed insoluble pellets at the bottom of tubes and were able to be reconstituted to soluble proteins immediately when PBST is added. Among the tested ratios, most of Fab fragments (99.1%) were bound to HDS at the ratio of 1:0.1 (Fab fragment : HDS, w/w) (Figure 2.4). Interestingly, less proteins were bound to HDS at the higher ratios (1:0.2 – 1:1). This may be due to repelling force between highly negatively charged HDS polymers. This optimal ratio (1:0.1) of binding is ideal since only 10 % mass of HDS is needed to capture Fab fragments, therefore, not so much HDS needs to be encapsulated in PLGA microspheres.

2.4.3.2 Active self-encapsulating PLGA microspheres with HDS and $ZnCO_3$

The formulations developed initially for lysozyme and VEGF in our lab contained 3 % trehalose (w/w of polymer) as a porosigen and 4 % HDS as a trapping agent in an initial inner water phase and 3 % $MgCO_3$ as an antacid. Therefore, half milliliter of 2 mg/mL Fab fragments were loaded into 20 mg of this formulation for 48 h at 24°C. Loading and encapsulation efficiency were measured by quantifying the remaining proteins in the supernatants with SE-HPLC, which were 1.8 % and 36.9 %, respectively

(Figure 2.5 A and B). After the active self-encapsulation, *in vitro* release study was performed at the particle concentration of 3 mg/mL in PBST containing 1 % BSA for ELISA analysis. Considering the loading and the particle concentration in release study were low, measurement of release by SE-HPLC was not performed due to its low limit of detection. Release of immunoreactive Fab fragments from this formulation almost stopped at 34 % on day 7 (Figure 2.5 C). $MgCO_3$ was known to maintain the microenvironmental pH in PLGA at around 7 [26]. On the other hand, it can be extrapolated that Fab fragment mimicking ranibizumab is stable at pH 5.5 which is the pH of the commercial Lucentis® formulation. Therefore, $ZnCO_3$ (6 %) which maintains the microenvironmental pH in PLGA at 5 - 6 [26] was encapsulated in the HDS-PLGA microspheres instead of $MgCO_3$. After the active self-encapsulation, it was observed by SEM that pores of the microspheres were closed and surface became smooth (Figure S2.2). Loading and encapsulation efficiency were slightly reduced to 1.2 % and 23.4 %, respectively (Figure 2.5 A and B), however, release of immunoreactive Fab fragments was continuous throughout the whole release study and by day56, the total cumulative release was 99.1 % of the loaded protein (Figure 2.5 C). This result showed the control of microenvironmental pH in PLGA can be a strategy to stabilize the encapsulated proteins and to result in continuous and complete release. However, loading and encapsulation efficiency were low, so these parameters still need to be improved. In addition, initial burst release on day1 from the HDS-PLGA microspheres with $ZnCO_3$ was 41.7 %, and then release rate slowed down. The release rate needs to be near zero-order to maintain the concentration of antibodies at a constant level in the target site.

2.4.3.3 Effect of $ZnCO_3$ content on loading

In order to increase loading and encapsulation efficiency, the effect of $ZnCO_3$ content in microspheres on loading was investigated. The HDS-PLGA microspheres studied above which contain 6 % $ZnCO_3$ resulted in almost complete release, therefore, 6 % $ZnCO_3$ is thought to be enough to stabilize the encapsulated proteins. However, it may be possible that high content of the basic salt increase pH in the pores during the active loading, thus resulting in low loading of Fab fragments as efficient loading occurs at pH in between the pKa of trapping agents and pI of proteins. Therefore, the content of $ZnCO_3$ was reduced to 0, 3 or 4.5 %. As expected, HDS-PLGA microspheres without ZnCO3 showed the highest loading (2.7 %) among those probably because loading pH in the microspheres did not increase. Interestingly, however, loadings in the microspheres with 3 % and 4.5 % $ZnCO_3$ were 0.9 % and 1.2 %, which were slightly lower than one (1.3 %) with 6 % $ZnCO_3$ at the same condition. Overall, changing the content of $ZnCO_3$ did not much enhance both the loading and encapsulation efficiency (Figure 2.6 A).

2.4.3.4 Effect of loading buffer pH on loading

Similar to changing the basic salt content, the pH of the loading buffer was changed to test the effect on loading parameters. In addition to the initial pH 5.5 of 10 mM histidine buffer, loading buffers of pH 4.5, 5.0 (10 mM acetate buffer) and 6.0 (10 mM histidine buffer) were tested with all the other condition as previously used. However, the resulting loadings (1.5 %, 1.6 %, 1.3 % and 1.5 % for pH 4.5, 5.0, 5.5 and 6.0, respectively) in those conditions did not appear to exhibit a pH-dependent pattern (Figure 2.6 B). These pH values were the initial pH of loading buffers, and it was observed later that the final pH of loading solutions after adding the proteins were all

similar (pH ~5.5) since the protein by itself has buffering capacity. However, adjusting final pH to the desired values was not performed since the addition of extreme pH adjusting solutions would destabilize the proteins.

2.4.3.5 Effect of HDS content on loading

As shown in Figure 2.4, Fab-HDS binding (99.1%) was the highest at 1:0.1 in the loading buffer (10 mM histidine buffer, pH 5.5) and it gradually reduced at the lower and higher ratios. Thus, there should be a certain ratio at which most HDS is available for binding of Fab fragments in microspheres. Since the encapsulation efficiency of HDS in microspheres is unknown, varying amount of HDS (0.3 % - 8 %, w/w of PLGA) was encapsulated and loadings of Fab fragments into these formulations were measured (Figure 2.6 C). A formulation with 1 % HDS resulted in the highest loading (2.1 %) and ones with the lowest (0.3 %) and highest (8 %) HDS content showed the lower loadings, which are 0.6 % and 1 %, respectively. It is supposed that the 1 % HDS content gives the optimal binding ratio with the proteins in loading solution as shown in the binding profile of Figure 2.4. Overall, loading and encapsulation efficiency were not significantly enhanced as desired.

2.4.3.6 Effect of Fab concentration on loading

Lastly, the effect of Fab fragment concentration in the loading buffer on loading/efficiency was studied. Formulations with 1 % and 2 % HDS were chosen because they demonstrated relatively higher loading of Fab fragments. Other conditions were fixed to the initial ones (10 mM histidine buffer, pH 5.5, and 6 % $ZnCO_3$). Fab fragments of three different concentrations (4, 8, 16 mg/mL) in the fixed volume of loading buffer (0.125 mL) were loaded into 5 mg of 1 % and 2 % HDS-PLGA

microspheres through the same active self-encapsulation process as above. Higher concentration of proteins in loading solutions resulted in higher loading and formulations with 1 % HDS showed slightly higher loading than ones with 2 % HDS at the same loading concentration as expected (Figure 2.7). Loading in microspheres with 1 % HDS at 16 mg/mL Fab fragment was the highest (6.4 %) which seems promising, however, encapsulation efficiency was only 15.7 % which is the lowest among the same formulations. On the contrary, the formulation loaded with the lowest concentration (4 mg/mL) of proteins showed the lowest loading (2.9 %) and the highest encapsulation efficiency (29.3 %). This opposite trend of loading and encapsulation efficiency was also observed in 2 % HDS microspheres. Considering all the resulting loadings and encapsulation efficiencies, changing the parameters above did not improve both loading and encapsulation efficiency simultaneously to the desired levels.

2.4.4 Evaluating whole antibodies of bevacizumab

Papain-digested Fab fragment from bevacizumab had been used because it mimics ranibizumab (Lucentis®) which is an officially approved drug for wet AMD at a much lower cost and whole antibody is known to be prone to aggregation induced by agitation [18,19] which is a step of active self-encapsulation. However, it is difficult to control quality of enzymatically produced Fab fragments in laboratory settings and considerable amount of the papain-digested Fab fragments dimerizes depending on concentration. From the soluble Fab fragment standards, the monomer content was measured by SE-HPLC, which only ranged from 56.0 to 66.5 % (Figure S2.3), and it is unknown how this considerable dimerization affects stability and activity of the proteins.

In order to avoid these uncertainties, we decided to use the whole antibody of bevacizumab instead of Fab fragments for all the following studies.

2.4.5 Screening trapping agents for whole antibody

From the above studies, it was revealed that HDS is promising as a trapping agent for active self-encapsulation of the therapeutic antibodies, but has some drawbacks which are low loading or low encapsulation efficiency, and undesirable release kinetics. Therefore, other trapping agents were tested as well. Several properties such as biocompatibility, biodegradability, and anionic charge property at loading pH were desired as selection criteria for trapping agents. Consequently, the following anionic polymers were chosen to test abilities as trapping agents: poly(acrylic acid) (PAA), poly(methacrylic acid) (PMAA), poly(styrenesulfonic acid) (PSSA), pectin, and carrageenan. These are commonly researched materials for drug delivery and meet the desirable criteria [27–31]. Firstly, their binding ability to bevacizumab was tested with the same condition as in Fab-HDS binding assay done previously (Section 2.3.5). Like HDS, bevacizumab bound optimally to the polymers at a specific ratio, except for PSSA to which most proteins bound at and beyond a certain ratio (Figure 2.8). The optimal ratios at which most proteins bound to the trapping agents ranged from 1:0.1 to 1:0.5 (bevacizumab:trapping agent, w/w) which are acceptable because the trapping agents do not need to be encapsulated more than proteins in microspheres. Next, it was tested how much active bevacizumab can be recovered from the complexes after reconstitution in PBST. Among those complexes, the reconstituted bevacizumab from PAA, PMAA and pectin was completely soluble (101.7 %, 103.8 % and 104.0 %, respectively) and protein bound to PAA demonstrated the highest immunoreactivity (90.7 %) (Figure 2.9).

Therefore, PAA was chosen to be encapsulated as another trapping agent in PLGA microspheres because it demonstrated high protein binding and desired properties of released proteins in terms of solubility and immunoreactivity. PAA was encapsulated at 4 % and 8 % in PLGA microspheres with 6 % $ZnCO_3$ and bevacizumab was loaded with the same active self-encapsulation process as before. Unfortunately, however, loadings and encapsulation efficiencies were extremely low, which were 0.27 % and 2.7 % for 4 % PAA formulation; and 0.16 % and 1.6 % for 8 % PAA formulation (Figure 2.10). Release study was not performed because the concentration of released proteins would be too low to be measured.

2.5 Conclusions

In this chapter, we demonstrated that anionic polymers can serve as trapping agents for the anti-VEGF antibodies to develop active self-encapsulating PLGA microspheres. Ca-alginate enabled high loading and encapsulation efficiency of the proteins, but the release stopped after high initial burst release on day 1, which is undesirable. HDS-PLGA microspheres containing $ZnCO_3$ as an antacid showed continuous and complete release of the immunoreactive anti-VEGF Fab fragments by day56. Despite changing several formulation parameters, their low loading and encapsulation efficiency were not significantly improved and the release kinetics needs to be more near zero-order to maintain the concentration of antibodies at a constant level in the target site. In an attempt to solve these issues, other anionic polymers were screened as trapping agents and active self-encapsulating PAA-PLGA microspheres were prepared, however, they resulted in very low loading and encapsulation efficiency.

In conclusion, our data suggested that active self-encapsulating PLGA microspheres were not suitable as controlled release systems of bevacizumab for wet AMD since they did not simultaneously meet all the criteria: high loading, high encapsulation efficiency, and near zero-order release of the immunoreactive antibodies even though they have been successfully utilized for controlled release of other protein drugs. Thus, we decided to investigate other strategies e.g. PLGA millicylindrical implants as controlled release formulations for bevacizumab as discussed in the next chapters.

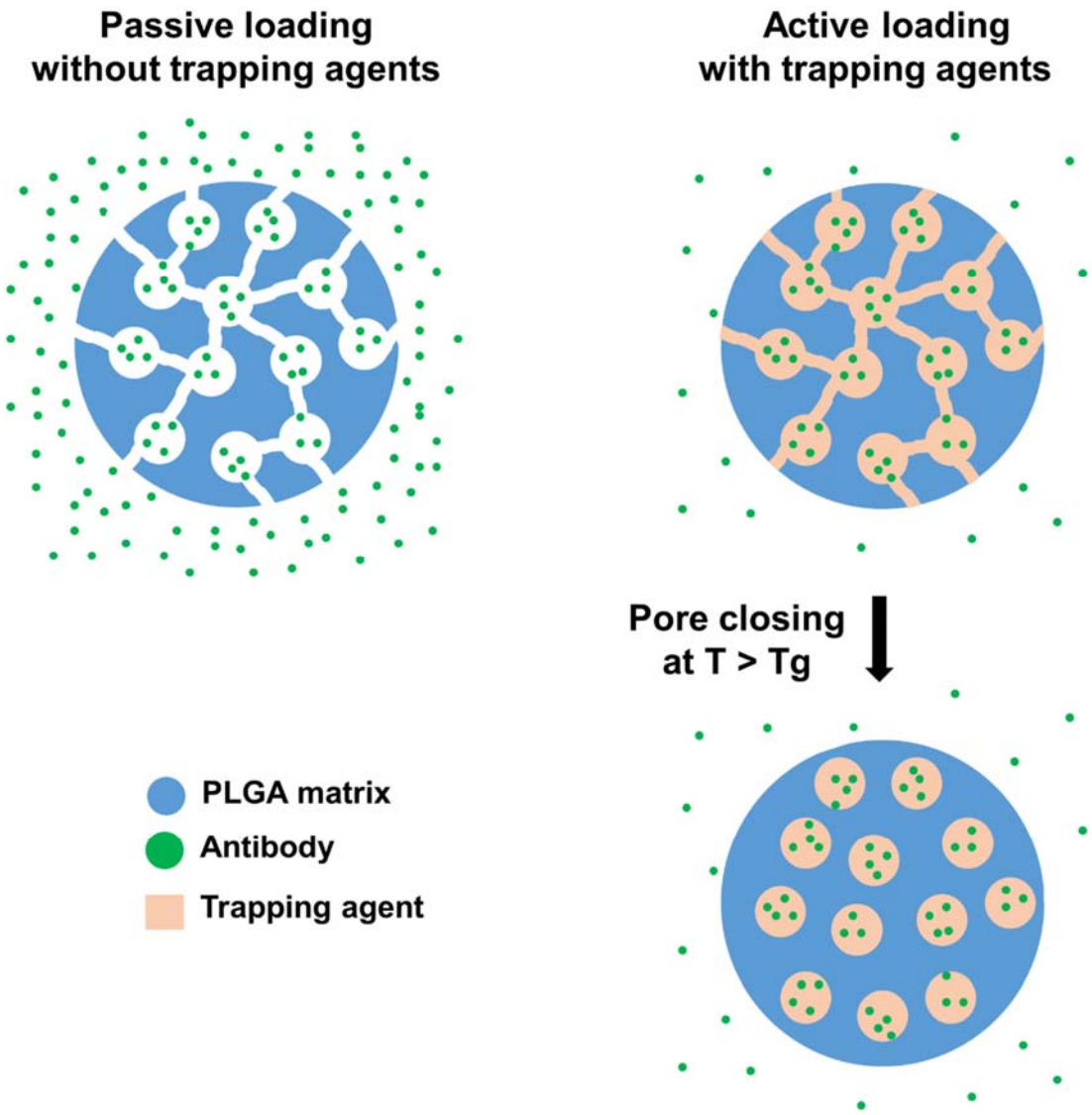

Figure 2.1: Loading schematic comparison of passive loading and active self-encapsulation in PLGA microspheres.

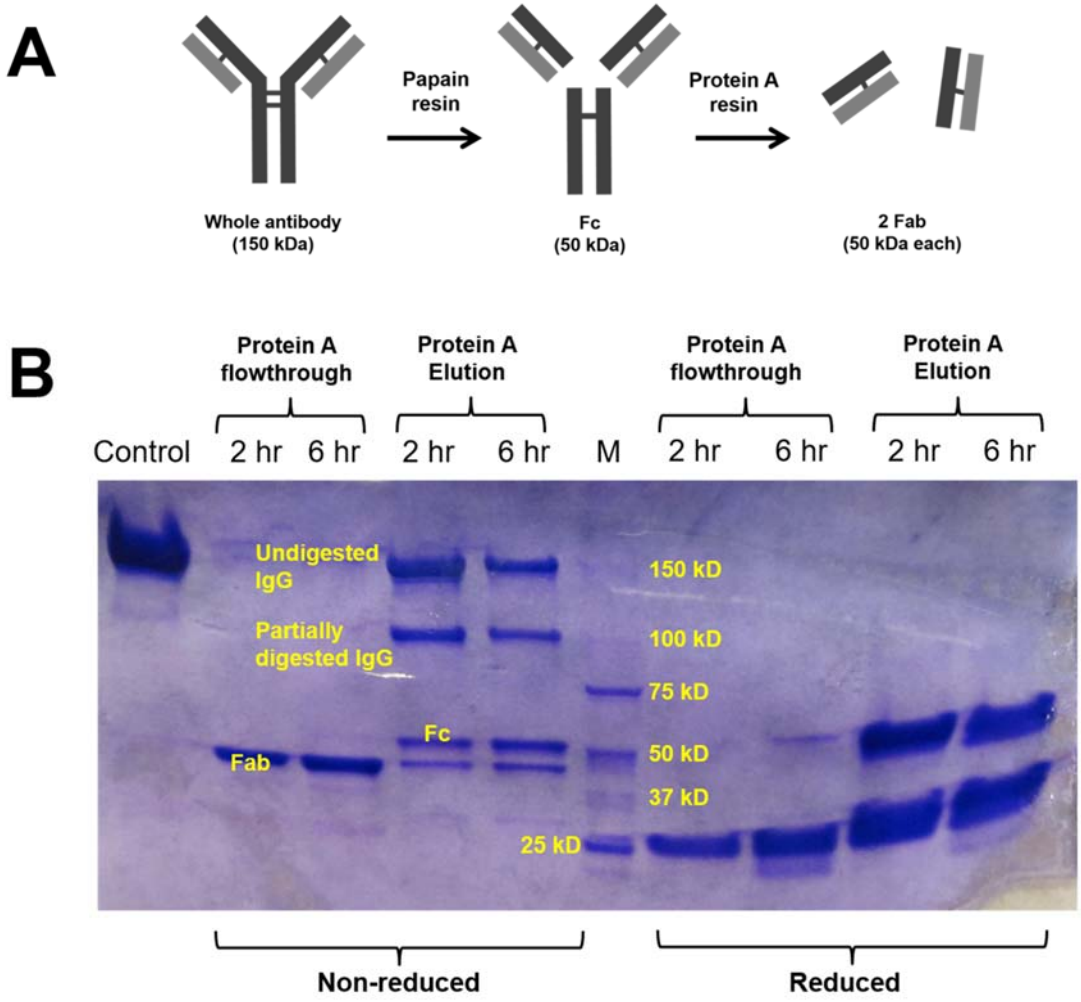

Figure 2.2: Preparation of Fab fragments from bevacizumab. *Schematic for digesting Fab fragments using immobilized papain. Modified from the manual of Pierce™ Fab Preparation Kit (A). SDS-PAGE of non-reduced and reduced proteins from papain digestion of bevacizumab (B).*

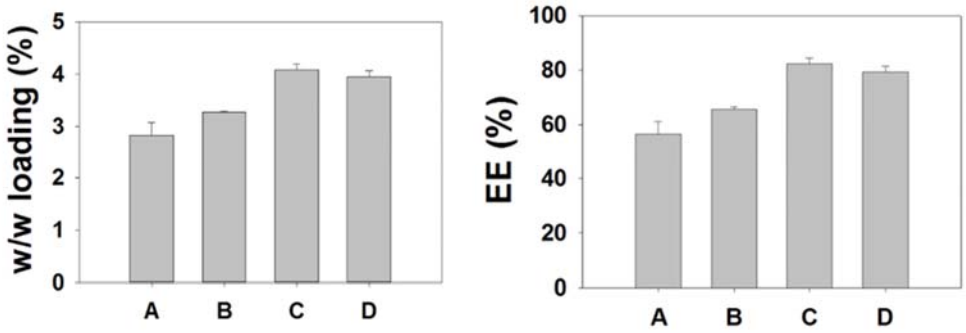

Figure 2.3: Loading (w/w) and encapsulation efficiency of Fab fragments into Ca-alginate PLGA microspheres*. Each formulation has an inner water phase (400 µL) of (A)20 mg of Ca-alginate powders dispersed in 50 % trehalose solution, (B)20 mg of Ca-alginate powders dispersed in 10 % trehalose solution, (C)20 mg of Ca-alginate powders dispersed in dH2O, and (D)40 mg of Ca-alginate powders dispersed in 10 % trehalose solution. The values are expressed as mean ± SD, n=2.*

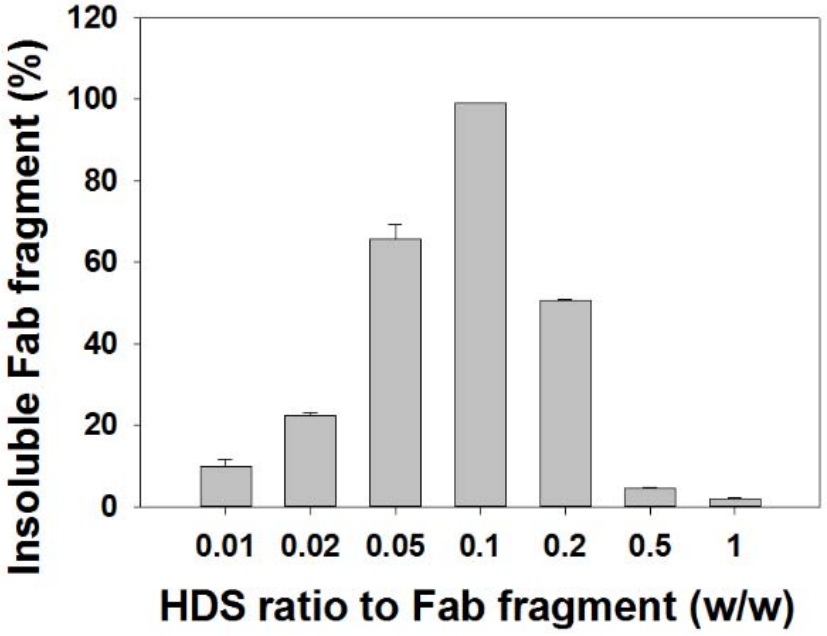

Figure 2.4: Fab-HDS binding profile. *Fab fragments were mixed with HDS at different mass ratios and incubated for 1 h at room temperature. Soluble free Fab fragments were quantified by SE-HPLC after centrifugation. The values are expressed as mean ± SD, n=2.*

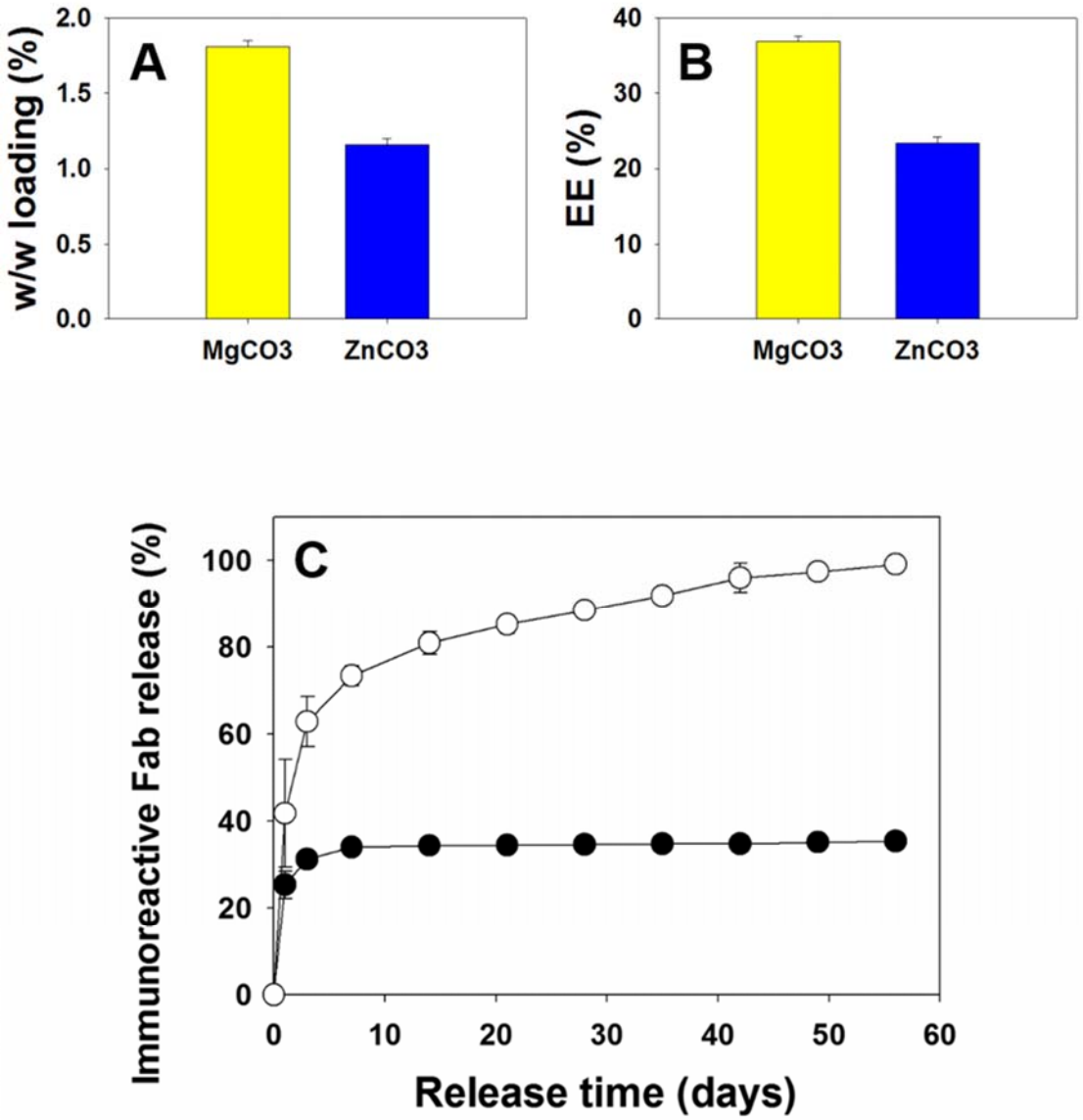

Figure 2.5: Effect of base on HDS-PLGA formulations. *Loading (w/w, A), encapsulation efficiency (B) of Fab fragment, and immunoreactive Fab fragment release kinetics of HDS-PLGA microspheres containing 3 % $MgCO_3$ (yellow, ●) and 6 % $ZnCO_3$ (blue, ○) as an antacid. The values are expressed as mean ± SD, n=3.*

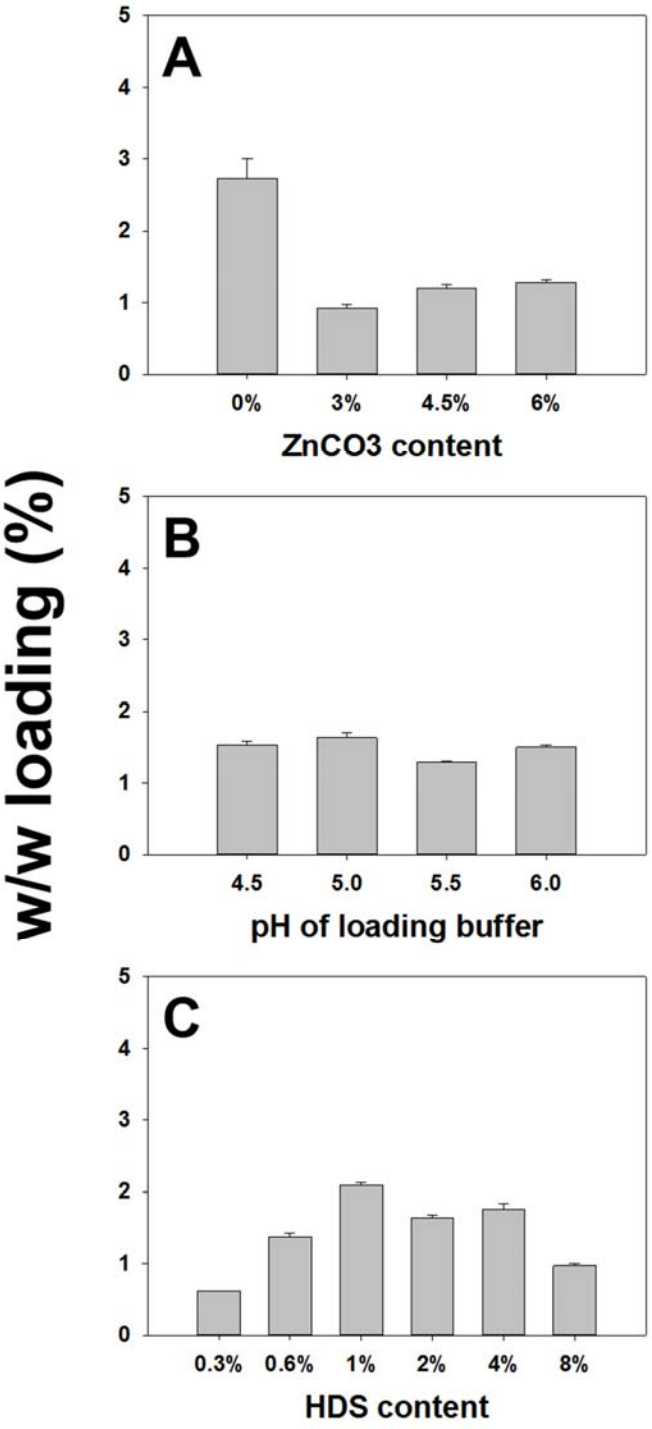

Figure 2.6: Effect of formulation parameters for HDS-PLGA. *ZnCO3 content (A), pH of loading buffer (B), and HDS content (C) on loading of Fab fragments. The values are expressed as mean ± SD, n=2.*

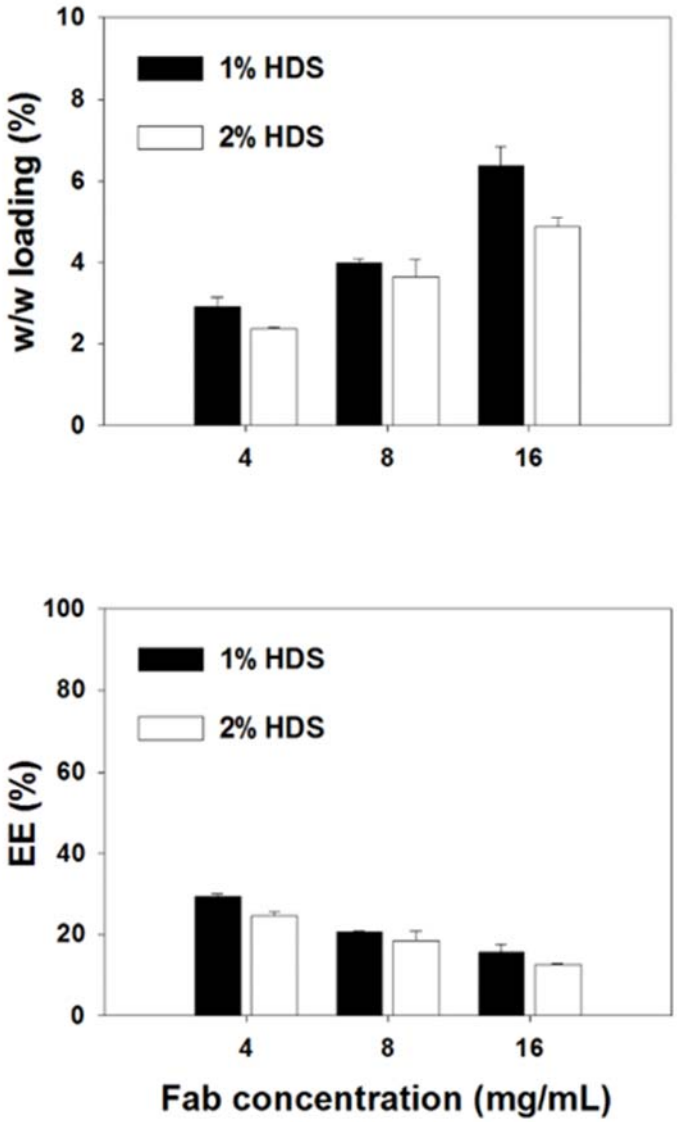

Figure 2.7: Effect of Fab fragment concentration in loading solution on loading (w/w) and encapsulation efficiency. *Fab fragments were loaded at different concentration into HDS-PLGA microspheres containing 1 % HDS (black) and 2 % HDS (white). The values are expressed as mean ± SD, n=2.*

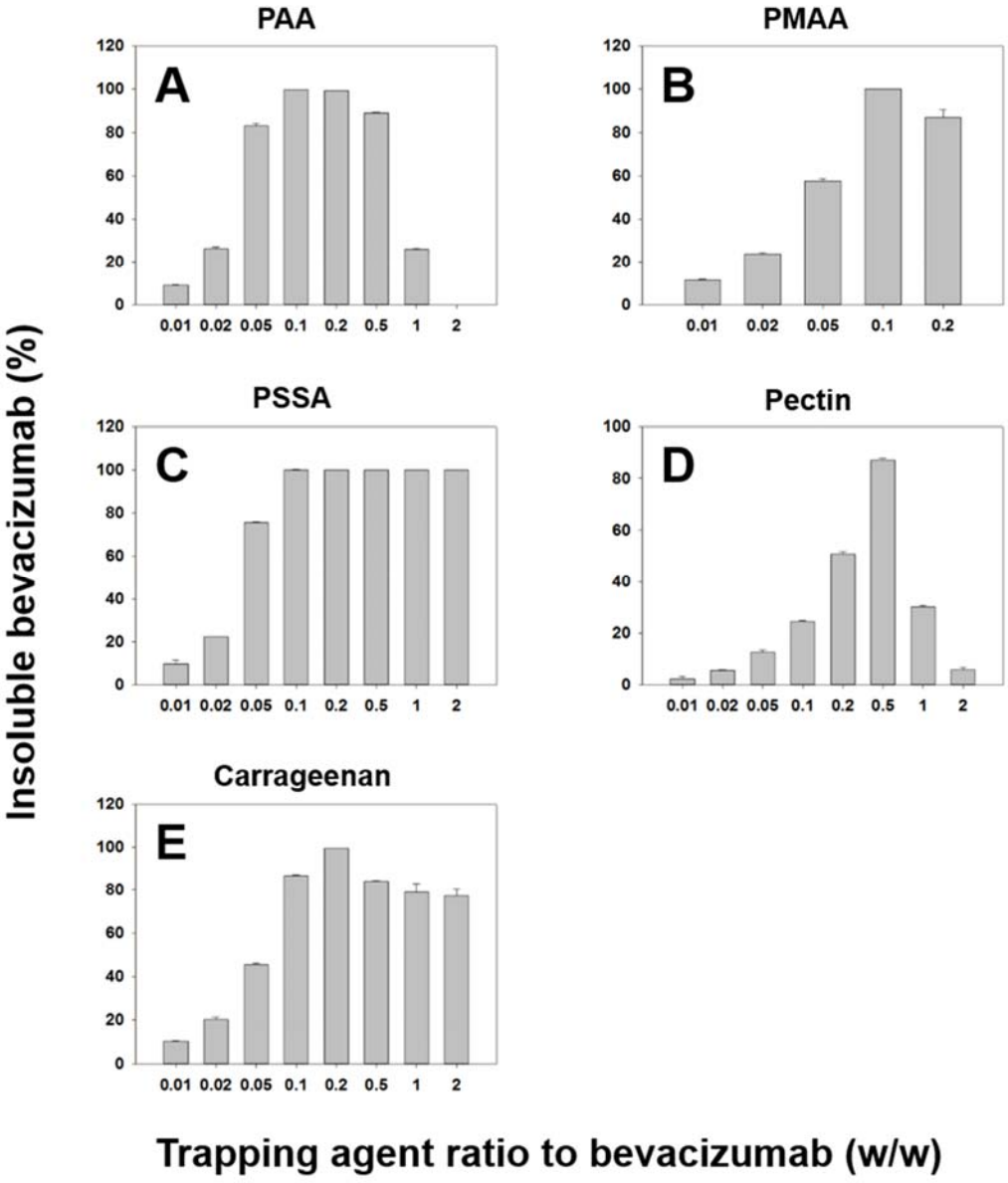

Figure 2.8: Bevacizumab-trapping agent binding profiles. *Bevacizumab were mixed with PAA (A), PMAA (B), PSAA (C), pectin (D), and carrageenan (E) at different mass ratios and incubated for 1 h at room temperature. Soluble free bevacizumab was quantified by SE-HPLC after centrifugation. The values are expressed as mean ± SD, n=2.*

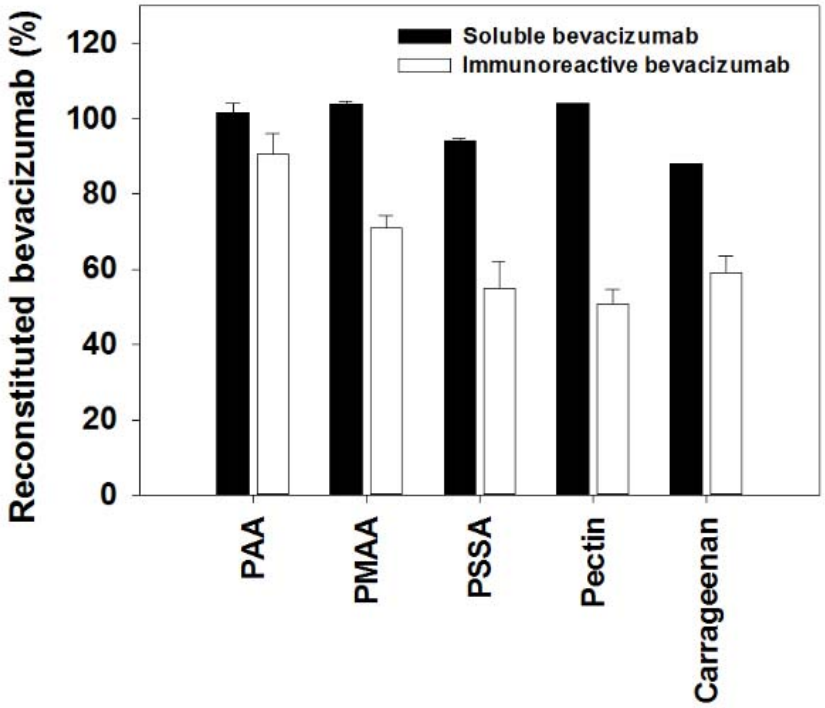

Figure 2.9: Reconstituted bevacizumab from complexes of trapping agents.
Bevacizumabs bound to trapping agents which are PAA (1:0.1), PMAA (1:0.1), PSSA (1:0.1), pectin (1:0.5) and carrageenan (1:0.2) were reconstituted in PBST and their solubility (black bars) and immunoreactivity (white bars) were analyzed by SE-HPLC and ELISA. The values are expressed as mean ± SD, n=2.

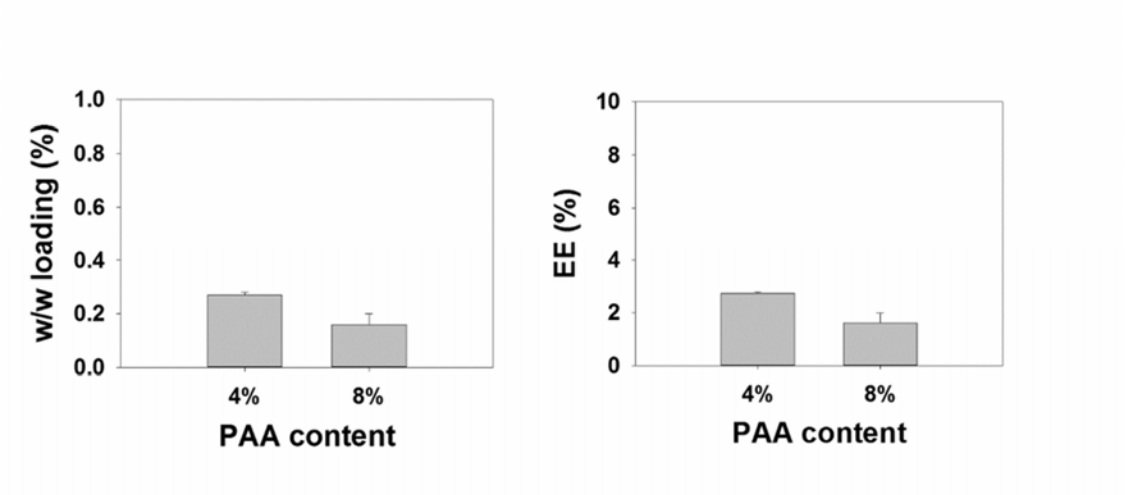

Figure 2.10: Loading (w/w) and encapsulation efficiency of bevacizumab in 4 % and 8 % PAA-PLGA microspheres. *The values are expressed as mean ± SD, n=2.*

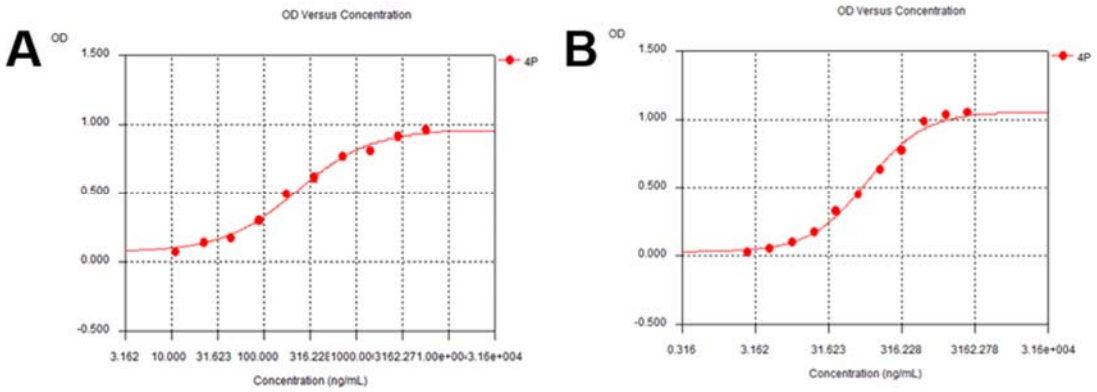

Figure S2.1: ELISA standard curves of Fab fragments (A) and whole antibodies of bevacizumab (B).

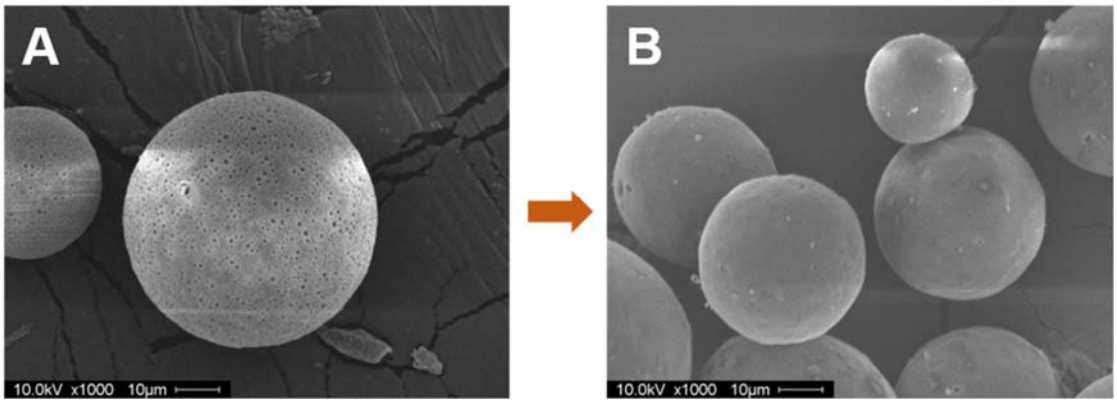

Figure S2.2: SEM images of HDS-PLGA microspheres containing 6 % ZnCO3 before (A) and after (B) self-encapsulation process of Fab fragments.

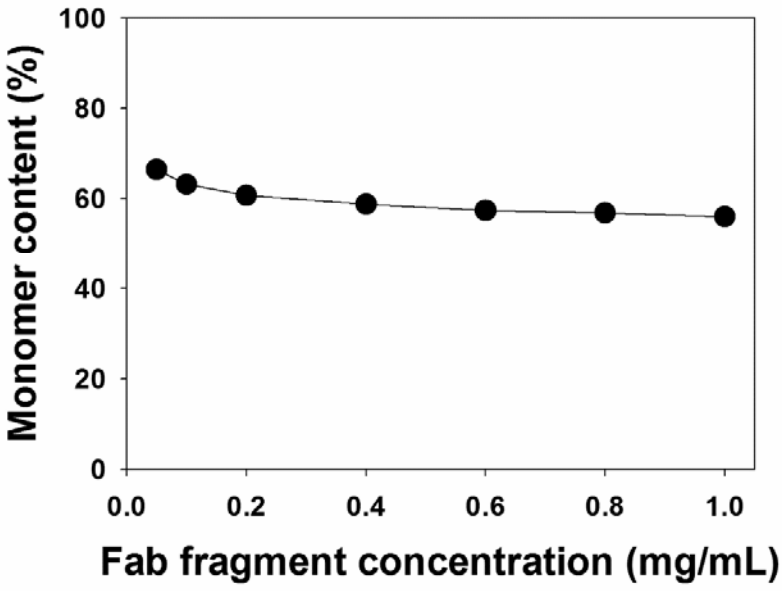

Figure S2.3: Monomer content as a function of concentration of Fab fragments. *Monomer content (%) of Fab fragments prepared by papain digestion is dependent on concentration.*

2.6 References

[1] J. Shao, M.M. Choudhary, A.P. Schachat, Neovascular age-related macular degeneration, Dev. Ophthalmol. 55 (2015) 125–136. doi:10.1159/000438969.

[2] J.L. Kovach, S.G. Schwartz, H.W. Flynn, I.U. Scott, Anti-VEGF treatment strategies for wet AMD, J. Ophthalmol. 2012 (2012). doi:10.1155/2012/786870.

[3] K.M. Droege, P.S. Muether, M.M. Hermann, A. Caramoy, U. Viebahn, B. Kirchhof, S. Fauser, Adherence to ranibizumab treatment for neovascular age-related macular degeneration in real life, Graefe's Arch. Clin. Exp. Ophthalmol. 251 (2013) 1281–1284. doi:10.1007/s00417-012-2177-3.

[4] K.G. Falavarjani, Q.D. Nguyen, Adverse events and complications associated with intravitreal injection of anti-VEGF agents: a review of literature., Eye (Lond). 27 (2013) 787–94. doi:10.1038/eye.2013.107.

[5] G. Ma, Microencapsulation of protein drugs for drug delivery: Strategy, preparation, and applications, J. Control. Release. 193 (2014) 324–340. doi:10.1016/j.jconrel.2014.09.003.

[6] S.P. Schwendeman, R.B. Shah, B.A. Bailey, A.S. Schwendeman, Injectable controlled release depots for large molecules, J. Control. Release. 190 (2014) 240–253. doi:10.1016/j.jconrel.2014.05.057.

[7] S. Mohammadi-Samani, B. Taghipour, PLGA micro and nanoparticles in delivery of peptides and proteins; problems and approaches., Pharm. Dev. Technol. 7450 (2014) 385–393. doi:10.3109/10837450.2014.882940.

[8] R. a Jain, The manufacturing techniques of various drug loaded biodegradable poly(lactide-co-glycolide) (PLGA) devices, Biomaterials. 21 (2000) 2475–2490. doi:10.1016/S0142-9612(00)00115-0.

[9] G. Zhu, S.R. Mallery, S.P. Schwendeman, Stabilization of proteins encapsulated in injectable poly (lactide-co-glycolide), Nat. Biotechnol. 18 (2000) 52–57. doi:10.1038/71916.

[10] S.E. Reinhold, K.G.H. Desai, L. Zhang, K.F. Olsen, S.P. Schwendeman, Self-healing microencapsulation of biomacromolecules without organic solvents, Angew. Chemie - Int. Ed. 51 (2012) 10800–10803. doi:10.1002/anie.201206387.

[11] K.G.H. Desai, S.P. Schwendeman, Active self-healing encapsulation of vaccine antigens in PLGA microspheres, J. Control. Release. 165 (2013) 62–74. doi:10.1016/j.jconrel.2012.10.012.

[12] K.G.H. Desai, S. Kadous, S.P. Schwendeman, Gamma irradiation of active self-healing PLGA microspheres for efficient aqueous encapsulation of vaccine antigens, Pharm. Res. 30 (2013) 1768–1778. doi:10.1007/s11095-013-1019-2.

[13] R.B. Shah, S.P. Schwendeman, A biomimetic approach to active self-microencapsulation of proteins in PLGA, J. Control. Release. 196 (2014) 60–70.

doi:10.1016/j.jconrel.2014.08.029.

[14] Z. Gaozhong, S.P. Schwendeman, Stabilization of proteins encapsulated in cylindrical poly(lactide-co- glycolide) implants: Mechanism of stabilization by basic additives, Pharm. Res. 17 (2000) 351–357. doi:10.1023/A:1007513425337.

[15] D.J. Pieramici, M.D. Rabena, Anti-VEGF therapy: comparison of current and future agents., Eye (Lond). 22 (2008) 1330–1336. doi:10.1038/eye.2008.88.

[16] L. Liu, D.A. Ammar, L.A. Ross, N. Mandava, M.Y. Kahook, J.F. Carpenter, Silicone oil microdroplets and protein aggregates in repackaged bevacizumab and ranibizumab: Effects of long-term storage and product mishandling, Investig. Ophthalmol. Vis. Sci. 52 (2011) 1023–1034. doi:10.1167/iovs.10-6431.

[17] J.S. Andrew, E.J. Anglin, E.C. Wu, M.Y. Chen, L. Cheng, W.R. Freeman, M.J. Sailor, Sustained release of a monoclonal antibody from electrochemically prepared mesoporous silicon oxide, Adv. Funct. Mater. 20 (2010) 4168–4174. doi:10.1002/adfm.201000907.

[18] I.C. Shieh, A.R. Patel, Predicting the Agitation-Induced Aggregation of Monoclonal Antibodies Using Surface Tensiometry, Mol. Pharm. 12 (2015) 3184–3193. doi:10.1021/acs.molpharmaceut.5b00089.

[19] B.M. Teska, J.M. Brake, G.S. Tronto, J.F. Carpenter, Aggregation and Particle Formation of Therapeutic Proteins in Contact With a Novel Fluoropolymer Surface Versus Siliconized Surfaces: Effects of Agitation in Vials and in Prefilled Syringes, J. Pharm. Sci. 105 (2016) 2053–2065. doi:10.1016/j.xphs.2016.04.015.

[20] H. Nomoto, F. Shiraga, N. Kuno, E. Kimura, S. Fujii, K. Shinomiya, A.K. Nugent, K. Hirooka, T. Baba, Pharmacokinetics of bevacizumab after topical, subconjunctival, and intravitreal administration in rabbits, Investig. Ophthalmol. Vis. Sci. 50 (2009) 4807–4813. doi:10.1167/iovs.08-3148.

[21] S. Kaja, J.D. Hilgenberg, E. Everett, S.E. Olitsky, J. Gossage, P. Koulen, Effects of dilution and prolonged storage with preservative in a polyethylene container on Bevacizumab (Avastin???) for topical delivery as a nasal spray in anti-hereditary hemorrhagic telangiectasia and related therapies, Hum. Antibodies. 20 (2011) 95–101. doi:10.3233/HAB-2011-0244.

[22] S.K. Li, M.R. Liddell, H. Wen, Effective electrophoretic mobilities and charges of anti-VEGF proteins determined by capillary zone electrophoresis, J. Pharm. Biomed. Anal. 55 (2011) 603–607. doi:10.1016/j.jpba.2010.12.027.

[23] C. Magdelaine-Beuzelin, C. Pinault, G. Paintaud, H. Watier, Therapeutic antibodies in ophthalmology: Old is new again, MAbs. 2 (2010) 176–180. doi:10.4161/mabs.2.2.11205.

[24] D. Jain, D. Bar-Shalom, Alginate drug delivery systems: application in context of pharmaceutical and biomedical research., Drug Dev. Ind. Pharm. 40 (2014) 1576–84. doi:10.3109/03639045.2014.917657.

[25] E. Ruvinov, S. Cohen, Alginate biomaterial for the treatment of myocardial

infarction: Progress, translational strategies, and clinical outlook. From ocean algae to patient bedside., Adv. Drug Deliv. Rev. 96 (2016) 54–76. doi:10.1016/j.addr.2015.04.021.

[26] P. Dissertations, The microclimate in poly (lactide-co-glycolide) microspheres and its ..., (2000).

[27] T. Marras-Marquez, J. Peña, M.D. Veiga-Ochoa, Robust and versatile pectin-based drug delivery systems, Int. J. Pharm. 479 (2015) 265–276. doi:10.1016/j.ijpharm.2014.12.045.

[28] L. Li, R. Ni, Y. Shao, S. Mao, Carrageenan and its applications in drug delivery, Carbohydr. Polym. 103 (2014) 1–11. doi:10.1016/j.carbpol.2013.12.008.

[29] D. Das, P. Ghosh, S. Dhara, A.B. Panda, S. Pal, Dextrin and poly(acrylic acid)-based biodegradable, non-cytotoxic, chemically cross-linked hydrogel for sustained release of ornidazole and ciprofloxacin, ACS Appl. Mater. Interfaces. 7 (2015) 4791–4803. doi:10.1021/am508712e.

[30] P. Yang, D. Li, S. Jin, J. Ding, J. Guo, W. Shi, C. Wang, Stimuli-responsive biodegradable poly(methacrylic acid) based nanocapsules for ultrasound traced and triggered drug delivery system, Biomaterials. 35 (2014) 2079–2088. doi:10.1016/j.biomaterials.2013.11.057.

[31] J.P.K. Tan, Q. Wang, K.C. Tam, Control of burst release from nanogels via layer by layer assembly, J. Control. Release. 128 (2008) 248–254. doi:10.1016/j.jconrel.2008.03.012.

Chapter 3: PLGA millicylindrical implants of bevacizumab

3.1 Abstract

To reduce the administration frequency of bevacizumab for wet age-related macular degeneration (wet AMD), poly(lactic-co-glycolic acid) (PLGA) millicylindrical implants were evaluated as sustained release formulations of the protein. To prepare PLGA implants, an anhydrous solvent-extrusion method in which drug powders are suspended in PLGA/acetone solution was employed. The powders directly lyophilized and ground from commercial Avastin® solution without any change in the composition resulted in high recovery when re-dissolved in the aqueous buffer (99 %) and extracted from implants (97 %). The implants loaded with 15 % bevacizumab from this powder released 94 % of the encapsulated proteins in 1 day, which is undesirable. In order to reduce this initial burst and to slow down the release, trehalose was removed through buffer exchange since its abundance increases the volumetric loading of total drug powder above the percolation threshold. However, the recovery of protein from the trehalose free powder was only 67 % when the powder was reconstituted in the aqueous buffer, and only 58 % was recovered by extracting the protein from the implants. The release rate was slower, but the total cumulative release was only 53 % out of the soluble extracted loading, suggesting that trehalose has anti-aggregation effects during the powder and implant preparation and during release. With the powder containing trehalose, dependency of release rate on loading was tested and the implant loaded with 3 % bevacizumab showed the most promising release kinetics among the implants. To

increase the loading of bevacizumab while maintaining a continuous release profile and preventing aggregation, the effort to optimize trehalose content in the powder was made. It was found that a 1.5:1 ratio (trehalose : bevacizumab, w/w) still prevents aggregation of bevacizumab and yielded adequate recovery of soluble protein from cryomilled powder. With the optimized trehalose content in the powder, the implants of various powder loading were tested and the release rate was slower than the initial implants with the corresponding loading of bevacizumab from Avastin® solution. The implant loaded with 6 % bevacizumab with the optimized trehalose content showed a biphasic release profile with the total cumulative release of 81 % which was the best release profile among the tested implants. Hence, despite improvement in stability of the mAb during encapsulation, further work is needed to achieve near zero-order release of stable mAb, thus maintaining the concentration of bevacizumab longer in the therapeutic window at the target site.

3.2 Introduction

Over the past decade, anti-vascular endothelial growth factor (VEGF) therapy has been a common treatment strategy for wet AMD [1]. In wet AMD, overexpression of VEGF is responsible for abnormal growth of blood vessels under the macula, resulting in central vision loss [2]. Therefore, inhibition of VEGF activity by anti-VEGF agents is a key to treat wet AMD. Macugen® (pegaptanib, anti-VEGF aptamer) which is the first FDA-approved anti-VEGF agent for wet AMD in 2004 was able to slow down progression of the disease, but did not improve visual acuity significantly [3]. Later developed anti-VEGF protein formulations for wet AMD, which are Lucentis®

(ranibizumab, anti-VEGF monoclonal antibody Fab fragment) and Eylea® (aflibercept, a recombinant fusion protein consisting of portions of human VEGF receptors 1 and 2 extracellular domains fused to the Fc portion of human IgG1), demonstrated better results compared to Macugen®, and are currently the most used drugs for wet AMD [1,4]. Another anti-VEGF agent which is one of the most used drugs for the disease is Avastin® (bevacizumab, anti-VEGF whole monoclonal antibody). It is officially approved for intravenous infusion to treat certain types of cancer, however has also been widely used off-label for intravitreal injection to treat wet AMD due to its lower price relative to Lucentis® and Eylea® [1,5]. The intravitreal injection of these anti-VEGF agents is usually given once a month (every 4 weeks), but this is very inconvenient for patients [6] and may induce infection, inflammation, and hemorrhage [7]. Therefore, if one can extend the therapy duration, and thus reduce administration frequency, it will reduce the associated inconvenience and risks.

In the previous chapter, the efforts to increase loading and encapsulation efficiency of bevacizumab with the active self-encapsulating PLGA microspheres were not successful. In order to overcome the issues, in this chapter, PLGA millicylindrical implants were employed as depot systems for sustained release of bevacizumab. Loading of drugs into PLGA implants is accomplished by simply suspending drug powders in the PLGA/acetone solution, so the encapsulation efficiency is theoretically 100 %, and any desired loading can be achieved [8,9]. Ozurdex®, a PLGA implant, is an FDA-approved intravitreal injectable device for controlled release of dexamethasone [10], providing a clinical precedent for use of PLGA implants in the eye. The device is intravitreally injected via a special pen-like applicator without any surgical incisions.

One of the main drawbacks of PLGA formulations for protein encapsulation is the formation of an acidic microenvironment during release due to the degraded acid byproducts in the polymer, which easily destabilizes the encapsulated proteins and results in incomplete release. This issue has been overcome by co-encapsulation of poorly soluble basic salts to neutralize the acids and to achieve a more continuous and higher total protein release [8,11,12]. Similarly, the use of anhydrous microencapsulation when preparing millicylindrical devices similar to Ozurdex® was developed by our group in order to minimize the stress during encapsulation of the organic solvent contact with a mobilized protein as occurs during common methods of encapsulation [12–14]. In order to encapsulate water-soluble proteins in PLGA implants, the micronized protein powder is first suspended in PLGA solution. Drying (e.g. lyophilization) and milling processes, which also can damage proteins, are needed to prepare protein powder for encapsulation. To protect proteins from damage by these stresses, stabilizers need to be co-incorporated. Sugars such as trehalose and sucrose have been widely used in protein formulations as stabilizers. Although the stabilizing mechanism of sugars for proteins has not been fully understood, three theories have been proposed, which are the “vitrification”, “preferential exclusion” and “water replacement” theories [15–17].

High loading of any water-soluble components in the polymer results in faster release [18,19]. Therefore, in this chapter, dependency of release rate on loading was tested, and we sought to optimize the ratio of sugar to protein so that both high stability and desirable release rate of bevacizumab would be possible at the same time.

3.3 Materials and Methods

3.3.1 Materials

The Avastin®, commercial solution of bevacizumab was purchased from the University of Michigan Hospital pharmacy and used within its shelf-life period. PLGA 50:50 (inherent viscosity = 0.64 dL/g and Mw = 54.3 kDa, ester terminated) was purchased from LACTEL Absorbable Polymers (Birmingham, AL). Trehalose dihydrate (trehalose), $MgCO_3$, guanidine hydrochloride, DL-dithiothreitol (DTT), ethylenediamine-tetraacetic acid (EDTA), Na_2HPO_4 and NaH_2PO_4, were purchased from Sigma-Aldrich Chemicals (St. Louis, MO). Tween 80 (10%), acetone, KH_2PO_4, K_2HPO_4, KCl, phosphate buffered saline (PBS), Amicon Ultra-15 Centrifugal Filter Units (10,000 MWCO), silicone rubber tubing, and Coomassie plus reagent were purchased from Fisher Scientific (Hanover Park, IL).

3.3.2 Preparation of bevacizumab powder

The buffer of Avastin® solution containing bevacizumab and excipients was exchanged into 51 mM sodium phosphate buffer (pH 6.2) by using Amicon Centrifugal Filter Units (10,000 MWCO) to remove trehalose. Then, different levels of trehalose were added (weight of trehalose : weight of bevacizumab = 0, 0.1, 0.5, 1 and 1.5 : 1) and the solution was diluted with 51 mM sodium phosphate buffer (pH 6.2) for the final bevacizumab concentration of 5 or 25 mg/mL and lyophilized. The solid was then ground by CryoMill (Retsch, Germany) at 30 Hz for 30 min and sieved through 90-μm screen (Newark Wize Wearing, Newark, NJ). High trehalose content protein powder was prepared (ratio of 2.4 to 1, trehalose : bevacizumab) by lyophilizing the commercial Avastin® solution without buffer exchange, and then ground and sieved.

3.3.3 Preparation of PLGA millicylindrical implants with bevacizumab

The resulting bevacizumab powder was suspended into 50 % (w/w) PLGA solution in acetone with 3% (w/w) $MgCO_3$ in a 2 mL centrifuge tube, then mixed and transferred into a 3 mL syringe. The suspension was extruded into silicone rubber tubing (I.D. = 0.8 mm), then dried at room temperature for 48 h followed by vacuum drying at 40°C and -23 in. Hg vacuum for an additional 48 h. The final dried implants were obtained by removal of silicone tubing and were cut into segments of a desired length for future use.

3.3.4 Measurement of bevacizumab loading in implants

Implants (3-5 mg) were dissolved in 1 mL of acetone for 1 h and centrifuged to precipitate out the proteins. PLGA, dissolved in supernatant, was removed and the protein pellet was washed with acetone and centrifuged three times more to remove any residual PLGA. The pellet was then air dried, reconstituted in 1 mL of PBST (phosphate buffered saline with 0.02 % Tween-80, pH 7.4) at 37°C overnight and analyzed by size-exclusion high-performance liquid chromatography (SE-HPLC). The condition of SE-HPLC to quantify monomer and soluble aggregates was followed as previously described [20] with slight modifications. The mobile phase (0.182 M KH_2PO_4, 0.018 M K_2HPO_4, and 0.25 M KCl, pH 6.2) was run at a flow rate of 0.5 mL/min through a column (TSK-GEL G3000SWxl; Tosoh Bioscience, Japan), and elution was monitored at 280 nm. The volume of injection was 50 µL, and the running time was 30 minutes. All samples for SE-HPLC were filtered through 0.45 µm protein low binding filter. Extracted loading and loading efficiency were calculated by the following equations.

$$\text{Extracted loading (\%)} = \frac{\text{Weight of extracted bevacizumab}}{\text{Weight of total implant}} \times 100\ \%$$

$$\text{Loading efficiency (\%)} = \frac{\text{Extracted loading}}{\text{Theoretical loading}} \times 100\ \%$$

3.3.5 *In vitro* release study of bevacizumab from implants

Implants (1 cm long, 6-8 mg) were added in 1.5 mL centrifuge tubes with 1 mL of PBST and incubated at 37°C without agitation, as agitation was found to cause insoluble aggregation of the antibody [21,22]. The release medium was replaced with fresh medium at select time points. The amount of released bevacizumab at each time point was measured by SE-HPLC and calculated as percentage of the released amount out of the extracted loading of soluble bevacizumab

3.3.6 Evaluation of residual bevacizumab in implants

At the end of release study, the remaining bevacizumab was extracted by the same procedure used to measure protein loading after lyophilizing the remaining polymer. The protein pellet was then reconstituted in PBST and incubated at 37°C overnight to determine the soluble fraction of the protein remained in the polymer. After centrifugation, the supernatant was collected and the remaining insoluble precipitates were dissolved in denaturing solvent (6 M guanidine hydrochloride/1 mM EDTA) at 37°C for 1 h to determine non-covalent protein aggregates. After centrifuging and collecting supernatant, the remaining insoluble precipitates were dissolved again in denaturing/reducing solvent (6 M guanidine hydrochloride /1 mM EDTA/10 mM DL-

dithiothreitol) to measure covalent protein aggregates formed by disulfide bonds. Concentration of protein aggregates in each step was measured by Coomassie plus protein assay. All measurements were performed in triplicate and bevacizumab standards were dissolved in the same solvent used for each analysis.

3.3.7 Measurement of the effect of trehalose on aggregation of bevacizumab in powders

Bevacizumab powder with the various ratios of trehalose to bevacizumab (0, 0.1, 0.5, 1, 1.5 and 2.4:1) were dissolved in PBST at 37°C overnight. The soluble fraction of protein was measured by SE-HPLC to determine the effect of trehalose on aggregation of bevacizumab.

3.3.8 Scanning electron microscopy (SEM)

The surface morphology of PLGA microspheres was examined by Hitachi S3200N scanning electron microscope (Hitachi, Japan) (Figure S3.1). The microspheres were first fixed on a brass stub using double sided adhesive carbon tape and then were made electrically conductive by coating with a thin layer of gold (~ 5 nm) for 120 s at 40 W. The images of microspheres were taken at an excitation voltage of 8 - 20 kV.

3.4 Results and Discussion

3.4.1 Evaluation of bevacizumab loaded implants with trehalose

PLGA implants were formulated for sustained local delivery of bevacizumab. First, commercial Avastin® solution was lyophilized as is, then ground and sieved to prepare the bevacizumab powder. The formulation of Avastin® originally contains 2.4

times as much trehalose as bevacizumab, polysorbate 20, and buffer salts as excipients, as shown in Table 3.1. Bevacizumab lyophilized from the original Avastin® solution without any changes in its composition was loaded into PLGA implants at 15 % which is equivalent to 55.4 % loading of total protein powder due to the excipients. For all formulations, a poorly soluble base, $MgCO_3$ was also added into implants at 3 % (w/w) as an antacid to stabilize loaded proteins by preventing low pH degradation created by acid by-products from degradation of PLGA during release [8,12]. When the powder was simply dissolved in PBST, 99 % of soluble bevacizumab was recovered. Of the extracted powder from the implants, 97 % was soluble in PBST (Figure 3.1 A). Therefore, it is concluded that bevacizumab from the powder and extract is quite stable in terms of aggregation propensity. But most of the loaded proteins (94 %) were released on day 1 (Figure 3.1 B). It is thought that there is a percolation threshold of the bevacizumab loading, far below 15 %. Above the percolation threshold, the majority of drug particles are connected to each other and create water channels rapidly due to their high water solubility, so when water uptake starts at the beginning of release study the drug molecules will diffuse out through the rapidly formed water channels, thus creating the high initial burst release [18,19].

3.4.2 Evaluation of bevacizumab loaded implants without trehalose

Therefore, to reduce the release rate while maintaining the protein loading, the osmotically active trehalose, which occupies 64.9 % mass of the protein powder lyophilized from the original Avastin® solution (Table 3.1), was removed by buffer-exchange into 10 mM histidine buffer which was a loading buffer for the active self-encapsulating PLGA microspheres in Chapter 2. Without trehalose, 67 % of soluble

bevacizumab was recovered when the powder was dissolved in PBST, and only 58 % extracted protein was soluble from the implant after encapsulation, which is equivalent to 8.7 % extracted loading (Figure 3.2 A). This implant batch showed very slow release during the release study period and released only 31 % bevacizumab out of theoretical loading (15 %) by the end of release (Figure 3.2 B and Table 3.2), which is still only 53 % of the extracted loading (8.7 %). To analyze the remaining protein in polymer, the antibody was extracted from the implants after the release study. Non-covalent aggregate and covalent aggregate by disulfide bonds were 40 % and 35 %, respectively, with a total recovery of 106 % (Table 3.2). Aggregation of bevacizumab during cryomilling, preparation of implants, and the release study is thought to be attributed to the absence of trehalose in the drug powders since the extracted loading efficiency and total cumulative release of the implants with the presence of trehalose were both significantly higher.

3.4.3 Dependency of release kinetics of bevacizumab with trehalose on loading

From the formulations with and without trehalose, it is concluded that the presence of trehalose prevents aggregation of bevacizumab during cryomilling, implant preparation, and the release study. However, the implant loaded with 15 % bevacizumab and all the Avastin® excipients demonstrated high initial burst release due to the loading well above the percolation threshold. therefore, the implants with 3, 6, and 10 % loadings (w/w) of bevacizumab which are equivalent to 11.1, 22.2, and 37.0 % loading of total protein powder, respectively, were tested to evaluate dependency of release kinetics on loading. Extracted loading efficiencies calculated from extracted loadings ranged from 92 to 100 % (Table 3.3). Release rate of bevacizumab from these implants increased as protein loading increased (Figure 3.3). The initial burst release on day 1 from 10 and

15 % loaded implants were 66 and 94 %, and was significantly higher than ones from 3 and 6 % loaded implants, which were 7.0 and 4.6 %. Therefore, there must be the percolation threshold between 6 and 10 % bevacizumab loadings (22.2 and 37.0 % of total powder loadings). Above the percolation threshold, pure diffusion-through-channel release is expected to be the dominant release mechanism described in the section 3.4.1. Below the percolation threshold, on the other hand, drug particles are not connected in the polymer matrix, and thus form isolated water pores when water dissolves the drug particles. The isolated water pores start to swell because of osmotic pressure created by the osmotically active water-soluble components of drug powders and induce more water uptake. Finally, the swollen pores are ruptured and form microcracks which connect the adjacent pores, and then the drug molecules can be released through the interconnected pores. These steps involved in the formation of channels with microcracks induced by osmotic pressure are relatively slower than those formed when above the percolation threshold, thus acting as rate limiting step for drug release [18,19]. Therefore, the initial burst release is relatively low and following release rate is also slow because it is dominantly driven by osmotic pressure. The implants loaded with 3 % bevacizumab showed the most promising release profile which was continuous for 6 weeks with low initial burst and 62 % of total cumulative release. The incomplete total release from implants with lower loading is attributed to less homogeneous diffusion of $MgCO_3$ into the pores formed by drug particles which creates some acidic pores by polymer degradation during release period, thus finally destabilizing proteins [23]. Most of the residual proteins analyzed by extraction were non-covalent aggregates, which was 14 % and total recovery was 72 % (Table 3.4).

As a control, the implant loaded with 15 % of buffer-exchanged (trehalose-removed) bevacizumab into 51 mM sodium phosphate (pH 6.2) which is the buffer of Avastin® solution, not into 10 mM histidine buffer as in the above section, was also tested for comparison. Only 60 % soluble protein was recovered from the implant after encapsulation, which is equivalent to 9.0 % extracted loading (Table 3.3). The implant demonstrated very slow release during the whole release study period and released only 22 % bevacizumab out of the soluble extracted loading by the end of release, as seen in Figure 3.3 and Table 3.4. Therefore, it was reaffirmed that trehalose works as a stabilizer against aggregation of the proteins. To analyze the remaining protein in polymer, the antibody was extracted from the implants after the release study. Soluble residual protein in PBST, non-covalent aggregate and covalent aggregate by disulfide bonds were 1.3 %, 40 % and 1.6 %, respectively, with a total recovery of only 56 % (Table 3.4). The remaining protein, which was not recovered, could have formed insoluble aggregates e.g. covalent non-disulfide bonds, or hydrolysis products not detected by the SE-HPLC in the release media.

3.4.4 Effect of trehalose on aggregation of bevacizumab in powders

The presence of trehalose in the drug powder stabilized bevacizumab in the implants, but it also increased release rate undesirably since the commercial Avastin® has considerable amount of trehalose compared to bevacizumab, whose weight ratio is 2.4:1 (2.4:1 powder). Therefore, we sought to optimize the ratio so that both high stability and desirable release rate of bevacizumab would be possible at the same time. To determine the optimal ratio of trehalose to bevacizumab in the protein powder, buffer-exchanged bevacizumab was mixed with trehalose at various ratios before preparing the micronized

drug powder, as used for encapsulation. Then, the soluble protein in the powder when dissolved in PBST was measured by SE-HPLC (Figure 3.4 and Figure S3.2). The powder prepared from commercial Avastin® resulted in 99 % recovery of soluble bevacizumab and 98.0 % was recovered from the powders with the reduced ratio of 1.5:1 w/w trehalose : protein (1.5:1 powder). Further reducing trehalose in the powder at a trehalose : protein level of 1:1 resulted in only 76 % bevacizumab solubilized and the absence of trehalose resulted in only 70 % soluble protein in the powder. Therefore, the 1.5:1 powder was selected for the next step preparation of implants to maintain the stability of bevacizumab while slowing down the release.

3.4.5 Evaluation of implants with optimized trehalose content

To compare release rate of the implants prepared with 1.5:1 w/w trehalose : bevacizumab powder to the previous set of implants with 2.4:1 powder, implants having the same loading of bevacizumab (3,6,10 and 15 %) were tested. Loading efficiencies of extracted soluble bevacizumab ranged from 91 – 94 %, which were slightly lower than the implants with 2.4:1 powder (Table 3.5). The release rate of each implant with the same bevacizumab loading as in the implants with 2.4:1 powder was slower as expected due to lower total powder loadings (8.3, 16.7, 27.8 and 41.7 %, respectively) with reduced trehalose content (Figure 3.5). Release rate from 3 % bevacizumab loaded implant was very slow and total cumulative release was only 21 % when it stopped on day 42. The implants loaded with 10 and 15 % bevacizumab loading released their proteins very fast as expected because their total powder loading (27.8 and 41.7 %) clearly exceeded the percolation threshold in the polymer matrix. From evaluating the initial release from the previous set of the implants with the 2.4:1 powder, the percolation

threshold was likely in the range between 22.2 and 37.0 % of total powder loading. The implant loaded with 6 % of bevacizumab also showed low initial burst release (7.2 %) on day 1 since the total solids loading was lower than the assumed percolation threshold. Among this set of implants, one loaded with 6 % bevacizumab showed the most promising overall release profile, although the release rate was not constant as desired during the whole release period for an ideal formulation. The trehalose content cannot be reduced any further due to instability of bevacizumab in the powder, and therefore, other strategies are needed to achieve high loading and near zero-order release profile at the same time.

3.5 Conclusions

In this study, bevacizumab was loaded into PLGA millicylindrical implants to reduce its administration frequency. We demonstrated that trehalose in the bevacizumab powder directly lyophilized from the commercial Avastin® formulation prevents the proteins from aggregation in the powders and PLGA implants. With the absence of trehalose, a significant portion of bevacizumab was aggregated during the preparation of powders and implants, and the release study. With trehalose added, despite its stabilizing effect, the implants loaded with 10 % or higher bevacizumab resulted in undesirably fast release since the water-soluble trehalose occupies the most weight of drug powder, and the total drug powder loading was above the percolation threshold. The implants loaded with 3 % bevacizumab showed the most promising release kinetics, but the loading and incomplete total cumulative release still need to be improved. To increase loading while maintaining a good release kinetics and stability of the proteins, the lower contents of

trehalose in the drug powder were tested and it was found that the ratio of 1.5:1 (trehalose : bevacizumab) provides the comparable anti-aggregation effect. From this optimized content of trehalose, the implants with various loadings (3, 6, 10, and 15 %) of bevacizumab were evaluated and exhibited the same dependency of release rate on loading with slightly slower release.

In conclusion, trehalose was found to have anti-aggregation effect for bevacizumab and the release kinetics can be controlled by changing the loading of total drug powders. In order to increase loading and simultaneously to improve the release kinetics, further optimizations will be needed, and those efforts will be discussed in the next chapter.

Table 3.1: Composition in 4 mL of Avastin® solution.

Composition	Weight (mg)	Dry weight percentage (%)
Bevacizumab	100	27.1
Trehalose dihydrate	240	64.9
Polysorbate 20	1.6	0.4
Sodium phosphate, monobasic, monohydrate	23.2	6.3
Sodium phosphate, dibasic, anhydrous	4.8	1.3

Table 3.2: Summary of cumulative release and aggregation behavior of proteins from the implants loaded with 15% bevacizumab of the powders with buffer exchange. *Data reported as mean ± SD, n=2.*

Cumulative release (%)	Non-covalent aggregate (%)	Covalent aggregate (%)	Total recovery (%)
31 ± 4	40 ± 6	35 ± 1	106 ± 4

Table 3.3: Loading of implants prepared from bevacizumab powder with and without trehalose. *Data reported as mean ± SD, n=3.*

Trehalose:bevacizumab in powder (w/w)	Theoretical loading (%)	Extracted loading (%)	Loading efficiency (%)
2.4:1	3	2.8 ± 0.2	92 ± 5
	6	6.0 ± 0.8	100 ± 13
	10	9.9 ± 0.6	99 ± 7
	15	14.5 ± 1.5	97 ± 11
0:1	15	9.0 ± 0.3	60 ± 3

Table 3.4: Summary of cumulative release and aggregation behavior of bevacizumab from implants prepared from protein powder with and without trehalose. *Data reported as mean ± SD, n=3.*

Trehalose :bevacizumab in powder (w/w)	Theoretical loading (%)	Cumulative release (%)	Soluble residue (%)	Non-covalent aggregate (%)	Covalent aggregate (%)	Total recovery (%)
2.4:1	3	57 ± 15	0	14 ± 5	0.9 ± 0.9	72 ± 18
0:1	15	13 ± 1	1.3± 2.3	40 ± 20	1.6 ± 1.7	56 ± 23

Table 3.5: Loading of implants prepared from bevacizumab powder with the ratio of 1.5:1 w/w trehalose:bevacizumab. *Data reported as mean ± SD, n=3.*

Trehalose:bevacizumab in powder (w/w)	Theoretical loading (%)	Extracted loading (%)	Loading efficiency (%)
1.5:1	3	2.7 ± 0.0	91 ± 1
	6	5.6 ± 0.2	93 ± 4
	10	9.2 ± 0.2	92 ± 3
	15	14.1 ± 0.7	94 ± 5

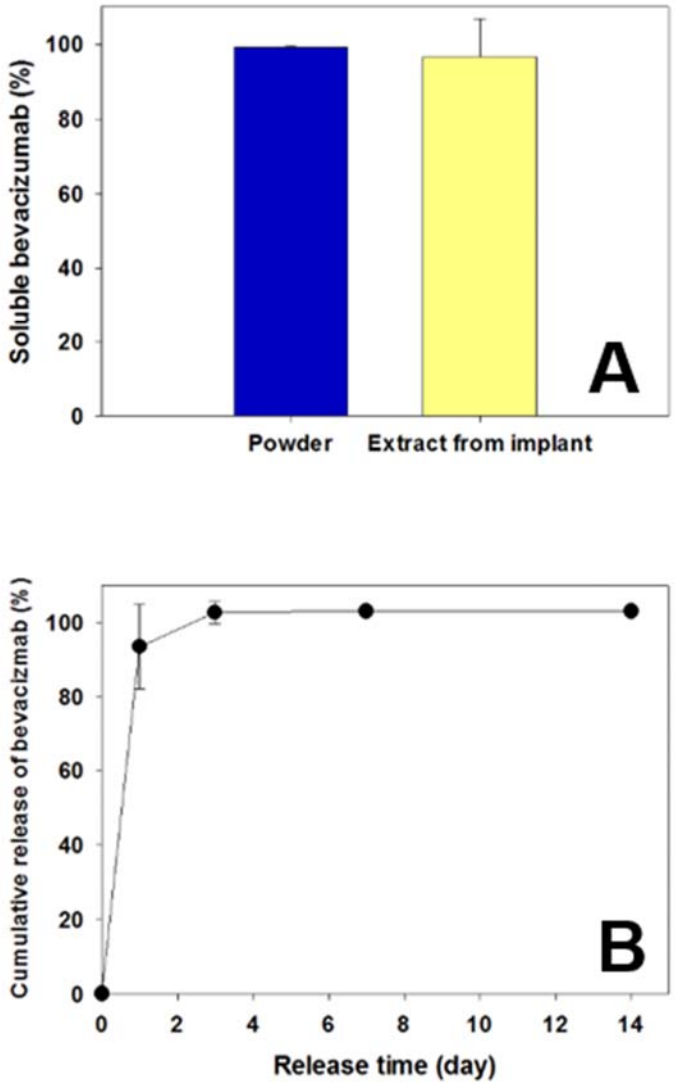

Figure 3.1: Recovery of soluble bevacizumab (A) from powder (blue bar) and extract from implant (yellow bar), and in vitro release study (B) of the implants loaded with 15% bevacizumab of the lyophilized Avastin® powders (trehalose : bevacizumab = 2.4:1, w/w). *Data reported as mean ± SD, n=2.*

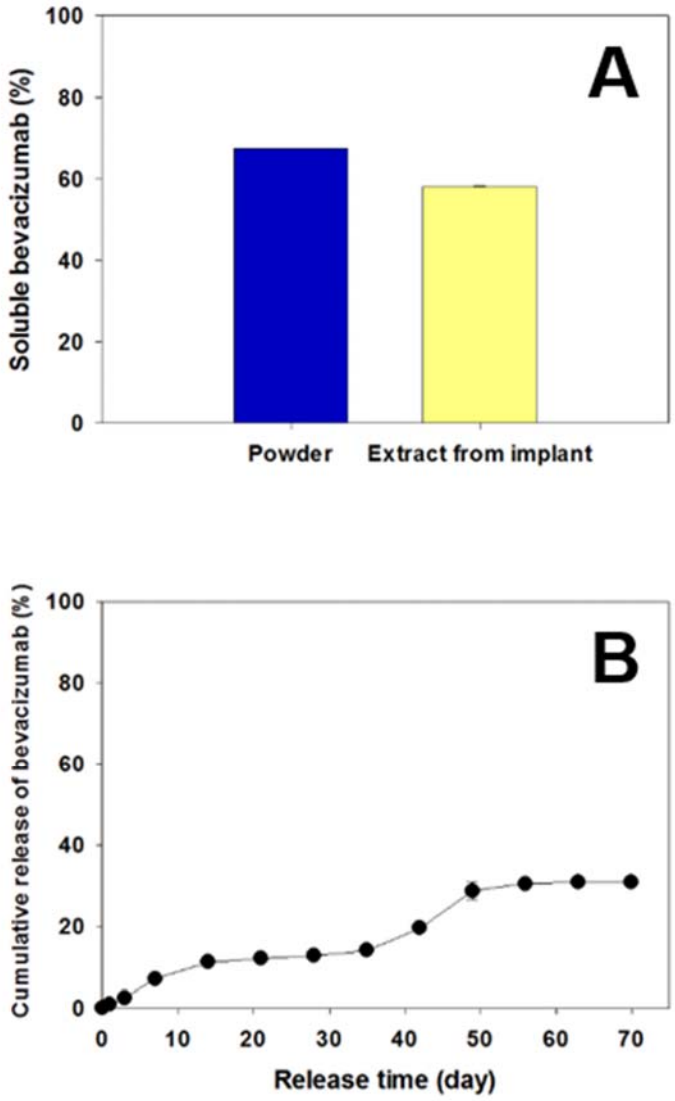

Figure 3.2: Recovery of soluble bevacizumab (A) from powder (blue bar) and extract from implant (yellow bar), and in vitro release study (B) of the implants loaded with 15% bevacizumab of the powders with buffer exchange (no trehalose). *Data reported as mean ± SD, n=2.*

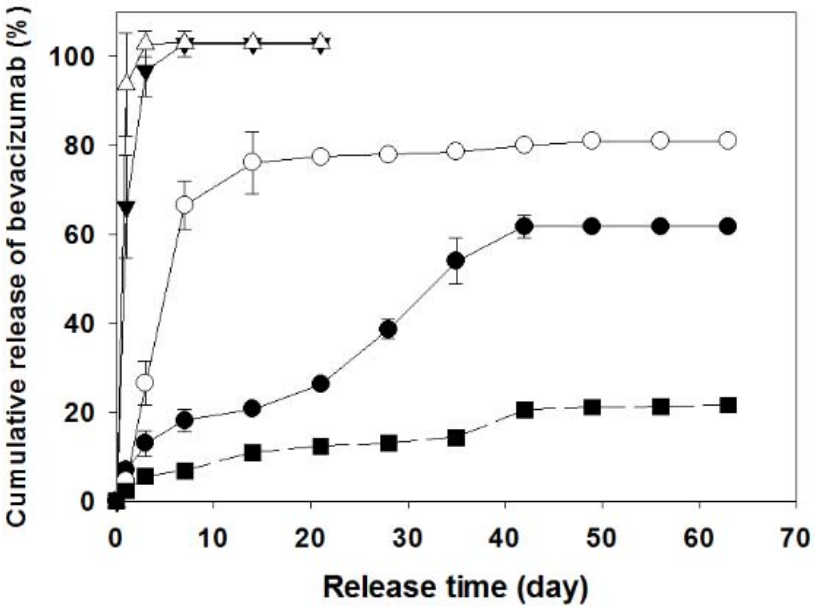

Figure 3.3: Release kinetics of bevacizumab from implants prepared with original Avastin® powder (solid line) and buffer-exchanged bevacizumab powder without trehalose (dashed line). *Theoretical loadings of each formulation were 3% (●), 6% (○), 10% (▼), 15% (Δ) and 15% (■). Symbols represent mean ± SD, n=3.*

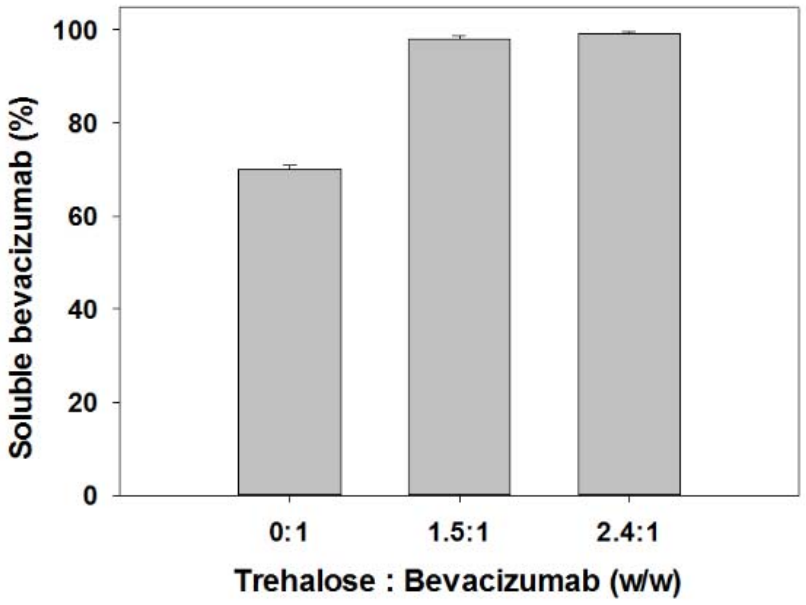

Figure 3.4: Soluble bevacizumab from cryomilled powder prepared with the different ratio of trehalose to bevacizumab (w/w). *Each bar represents mean ± SD, n=3.*

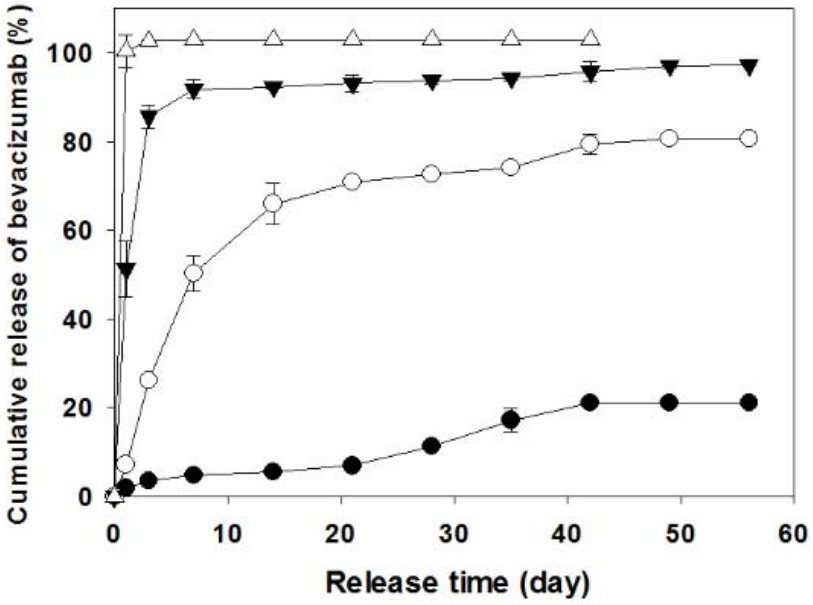

Figure 3.5: Release kinetics of bevacizumab from implants prepared with buffer-exchanged bevacizumab powder with the ratio of 1.5 to 1 w/w trehalose:bevacizumab and PLGA 75:25. *Theoretical loading of each formulation was 3% (●), 6% (○), 10% (▼), and 15%(Δ). Symbols represent mean ± SD, n=3.*

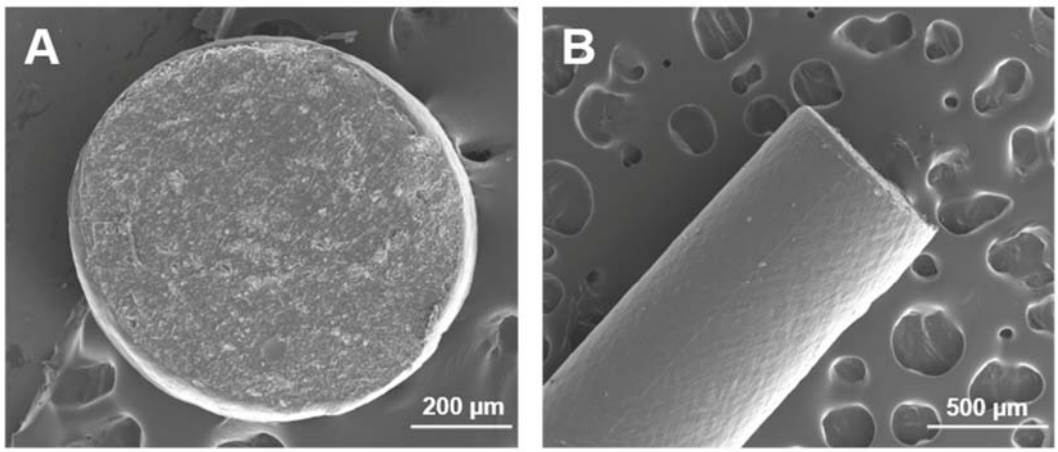

Figure S3.1: SEM images of PLGA millicylindrical implants (A: cross-section, B: lateral surface).

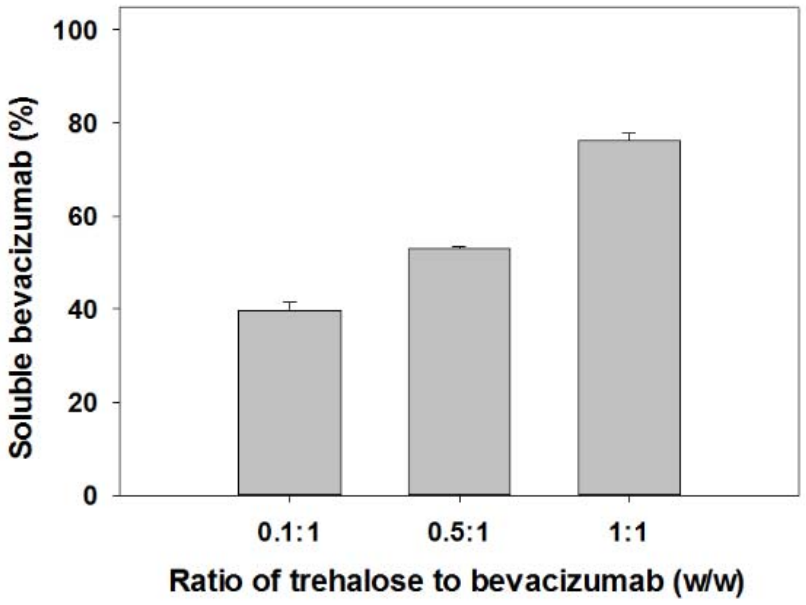

Figure S3.2: Soluble bevacizumab from powder prepared with the different ratios of trehalose to bevacizumab (w/w) prepared on a small scale. *Each bar represents mean ± SD, n=3.*

3.6 References

[1] J.L. Kovach, S.G. Schwartz, H.W. Flynn, I.U. Scott, Anti-VEGF treatment strategies for wet AMD, J. Ophthalmol. 2012 (2012). doi:10.1155/2012/786870.

[2] A.D. Kulkarni, B.D. Kuppermann, Wet age-related macular degeneration, Adv. Drug Deliv. Rev. 57 (2005) 1994–2009. doi:10.1016/j.addr.2005.09.003.

[3] M. V Emerson, A.K. Lauer, Emerging therapies for the treatment of neovascular age-related macular degeneration and diabetic macular edema, BioDrugs. 21 (2007) 245–257. doi:2145 [pii].

[4] E. Dhrami-gavazi, Q. Ghadiali, Aflibercept : a review of its use in the treatment of choroidal neovascularization due to age-related macular degeneration, (2015) 2355–2371. doi:10.2147/OPTH.S80040.

[5] N. Ferrara, A.P. Adamis, Ten years of anti-vascular endothelial growth factor therapy, Nat. Rev. Drug Discov. (2016) 1–19. doi:10.1038/nrd.2015.17.

[6] K.M. Droege, P.S. Muether, M.M. Hermann, A. Caramoy, U. Viebahn, B. Kirchhof, S. Fauser, Adherence to ranibizumab treatment for neovascular age-related macular degeneration in real life, Graefe's Arch. Clin. Exp. Ophthalmol. 251 (2013) 1281–1284. doi:10.1007/s00417-012-2177-3.

[7] K.G. Falavarjani, Q.D. Nguyen, Adverse events and complications associated with intravitreal injection of anti-VEGF agents: a review of literature., Eye (Lond). 27 (2013) 787–94. doi:10.1038/eye.2013.107.

[8] V. Milacic, S.P. Schwendeman, Lysozyme Release and Polymer Erosion Behavior of Injectable Implants Prepared from PLGA-PEG Block Copolymers and PLGA/PLGA-PEG Blends., Pharm. Res. 31 (2013) 436–448. doi:10.1007/s11095-013-1173-6.

[9] Y. Zhong, L. Zhang, A.G. Ding, A. Shenderova, G. Zhu, P. Pei, R.R. Chen, S.R. Mallery, D.J. Mooney, S.P. Schwendeman, Rescue of SCID murine ischemic hindlimbs with pH-modified rhbFGF/Poly(DL-lactic-co-glycolic acid) implants, J. Control. Release. 122 (2007) 331–337. doi:10.1016/j.jconrel.2007.05.016.

[10] N. Kuno, S. Fujii, Biodegradable intraocular therapies for retinal disorders: Progress to date, Drugs and Aging. 27 (2010) 117–134. doi:10.2165/11530970-000000000-00000.

[11] J. Kang, S.P. Schwendeman, Comparison of the effects of Mg(OH)2 and sucrose on the stability of bovine serum albumin encapsulated in injectable poly(D,L-lactide-co-glycolide) implants, Biomaterials. 23 (2002) 239–245. doi:10.1016/S0142-9612(01)00101-6.

[12] G. Zhu, S.R. Mallery, S.P. Schwendeman, Stabilization of proteins encapsulated in injectable poly (lactide-co-glycolide), Nat. Biotechnol. 18 (2000) 52–57. doi:10.1038/71916.

[13] T. Zhou, H. Lewis, R.E. Foster, S.P. Schwendeman, Development of a multiple-drug delivery implant for intraocular management of proliferative vitreoretinopathy, J. Control. Release. 55 (1998) 281–295. doi:10.1016/S0168-3659(98)00061-3.

[14] S.P. Schwendeman, M. Cardamone, M.R. Brandon, A. Klibanov, R. Langer, Stability of proteins and their delivery from biodegradable polymer microspheres, in: S. Cohen, H. Bernstein (Eds.), Microparticulate Syst. Deliv. Proteins Vaccines, Marcel Dekker, New York, 1996: pp. 1–49.

[15] N.K. Jain, I. Roy, Trehalose and protein stability, Curr. Protoc. Protein Sci. (2010) 1–12. doi:10.1002/0471140864.ps0409s59.

[16] L. Chang, D. Shepherd, J. Sun, D. Ouellette, K.L. Grant, X. Tang, M.J. Pikal, Mechanism of protein stabilization by sugars during freeze-drying and storage: Native structure preservation, specific interaction, and/or immobilization in a glassy matrix?, J. Pharm. Sci. 94 (2005) 1427–1444. doi:10.1002/jps.20364.

[17] N.K. Jain, I. Roy, Effect of trehalose on protein structure, Protein Sci. 18 (2009) 24–36. doi:10.1002/pro.3.

[18] B. Amsden, Review of osmotic pressure driven release of proteins from monolithic devices., J. Pharm. Pharm. Sci. 10 (2007) 129–43. http://www.ncbi.nlm.nih.gov/pubmed/17706172.

[19] B.G. Amsden, Y. Cheng, M.F.A. Goosen, A mechanistic study of the release of osmotic agents from polymeric monoliths, 3659 (1994).

[20] L. Liu, D.A. Ammar, L.A. Ross, N. Mandava, M.Y. Kahook, J.F. Carpenter, Silicone oil microdroplets and protein aggregates in repackaged bevacizumab and ranibizumab: Effects of long-term storage and product mishandling, Investig. Ophthalmol. Vis. Sci. 52 (2011) 1023–1034. doi:10.1167/iovs.10-6431.

[21] I.C. Shieh, A.R. Patel, Predicting the Agitation-Induced Aggregation of Monoclonal Antibodies Using Surface Tensiometry, Mol. Pharm. 12 (2015) 3184–3193. doi:10.1021/acs.molpharmaceut.5b00089.

[22] B.M. Teska, J.M. Brake, G.S. Tronto, J.F. Carpenter, Aggregation and Particle Formation of Therapeutic Proteins in Contact With a Novel Fluoropolymer Surface Versus Siliconized Surfaces: Effects of Agitation in Vials and in Prefilled Syringes, J. Pharm. Sci. 105 (2016) 2053–2065. doi:10.1016/j.xphs.2016.04.015.

[23] Z. Gaozhong, S.P. Schwendeman, Stabilization of proteins encapsulated in cylindrical poly(lactide-co- glycolide) implants: Mechanism of stabilization by basic additives, Pharm. Res. 17 (2000) 351–357. doi:10.1023/A:1007513425337.

Chapter 4: Coated PLGA implants for controlled release of bevacizumab

4.1 Abstract

Wet age-related macular degeneration (AMD) is a condition in which new abnormal blood vessels grow under the macula, thus displacing the macula from its normal position, and resulting in rapid central vision loss. The growth of abnormal blood vessels under the retina is stimulated by overexpression of vascular endothelial growth factor (VEGF), therefore, anti-VEGF therapies have been developed to treat wet AMD. Intravitreal injections of the anti-VEGF agents are typically given every 4 weeks, but this is very inconvenient and repeated injections may induce infection, inflammation and hemorrhage. Sustained release formulations of the anti-VEGF agents can reduce administration frequency for patient convenience and minimize the risks while maintaining the therapeutic concentration in the vitreous.

Poly (lactic-co-glycolic acid) (PLGA) is the most common and extensively researched polymer which has been used in several FDA-approved medical devices for long-term controlled release due to its biodegradability, biocompatibility and ability to provide desirable release kinetics. Injectable PLGA implants such as millicylinders has been used to deliver a number of stabilized protein drugs. Therefore, in this research, PLGA millicylindrical implants were employed to develop sustained release formulations of bevacizumab (Avastin®), a marketed anti-VEGF agent. To achieve near zero-order

release kinetics, with high loading of the protein and osmotically active excipients, the implants were coated with pure PLGA. Release kinetics of bevacizumab from implants with different PLGA concentrations in the coating solution were studied and it was observed that higher PLGA concentrations in a coating solution resulted in slower release of the antibodies. The implants coated with 30 % and 50 % PLGA demonstrated continuous *in vitro* release kinetics under physiological conditions over six weeks with total cumulative release of 82 ± 8 and 89 ± 4 % (mean ± SD, n=3), respectively. Analysis of the released antibodies by size-exclusion chromatography (SEC), enzyme-linked immunosorbent assay (ELISA) and circular dichroism (CD) showed little change in monomer content, immunoreactivity, and secondary structure during the 6-week release period.

4.2 Introduction

Wet AMD is a condition in which new abnormal blood vessels grow and leak fluid, or blood, behind the macula. This leads to macula displacement, and rapid central vision loss. AMD is a major cause of vision loss in developed countries, especially in people 60 or older. There are two forms of AMD: the wet and dry form. The wet form of AMD accounts for only 10 % of the cases, but is responsible for 90 % of vision loss, whereas the more common dry form results in relatively mild symptoms [1–4]. In wet AMD, the growth of abnormal blood vessels under the retina is stimulated by overexpression of VEGF. Therefore, anti-VEGF therapies have been developed to neutralize VEGF activity. The first FDA-approved anti-VEGF agent was Macugen® (pegaptanib, anti-VEGF aptamer) which slowed vision loss compared to conventional

treatment such as laser coagulation, or photodynamic therapy, however Macugen® did not improve visual acuity in patients [5]. The next FDA-approved, anti-VEGF, agent for wet AMD was Lucentis® (ranibizumab, anti-VEGF monoclonal antibody Fab fragment), which until recently was the leading product in the market owing to its ability to improve visual acuity significantly in wet AMD patients. On the other hand, Avastin® (bevacizumab, anti-VEGF whole monoclonal antibody), which is officially approved for various forms of cancer, has been used off-label extensively by clinicians since it shows similar efficacy to Lucentis® and a single equivalent dose of Avastin® for wet AMD is actually 40 times less expensive than that of Lucentis® [6,7]. Recently in 2011, Eylea® (aflibercept, a recombinant fusion protein consisting of portions of human VEGF receptors 1 and 2 extracellular domains fused to the Fc portion of human IgG1) was approved for wet AMD and is currently the most promising anti-VEGF agent since it demonstrates better outcomes than the other anti-VEGF antibodies [8]. The current dosing regimen of the anti-VEGF antibodies is monthly by intravitreal injection, but this is very inconvenient for patients [9] and repeated injections introduce risk of infection, inflammation and hemorrhage [10]. Therefore, sustained release formulations are needed to reduce administration frequency for improved patient compliance and convenience and minimize the risks by maintaining the therapeutic concentration longer at the target site.

PLGA is among the most commonly and extensively researched polymer biomaterials, and has been used in numerous FDA-approved medical devices for controlled release formulations due to its biodegradability, biocompatibility and ability to achieve desirable release kinetics [11]. Several forms of PLGA depots for controlled release of protein have been developed such as microspheres, nanoparticles, implants,

and films [12–15]. Among these different types of PLGA formulations, the PLGA implant has advantages over other forms namely in: high and easily controlled loading, high loading efficiency, minimally invasive injection, and anhydrous encapsulation of protein for additional stability. In terms of ocular delivery, there is a FDA-approved precedent: Ozurdex® is a PLGA implant for controlled release of dexamethasone into the eye [16]. In this study, therefore, PLGA implants were deemed a viable option and further investigated for controlled release of bevacizumab in the vitreous.

Desirable attributes of the bevacizumab loaded implants are high loading of the antibodies due to the limit of intravitreal injection volume and near zero-order release profile to maintain effective antibody concentration in the vitreous. Release kinetics of osmotically active agents from hydrophobic polymer matrix depends on a number of factors including the excipient loading [17,18]. Therefore, loading of the antibodies has to be adjusted to obtain desired release kinetics as well. To stabilize encapsulated proteins, additional osmolytes such as salts, and sugars may be needed, but these will affect the release kinetics of antibodies as well. These stabilizing parameters were described in Chapter 3. To achieve desired release kinetics, in addition to adjusting the loading, coating "core implants" (monolithic implants investigated in Chapter 3) with pure polymer has been utilized to sustain release of highly loaded antibiotics [19,20], testosterone, estradiol-17β [21], and bovine serum albumin [22].

In this chapter, polymer coated (or referred to simply as "coated") PLGA implants for anti-VEGF therapy were developed to achieve the desirable attributes with formulating anti-VEGF protein dosage forms. Several important elements were identified to achieve a formulation with desirable stability and controlled release of bevacizumab

from PLGA, namely: (a) developing a suitable PLGA coating method and optimizing it to achieve near zero-order and complete release (>80%); (b) incorporating a poorly soluble base to neutralize acids liberated from PLGA for protein stability combined with a PLGA of a suitable MW with end-capping to accomplish continuous release; (c) applying cryomilling for safely preparing protein powder for encapsulation; and (d) applying an anhydrous solvent extrusion technique to both stabilize the protein during encapsulation and to create cylindrical implants suitable for intravitreal injection. The studies below describe the formulation optimization that incorporate the above important elements, and the *in vitro* performance of the resulting coated PLGA millicylindrical implants for slow-release of stable bevacizumab.

4.3 Materials and Methods

4.3.1 Materials

Avastin®, commercial solution of bevacizumab, was purchased from the pharmacy and used within its shelf-life period. PLGA 50:50 (inherent viscosity = 0.64 dL/g and Mw = 54.3 kDa, ester terminated) was purchased from LACTEL Absorbable Polymers (Birmingham, AL). Trehalose dihydrate (trehalose), $MgCO_3$, guanidine hydrochloride, DL-dithiothreitol (DTT), ethylenediamine-tetraacetic acid (EDTA), Na_2HPO_4, NaH_2PO_4, anti-human IgG-alkaline phosphatase antibody produced in goat and p-nitrophenyl phosphate liquid substrate system (pNPP) were purchased from Sigma-Aldrich Chemicals (St. Louis, MO). Tween 80 (10%), acetone, KH_2PO_4, K_2HPO_4, KCl, phosphate buffered saline (PBS), Amicon Ultra-15 Centrifugal Filter Units (10,000 MWCO), silicone rubber tubing, and Coomassie plus reagent assay kit were purchased

from Fisher Scientific (Hanover Park, IL). Recombinant human vascular endothelial growth factor (VEGF) was a generous gift from Genentech.

4.3.2 Preparation of bevacizumab powder

The buffer of Avastin® solution containing bevacizumab and excipients was exchanged into 51 mM sodium phosphate buffer (pH 6.2) by using Amicon Centrifugal Filter Units (10,000 MWCO) to remove trehalose. Then, trehalose was added (weight of trehalose : weight of bevacizumab = 1.5 : 1) again and the solution was diluted with 51 mM sodium phosphate buffer (pH 6.2) for the final bevacizumab concentration of 25 mg/mL and lyophilized. The solid was then ground by CryoMill (Retsch, Germany) at 30 Hz for 30 min and sieved through 90-μm screen (Newark Wize Wearing, Newark, NJ).

4.3.3 Preparation of coated implants with bevacizumab

The resulting bevacizumab powder was suspended into 50 % (w/w) PLGA solution in acetone with 3% (w/w) $MgCO_3$ in a 2 mL centrifuge tube, then mixed and transferred into a 3 mL syringe. The suspension was extruded into silicone rubber tubing (I.D. = 0.8 mm), then dried at room temperature for 48 h followed by vacuum drying at 40°C and -23 in. Hg vacuum for an additional 48 h. The final dried implants were obtained by removal of silicone tubing and were cut into segments of desired length for future use. For coated implants, the core implants were put back into silicone tubing and pure PLGA solution at various concentrations in acetone within a 3 mL syringe was extruded over the core implants to coat the surface and dried in vacuum oven at room temperature for 48 h and at 40°C for an additional 48 h. Then, silicone tubing was removed and the final coated implants were cut for the following experiments.

4.3.4 Measurement of bevacizumab loading in implants

Implants (3-5 mg) were dissolved in 1 mL of acetone for 1 h and centrifuged to precipitate proteins. PLGA dissolved in supernatant was removed and the protein pellet was washed with acetone and centrifuged three times more to remove residual PLGA. The pellet was then air dried, reconstituted in 1 mL of PBST (phosphate buffered saline with 0.02 % Tween 80, pH 7.4) at 37°C overnight and analyzed by size-exclusion high-performance liquid chromatography (SE-HPLC). The condition of SE-HPLC to quantify monomer and soluble aggregates was followed as previously described [23] with slight modifications, which included the injection volume of 50 µL and filtration of all samples through 0.45 µm filter. Extracted loading and loading efficiency were calculated by the following equations.

$$\text{Extracted loading (\%)} = \frac{\text{Weight of extracted bevacizumab}}{\text{Weight of total implant}} \times 100\ \%$$

$$\text{Loading efficiency (\%)} = \frac{\text{Extracted loading}}{\text{Theoretical loading}} \times 100\ \%$$

4.3.5 *In vitro* release study of bevacizumab from implants

Implants (0.5 - 2 cm long, 3 - 14 mg) were added in 1.5 mL centrifuge tubes with 1 mL of PBST and incubated at 37°C without agitation, as agitation was found to cause insoluble aggregation of the antibody in the release media. The release medium was replaced with fresh medium at each time point. The amount of released bevacizumab at each time point was measured by SE-HPLC and calculated as percentage of the released amount out of the extracted loading of soluble bevacizumab. In certain instances, the

release media was also analyzed for protein structure and immunoreactivity, as described below.

4.3.6 Evaluation of residual bevacizumab in implants

At the end of release study, the remaining bevacizumab was extracted by the same procedure used to measure protein loading after lyophilizing the remaining polymer. The protein pellet was then reconstituted in PBST and incubated at 37°C overnight to determine the soluble fraction of the protein that remained in the polymer. After centrifugation, the supernatant was collected and the remaining insoluble precipitates were dissolved in denaturing solvent (6 M guanidine hydrochloride/1 mM EDTA) at 37°C for 1 h to determine non-covalent protein aggregates. After centrifuging and collecting supernatant, the remaining insoluble precipitates were dissolved in denaturing/reducing solvent (6 M guanidine hydrochloride /1 mM EDTA/10 mM DTT) to measure covalent protein aggregates formed by disulfide bonds. Concentration of protein aggregates in each step was measured by Coomassie plus protein assay. All measurements were performed in triplicate and bevacizumab standards were dissolved in the same solvent used for each analysis.

4.3.7 Enzyme linked immunosorbent assay (ELISA)

ELISA was performed to determine immunoreactivity of the released bevacizumab as described previously [24] with some modifications. Briefly, 96-well ELISA microplates were pre-coated with 50 µl of VEGF (0.5 µg/mL) solution in PBS (phosphate buffered saline, pH 7.4) at 4°C overnight. After washing with 350 µl of PBS four times, 100 µl of PBS containing 1 % BSA (bovine serum albumin) was added for blocking and incubated at room temperature for 2 h. After washing, 50 µl of bevacizumab

standards (0 ~ 2.56 μg/mL) and samples diluted in PBST containing 1 % BSA were added into each well and incubated at room temperature for 1 h. After washing, 50 μl of secondary antibody (alkaline phosphatase conjugated goat anti-human IgG) was added at 1: 1000 dilution in PBST containing 1 % BSA into each well and incubated for another 1 h. Detection was carried out by adding 50 μl of pNPP after washing. Color development was monitored with a plate reader (Dynex MRX II, Richfield, MN) every 10 min at 405 nm until R-squared value of the standard curve started decreasing.

4.3.8 Circular dichroism (CD)

CD was performed with Jasco J-815 CD spectrometer equipped with Jasco temperature controller (CDF-426S/15) and Peltier cell at 25 °C. The samples were diluted or buffer-exchanged into 51 mM sodium phosphate buffer (pH 6.2) and concentrated by using Amicon Centrifugal Filter Units (10,000 MWCO), so the final concentration ranged from 0.05 to 0.5 mg/mL for far UV measurements. The samples were measured in quartz cuvettes (Hellma) with a path length of 1 mm. The spectra were collected in continuous mode at a speed of 50 nm/min, bandwidth of 1 nm and a data integration time of 1sec and were averaged from 10 scans. The spectrum of blank 51 mM sodium phosphate buffer (pH 6.2) was subtracted from each spectrum by using the Jasco spectra manager software (Version 2.1). The raw data was converted to mean residue ellipticity (MRE) using the following equation:

$$[\boldsymbol{\theta}]_{\boldsymbol{mrw,\lambda}} = \boldsymbol{MRW} \times \frac{\boldsymbol{\theta_\lambda}}{\boldsymbol{10 \times d \times c}}$$

where is the θ_λ observed ellipticity in degree at wavelength λ, d is the path length in cm, c is the concentration in g/mL, and mean residue weight (MRW) in g/mol is 113 for

bevacizumab. The resulting CD spectra were smoothed using SigmaPlot software (Version 12.0, Systat Software, Inc.).

4.3.9 Confocal microscopy

The distribution of protein powder and PLGA coating in the coated implants was visualized using confocal microscopy. BSA labeled with Alexa Fluor® 488 (Thermo Fisher Scientific, Waltham, MA) was used as a fluorescent model protein. Regular BSA including 5 % of the fluorescent BSA was loaded at 10 % with trehalose and $MgCO_3$ into core implants as described before. To visualize and distinguish the PLGA coating from the fluorescent protein, Cyanine5 carboxylic acid dyes (Cy5, Lumiprobe, Hallandale Beach, FL) were dissolved at 10 µg/mL in PLGA/acetone solution, and the core implants were coated with the Cy5/PLGA solution as previously described. The dried implants were cut for cross-sectional images and placed on a clean glass slide. A clean glass cover slide was placed over the implant slices. To visualize lateral surface of implants, the dried or lyophilized implants from *in vitro* release study were placed on a glass slide. Samples were imaged using a confocal microscope (Nikon A1 Spectral Confocal Microscope) with excitation/emission wavelengths of 488/525 nm for the BSA labeled with Alexa Fluor® 488 and 640/700 nm for the Cy5 in PLGA coating.

4.4 Results and Discussion

4.4.1 Coated implants with pure PLGA for higher loading and improved continuous release

The strategy of reducing trehalose in the drug powder shown in the previous chapter had limitations for higher loading of bevacizumab, sustained release, and mAb stability. Therefore, a coating strategy was tested as a next step because they have been previously employed for high drug loading and sustained release in hydrophobic polymer implants [19–22]. As a coating method, simply extruding pure PLGA over the core implants in silicone tubing was used and the degree of coating was controlled by PLGA concentration in coating solution. Since the loading of bevacizumab needs to be high after coating, only 10 and 15 % loaded core implants were coated and tested. The extracted loadings of bevacizumab in uncoated, and 10, 30 and 50 % PLGA coated implants were 9.2, 9.0, 8.2, and 7.6 %, respectively. In addition, the diameters of uncoated, and 10, 30 and 50 % PLGA coated implants were 0.64, 0.64, 0.75, and 0.88 mm, respectively (Table 4.1). The extracted loadings of bevacizumab in the coated implants were lower than that of the uncoated implants, and a higher PLGA concentration in the coating solution resulted in lower extracted loading since the coating added more PLGA mass into the implants. Also as expected, a higher PLGA concentration (30 and 50 %) in the coating polymer solution resulted in thicker diameters of implants.

As a core, 10 % bevacizumab loaded implants with 1.5:1 powder were tested to determine how PLGA concentration in coating affected the release profile. Coated implants with 10 % PLGA showed slower release rate than the core implant and the implants coated with 30 and 50 % PLGA released bevacizumab even slower than the

10 % coated one and showed near zero-order release profiles for 6 weeks. The initial burst release on day 1 reduced from 51 % in uncoated implants to 14 % in 10 % PLGA coated ones, and 5.1 and 6.7 % in 30 and 50 % PLGA coated ones, respectively, Total cumulative releases from the uncoated and the 10, 30 and 50 % PLGA coated implants were 97, 92, 89, and 82 %, respectively (Figure 4.1 A). The implants coated with higher PLGA concentration than 50 % were not able to be tested because PLGA solution was too viscous to extrude over the core implants.

The release from the uncoated implants loaded with 10 % bevacizumab and 1.5:1 w/w trehalose : protein powder was fast and likely dominated by pure diffusion-through-channel since the drug particles above the percolation threshold were interconnected rapidly. By coating the lateral surface-wall of core implants, fast release of bevacizumab located near the surface was expected to occur primarily through the both open ends, thus resulting in lower initial burst release. The proteins located deeply into the middle of coated implants have much longer distance to the surface of both ends than that in uncoated implants whose maximum is only the radius of the implants. Hence, less complete channels from a drug particle to the surface in coated implants were formed even above the percolation threshold in core implants and resulted in low initial burst release and slower following release driven by slow formation of osmotic pressure-induced channels. Release rates of 30 and 50 % PLGA coated implants were similar during the whole release study period whereas release was faster in 10 % PLGA coated implants. Thus, 10 % PLGA coating was likely not thick enough to effectively coat the core implants completely during release, while PLGA at 30 % concentration or higher

coat the core implants sufficiently to prevent the release through the side walls before polymer mass loss occurs.

However, 50 % PLGA coated implants with 15 % bevacizumab loading of 1.5:1 powder still showed very high initial burst release (81 %) and near complete release after day 7. At this total powder loading (41.7 %) in core implants, most of the drug particles are thought to be closely interconnected, thus enabling the formation of water channels through the interconnected particles from both open ends rapidly once the implants are put in release medium. The coated implants with 10 % core loading of bevacizumab with 2.4:1 powder was also tested as a control. As expected, the initial burst release on day 1 was higher (24 %) than that (6.7 %) of the corresponding implant with 1.5:1 powder due to higher loading of osmotically active trehalose in core implants (Figure 4.1 B). By coating implants with pure PLGA, therefore, 30 and 50 % PLGA coated implants with 10 % bevacizumab loading of 1.5:1 powder were the best formulations among all the tested formulations for higher loading (8.2 and 7.6 %), more sustained release, and higher total cumulative release (89 and 82 %). The major residual proteins in polymer were non-covalent aggregates, which were 7.8 and 8.9 %, and total recoveries were 98 and 92 %, respectively (Table 4.2). It is important to note that a small difference in recovery and complete release was observed for the two different optimized coating conditions. It is possible that the thinner coating (from 30% polymer concentration), which was also sufficient to maintain the release, was able to reduce the diffusion barrier to water-soluble acids relative to the thicker coating (50%), slightly increase the microclimate pH to reduce aggregation and hydrolysis of the protein. Future studies will be aimed at

discerning these more subtle variations and also increasing duration of the release by increasing lactic content in the polymer.

4.4.2 Geometric analysis of powder distribution and PLGA coating

To visualize distribution of protein powder and PLGA coating on the cross-section of coated implants, confocal microscopy was performed. A commercial fluorescent (Alexa Fluor® 488) BSA was loaded into the core implants instead of bevacizumab to ensure high intensity of fluorescence. The powder with the green fluorescent BSA was homogeneously distributed on the cross-section of core implants, and a PLGA coating containing Cy5 dyes surrounded the core implants well in the both 30 % and 50 % PLGA coated implants (Figure 4.2). It was observed that the thickness of a PLGA coating was not consistent through the peripheral region and the PLGA coating of some parts invaded the region of core implants.

4.4.3 Stability of bevacizumab extracted and released from coated implants

To investigate the stability of released bevacizumab from these optimized implants, monomer content, immunoreactivity and conformational stability in secondary structure were evaluated via SE-HPLC, ELISA and CD. Intact bevacizumab originally shows a small dimer peak in size-exclusion chromatogram and the monomer content calculated by the following equation,

$$\text{Monomer content (\%)} = \frac{\text{AUC of a monomer peak}}{\text{AUC of total peaks}} \times 100\ \%$$

is dependent on the concentration of bevacizumab. Released proteins from the optimized formulations had a bit less monomer content than that of the corresponding concentration of intact bevacizumab, but it was maintained above 90 % during the whole period (Figure

4.3 A). Until 3-4 weeks of release, the monomer content decreased and slightly increased after then. It is speculated that formation of soluble dimers or oligomers from monomers resulted in the early decrease in monomer content and consumption of the soluble aggregates as nuclei for growth of higher order insoluble aggregates trapped in polymer caused the later increase in monomer content.

The immunoreactivity of extracted and released proteins from the coated implants was also measured to evaluate the binding activity against VEGF, which is a target antigen (Figure 4.3 B). It was calculated by the following equation,

$$\text{Immunoreactivity (\%)} = \frac{\text{Concentration from ELISA}}{\text{Concentration from SE} - \text{HPLC}} \times 100\ \%$$

, and measured at 115 and 102 % for extracts from 30 and 50 % PLGA coated implants, which means preparation of implants and extraction process did not decrease immunoreactivity of bevacizumab. For the release samples, it was maintained between 83 and 112 % for 30 % PLGA coated ones and between 89 and 105 % for 50 % PLGA coated ones until day 28. On day 42, it slightly decreased to 74 and 79 %, respectively.

Additionally, the far-UV CD spectra showed high conformational stability in the secondary structure of bevacizumab from powders, extracts, and release samples from 30 % (Figure 4.4 A) and 50 % (Figure 4.4 B) PLGA coated implants. Immunoglobulin G1 (IgG1), a subclass of bevacizumab, is known to have significant β-sheet structure characterized by broad negative peak at 218 nm in its far-UV CD spectrum [25], and all the spectra from each bevacizumab sample indicated insignificant changes in the secondary structure at the various stages. Therefore, it is concluded that released soluble

bevacizumab from the coated implants in a sustained manner also maintained the monomer content, immunoreactivity and secondary structure for 6 weeks.

4.4.4 Release kinetics of bevacizumab from coated implants of different lengths

The duration of bevacizumab release from the implants needs to be extended to longer than 6 weeks since at least 3-month releasing formulations are desired to reduce administration frequency of bevacizumab. Assuming complete insulation of the lateral surface of implants by the PLGA coating, the protein release will be slower and duration of release may become longer since the area of both open ends of the coated implants is constant regardless of the length of implants. To test this hypothesis, an *in vitro* study with the 30 % PLGA coated implants of three different lengths (0.5, 1 and 2 cm-long) was performed. However, except for the initial day 1-7 releases, the overall release rates of all the three implants were similar unlike our expectation (Figure 4.5). Therefore, the assumption of complete insulation of lateral surface might have been incorrect and the protein may still be released through the lateral surface of implants despite the polymer coating. In order to observe this, the coated implants with the fluorescent BSA and Cy5/PLGA coating from select time points of *in vitro* release study were visualized by confocal microscopy (Figure 4.6). As shown in Figure 4.6 A and B representing different lateral surface of the same piece of implant, the PLGA coating is not completely surrounding the core implant, therefore, the protein can be released though this uncoated part of the lateral surface. In addition, from the lateral surface images after day1, 3, 7 and 14 release (Figure 4.6 C, D, E and F), it is observed that pores are formed from the beginning of release study and become bigger, presumably due to swelling of the implants, along the release time. Therefore, the protein can be released through the pores

formed on the lateral surface of implants as well. This release phenomenon of proteins through the lateral surface of implants was observed in the cross-sectional images of the implants from day7 (Figure 4.6 G) and day14 (Figure 4.6 H) release. In these images, the fluorescent proteins are located more in the center of implants, and less in the peripheral region. Especially in the peripheral region near the surface of less coated part, more proteins seem to be released out compared to other peripheral regions. To slow down the release and extend the duration of release, a new method of coating procedure and/or a new coating material should be evaluated.

4.5 Conclusion

In this study, bevacizumab was loaded into coated PLGA implants and evaluated to develop sustained release formulation to reduce intravitreal administration frequency. By coating the core implants with PLGA, high loading (7.6-8.2 %, w/w) and continuous, near zero-order release over 6 weeks were achieved without a high initial burst release. Co-encapsulating trehalose and $MgCO_3$ as stabilizers also helped to achieve high total cumulative release (81.7-89.0 %). Bevacizumab released from these coated implants maintained the monomer content well above 90 % as well as its immunoreactivity, and secondary structure during the 6-week release period. It was observed by confocal microscopy that the proteins are also released through the lateral surface of the coated implants due to the non-uniform PLGA coating. Future work is directed towards evaluating the *in vivo* release kinetics and efficacy of the implants and improving the formulations to extend the duration of release to facilitate 3 month intervals between intravitreal injections. Finally, owing to the structural similarity of therapeutic

monoclonal antibodies, the coated PLGA implants, with the addition of appropriate disaccharides and antacids as stabilizers, have the potential to serve as delivery platforms for sustained release of other therapeutic monoclonal antibodies as well. Therefore, formulating other antibody drugs, which need sustained local delivery, with the described platform is a logical next step to pursue.

Table 4.1: Extracted loading and diameter of uncoated and coated implants.

Trehalose: bevacizumab in powder (w/w)	PLGA concentration in coating (%, w/w)	Theoretical loading in core implants (%)	Extracted loading (%)[a]	Diameter (mm)[a]
1.5:1	Uncoated	10	9.2 ± 0.2	0.64 ± 0.02
	10		9.0 ± 0.7	0.64 ± 0.01
	30		8.2 ± 1.1	0.75 ± 0.01
	50		7.6 ± 0.4	0.88 ± 0.01
	50	15	10.8 ± 0.3	N.D.
2.4:1	50	10	7.6 ± 0.8	N.D.

[a] Data reported as mean ± SD, *n*=3. N.D. = not determined.

Table 4.2: Mass balance of bevacizumab from in vitro release study of the coated implants prepared with 1.5:1 w/w trehalose : bevacizumab powder.

PLGA concentration in coating (%, w/w)	Cumulative release (%)	Soluble residue (%)	Non-covalent aggregate (%)	Covalent aggregate (%)	Recovery (%)
30	89 ± 4	0	7.8 ± 0.4	0.9 ± 0.3	98 ± 4
50	82 ± 8	0	8.9 ± 4.2	1.4 ± 1.6	92 ± 9

Data reported as mean ± SD, *n*=3

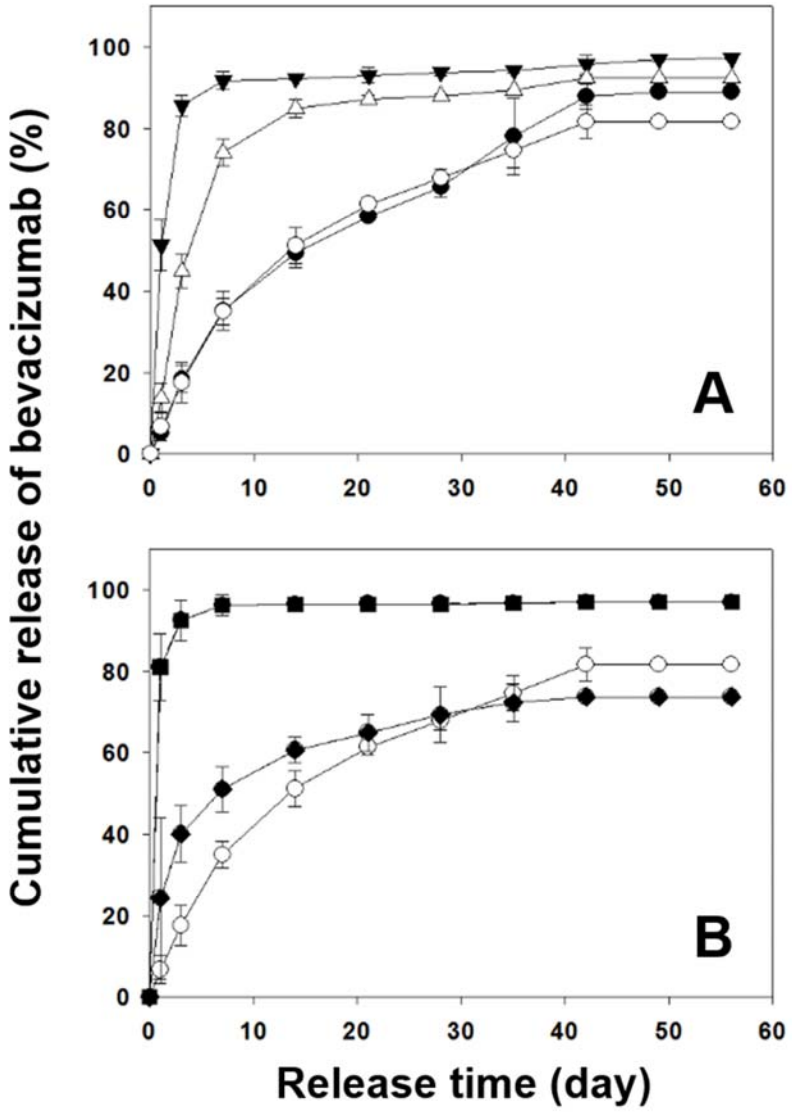

Figure 4.1: Release kinetics of bevacizumab from uncoated (▼) and coated (Δ, ○, ●, ■, ♦) implants. *Concentrations of PLGA solution for coating were 10 % (Δ), 30 % (●), and 50 % (○) for the core implants prepared with 10 % initial theoretical loading of buffer-exchanged bevacizumab powder with 1.5 to 1 w/w trehalose : bevacizumab (A). With 50 % PLGA in coating, release kinetics of different core implants loaded with 15% bevacizumab of the 1.5:1 powder (■), and loaded with 10 % bevacizumab of the original Avastin in the powder (♦) were compared to that of implants loaded with 10 % bevacizumab of the 1.5:1 powder (○) (B). Symbols represent mean ± SD, n=3.*

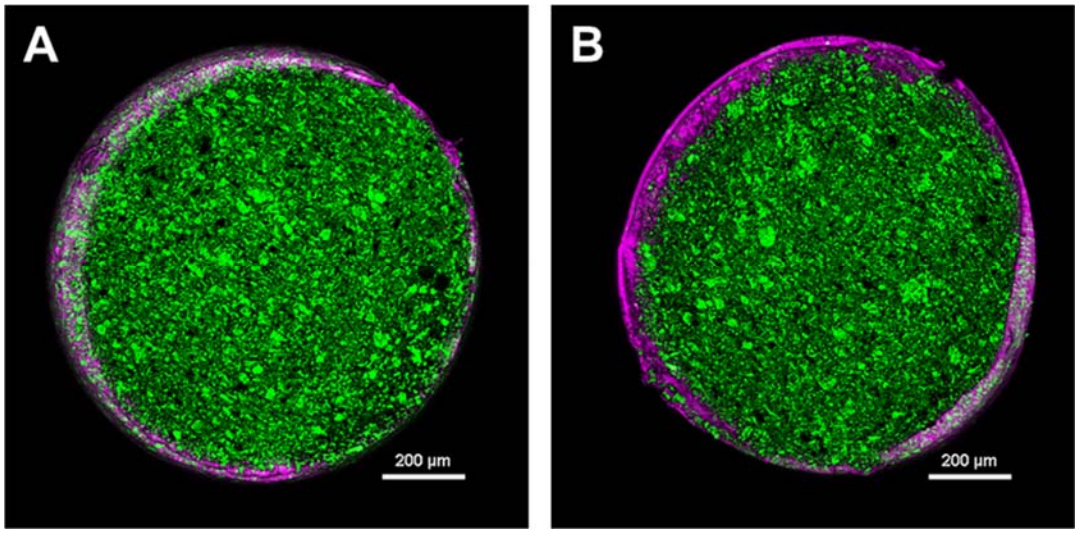

Figure 4.2: Cross-sectional images of 30 % (A) and 50 % (B) PLGA coated implants observed by confocal microscopy. *The green and the purple indicate protein powder and PLGA coating, respectively.*

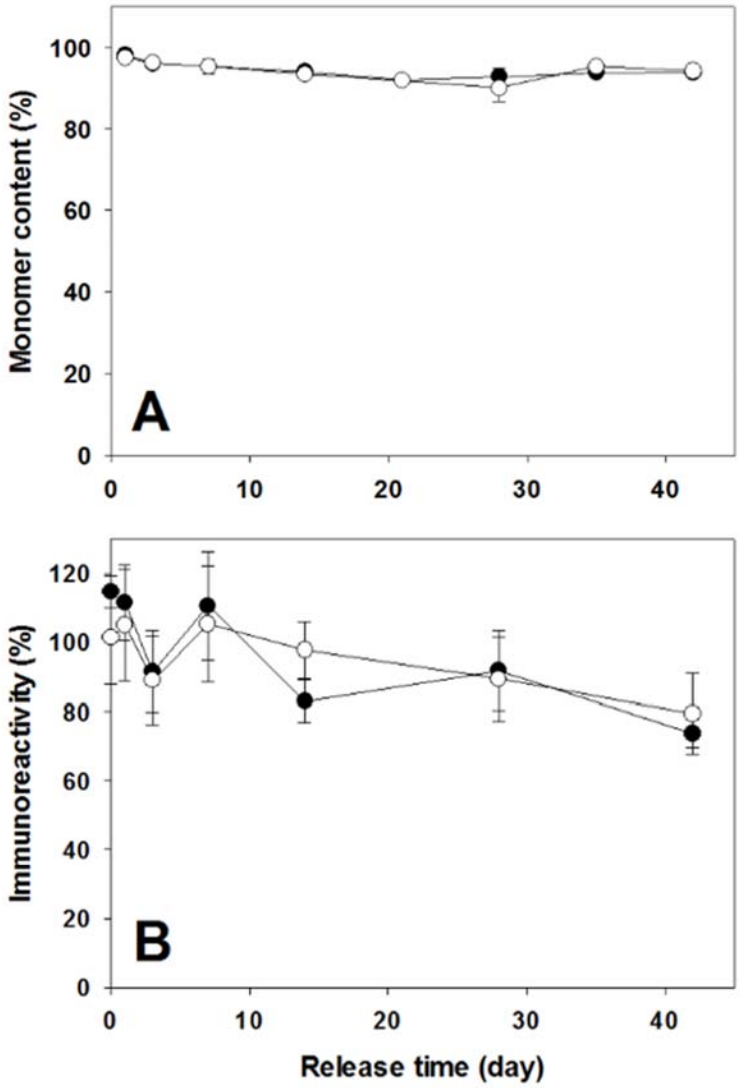

Figure 4.3: Monomer content (A) and immunoreactivity (B) of released bevacizumab from implants coated with 30 % w/w PLGA (●) and 50 %w/w PLGA (○). *Data are mean ± SD, n=3.*

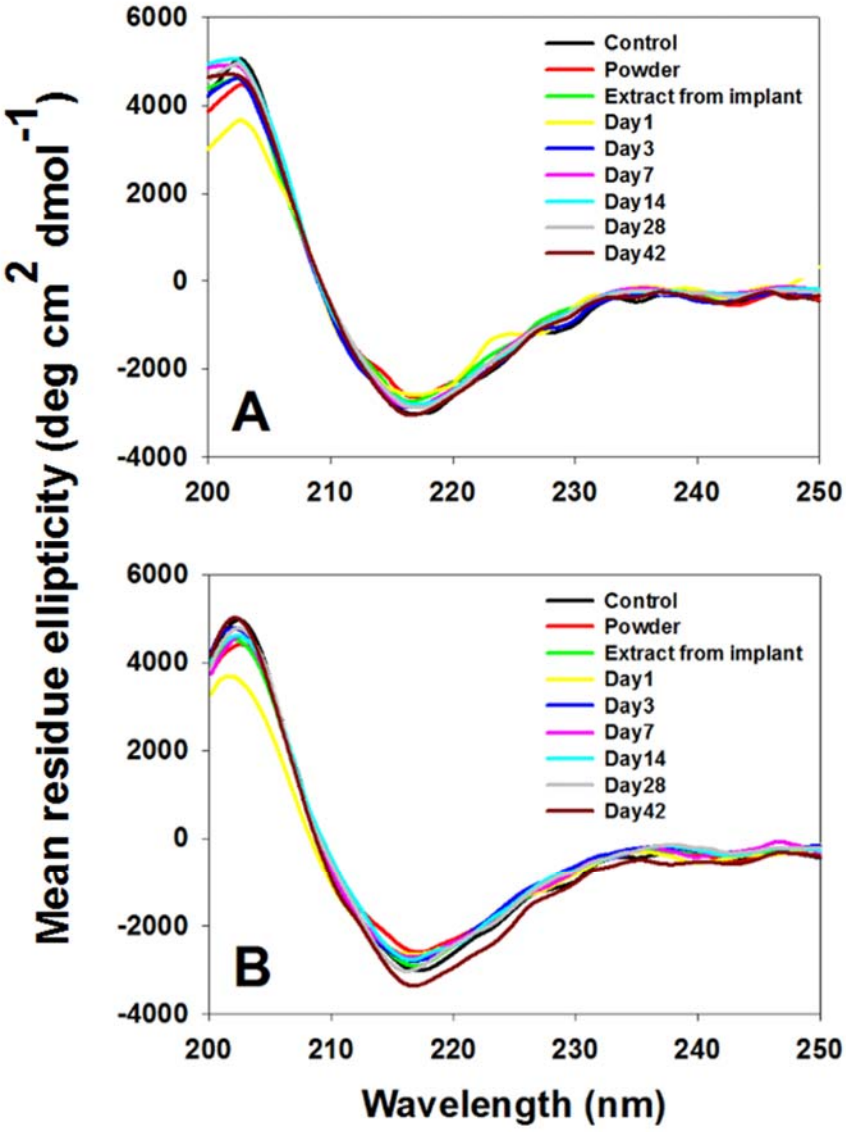

Figure 4.4: CD spectra of bevacizumab from Avastin® solution (control), 1:5 powder, extracts, and release samples at specific days of 30 % (A) and 50 % (B) PLGA coated implants. *Concentration of the protein measured by SE-HPLC was used to normalize all data.*

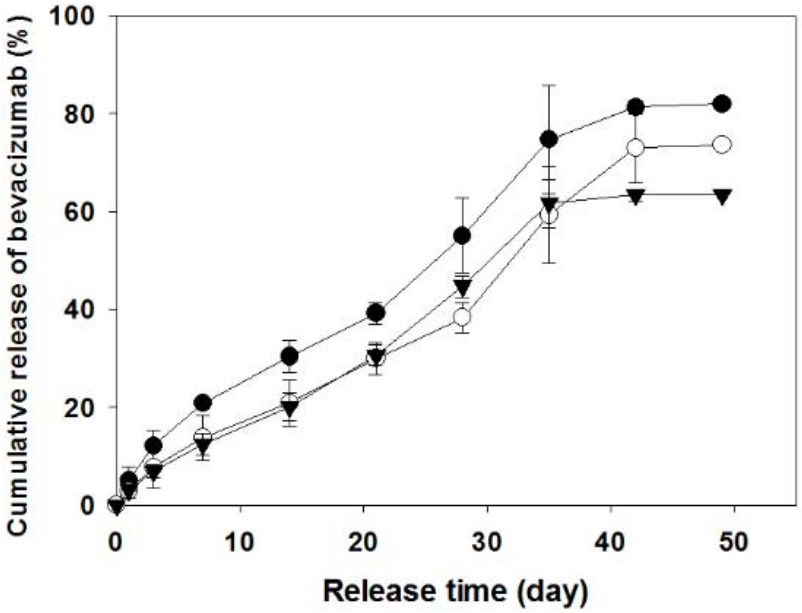

Figure 4.5: Release kinetics of bevacizumab from implants of different lengths (●: 0.5 cm, ○: 1 cm, ▼: 2 cm) prepared with 10 % initial theoretical loading of buffer-exchanged bevacizumab powder with 1.5 to 1 w/w trehalose:bevacizumab in the core implants and coated with 30 % PLGA. *Symbols represent mean ± SD, n=3.*

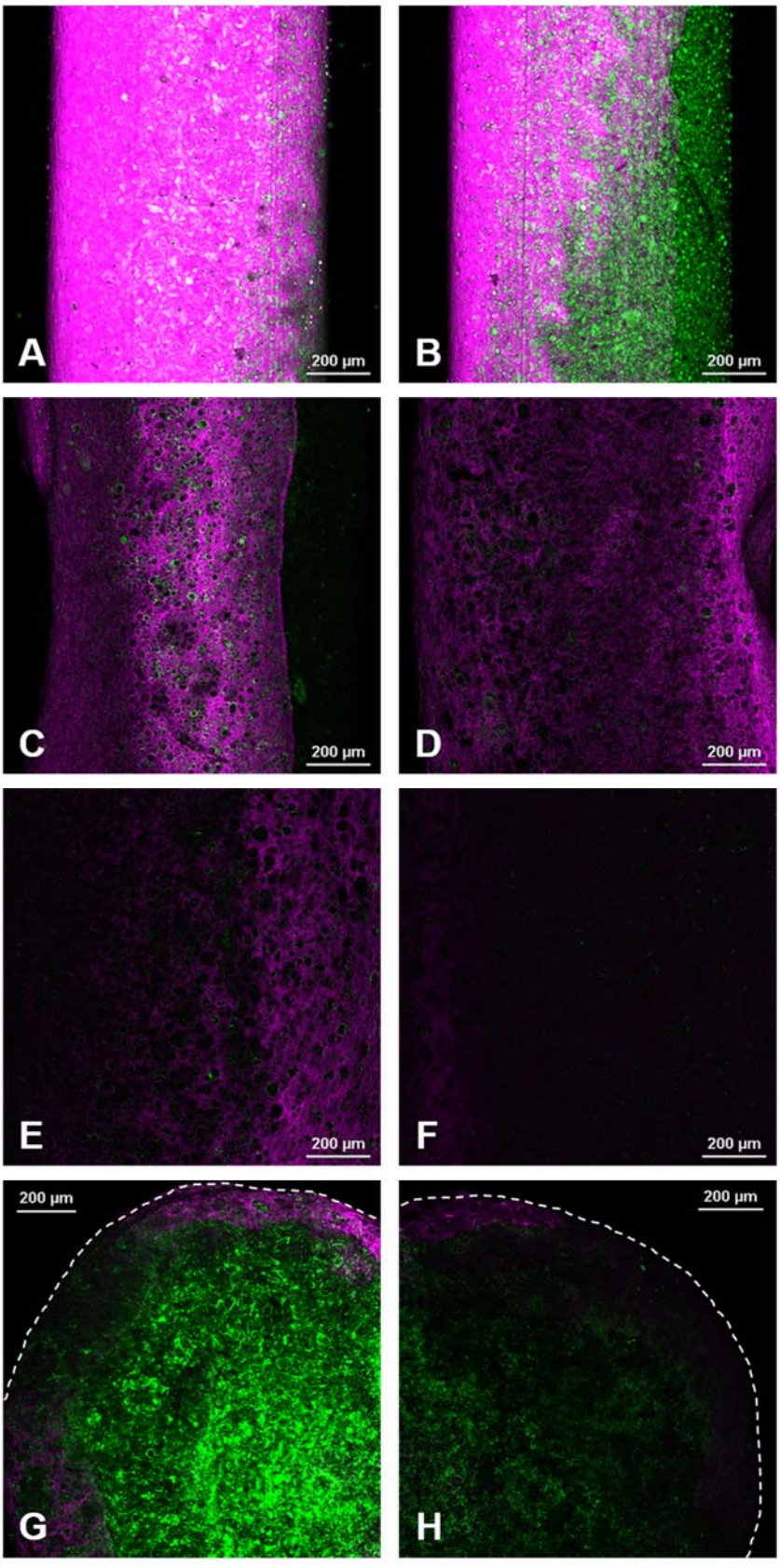
A
200 µm
B
200 µm
C
200 µm
D
200 µm
E
200 µm
F
200 µm
200 µm
G
200 µm
H

Figure 4.6: Distribution of Cy5/PLGA coating (purple) and fluorescent protein powder (green) on the lateral surface and cross-sections of coated implants during in vitro release study visualized by confocal microscopy. *A and B represent different lateral surface of the same implant before release study. C, D, E and F represent lateral surface of the coated implant after day1, 3, 7 and 14 release, respectively. G and H demonstrate cross-sections of the coated implants after day 7 and 14 release. The dotted white lines indicate borders of the implant cross-sections.*

4.6 References

[1] A.D. Singh, Gene- and Cell- Based Treatment Strategies for the Eye, (2015) 43–60. doi:10.1007/978-3-662-45188-5.

[2] A. V Chappelow, P.K. Kaiser, Neovascular age-related macular degeneration: potential therapies, Drugs. 68 (2008) 1029–1036. doi:6882 [pii].

[3] A.D. Kulkarni, B.D. Kuppermann, Wet age-related macular degeneration, Adv. Drug Deliv. Rev. 57 (2005) 1994–2009. doi:10.1016/j.addr.2005.09.003.

[4] B.A. Syed, J.B. Evans, L. Bielory, Wet AMD market, Nat. Rev. Drug Discov. (2012) 1–2. doi:10.1038/nrd3790.

[5] M. V Emerson, A.K. Lauer, Emerging therapies for the treatment of neovascular age-related macular degeneration and diabetic macular edema, BioDrugs. 21 (2007) 245–257. doi:2145 [pii].

[6] J.L. Kovach, S.G. Schwartz, H.W. Flynn, I.U. Scott, Anti-VEGF treatment strategies for wet AMD, J. Ophthalmol. 2012 (2012). doi:10.1155/2012/786870.

[7] N. Ferrara, A.P. Adamis, Ten years of anti-vascular endothelial growth factor therapy, Nat. Rev. Drug Discov. (2016) 1–19. doi:10.1038/nrd.2015.17.

[8] E. Dhrami-gavazi, Q. Ghadiali, Aflibercept : a review of its use in the treatment of choroidal neovascularization due to age-related macular degeneration, (2015) 2355–2371. doi:10.2147/OPTH.S80040.

[9] K.M. Droege, P.S. Muether, M.M. Hermann, A. Caramoy, U. Viebahn, B. Kirchhof, S. Fauser, Adherence to ranibizumab treatment for neovascular age-related macular degeneration in real life, Graefe's Arch. Clin. Exp. Ophthalmol. 251 (2013) 1281–1284. doi:10.1007/s00417-012-2177-3.

[10] K.G. Falavarjani, Q.D. Nguyen, Adverse events and complications associated with intravitreal injection of anti-VEGF agents: a review of literature., Eye (Lond). 27 (2013) 787–94. doi:10.1038/eye.2013.107.

[11] S.P. Schwendeman, R.B. Shah, B.A. Bailey, A.S. Schwendeman, Injectable controlled release depots for large molecules, J. Control. Release. 190 (2014) 240–253. doi:10.1016/j.jconrel.2014.05.057.

[12] R.B. Shah, S.P. Schwendeman, A biomimetic approach to active self-microencapsulation of proteins in PLGA, J. Control. Release. 196 (2014) 60–70. doi:10.1016/j.jconrel.2014.08.029.

[13] M.M. Pakulska, I.E. Donaghue, J.M. Obermeyer, A. Tuladhar, C.K. Mclaughlin, T.N. Shendruk, M.S. Shoichet, Encapsulation-free controlled release : Electrostatic adsorption eliminates the need for protein encapsulation in PLGA nanoparticles, (2016).

[14] V. Milacic, S.P. Schwendeman, Lysozyme Release and Polymer Erosion Behavior of Injectable Implants Prepared from PLGA-PEG Block Copolymers and

PLGA/PLGA-PEG Blends., Pharm. Res. 31 (2013) 436–448. doi:10.1007/s11095-013-1173-6.

[15] X. Qu, Y. Cao, C. Chen, X. Die, Q. Kang, A poly(lactide-co-glycolide) film loaded with abundant bone morphogenetic protein-2: A substrate-promoting osteoblast attachment, proliferation, and differentiation in bone tissue engineering, J. Biomed. Mater. Res. - Part A. 103 (2015) 2786–2796. doi:10.1002/jbm.a.35379.

[16] N. Kuno, S. Fujii, Biodegradable intraocular therapies for retinal disorders: Progress to date, Drugs and Aging. 27 (2010) 117–134. doi:10.2165/11530970-000000000-00000.

[17] B. Amsden, Review of osmotic pressure driven release of proteins from monolithic devices., J. Pharm. Pharm. Sci. 10 (2007) 129–43. http://www.ncbi.nlm.nih.gov/pubmed/17706172.

[18] B.G. Amsden, Y. Cheng, M.F.A. Goosen, A mechanistic study of the release of osmotic agents from polymeric monoliths, 3659 (1994).

[19] U.R.S.P. Wyss, Biodegradable Controlled Antibiotic Release Devices for Osteomyelitis: Optimization of Release Properties, (1994) 718–724.

[20] Xichen Zhang, U.P. Wyss, D. Pichora, M.F. a. Goosen, A mechanistic study of antibiotic release from biodegradable poly(d,1-lactide) cylinders, J. Control. Release. 31 (1994) 129–144. doi:10.1016/0168-3659(94)00011-5.

[21] X. Zhang, Controlled release of testosterone and estradiol- 17p from biodegradable cylinders, 29 (1994) 157–161.

[22] X. Zhang, U.P. Wyss, D. Pichora, B.G. Amsden, M.F.A. Goosen, Controlled release of albumin from biodegradable poly (DL-lactide) cylinders, J. Control. Release. 25 (1993) 61–69.

[23] L. Liu, D.A. Ammar, L.A. Ross, N. Mandava, M.Y. Kahook, J.F. Carpenter, Silicone oil microdroplets and protein aggregates in repackaged bevacizumab and ranibizumab: Effects of long-term storage and product mishandling, Investig. Ophthalmol. Vis. Sci. 52 (2011) 1023–1034. doi:10.1167/iovs.10-6431.

[24] J.S. Andrew, E.J. Anglin, E.C. Wu, M.Y. Chen, L. Cheng, W.R. Freeman, M.J. Sailor, Sustained release of a monoclonal antibody from electrochemically prepared mesoporous silicon oxide, Adv. Funct. Mater. 20 (2010) 4168–4174. doi:10.1002/adfm.201000907.

[25] V. Joshi, T. Shivach, N. Yadav, A.S. Rathore, Circular Dichroism Spectroscopy as a Tool for Monitoring Aggregation in Monoclonal Antibody Therapeutics, (2014).

Chapter 5: Conclusions, Significance and Future Work

The work presented in this dissertation takes aim at three requirements pertaining to successfully developing poly(lactic-co-glycolic acid) (PLGA) depot formulations of bevacizumab (or its Fab fragment) to reduce administration frequency for improved patient compliance and convenience, and to minimize risks of intravitreal injection for wet age-related macular degeneration (AMD): i) high w/w loading and loading efficiency of the antibodies due to the limited injection volume into the vitreous and improving the cost-effectiveness, ii) near zero-order and complete release of the antibodies for 3 months, and iii) minimal instability of the released antibodies for high efficacy and low immunogenicity.

Active self-encapsulation technology and utilizing poorly soluble basic salts to neutralize deleterious low pH in PLGA matrices were previously developed in our lab to achieve the above goals for other protein drugs [1,2]. Therefore, in Chapter 2, we applied those technologies to develop active self-encapsulating PLGA microspheres for the anti-VEGF antibodies. The previously utilized trapping agent for lysozyme [3], high molecular weight dextran sulfate (HDS) was employed since the HDS negative charge can entrap the positively charged antibodies. $ZnCO_3$ was co-encapsulated as an antacid and this resulted in continuous release of the immunoreactive antibodies for 56 days. But, w/w loading and loading efficiency were too low. Although several parameters (e.g. $ZnCO_3$ and HDS content, loading solution pH, and protein concentration in loading

solution) were adjusted, both loading (w/w) and loading efficiency were not significantly improved.

To increase the low loading and encapsulation efficiency observed in Chapter 2, in Chapter 3 PLGA millicylindrical implants were investigated. High w/w loading can be achieved using an anhydrous encapsulation procedure for proteins. Co-incorporation of trehalose afforded stabilization of the proteins against aggregation during powder preparation, but also contributed to faster release of the proteins due to its osmotic activity. Therefore, the ratio of trehalose and bevacizumab was optimized to sustain release of the protein while maintaining the stabilizing effect. For the desirable release rate, the loading of bevacizumab needed to be reduced to 3-6 %, but the total cumulative release was also reduced, indicating less than desired protein stability. The slower and less complete release from the implants with lower loading of water soluble and osmotically active trehalose can be explained by the percolation theory and an osmotic pressure-induced release mechanism. At the low loading below the percolation threshold, drug particles including substantial amount of osmotically active trehalose are dissolved and form isolated water pores after water start partitioning into polymer matrix. High osmotic pressure created in the water pores induces imbibition of more water, consequently, the water pores are ruptured and microcracks are formed. Subsequently, the microcracks interconnect the isolated water pores and form water channels to the surface of implant, thus enabling drug release. In this case, formation of the complete water channels to the surface is a slow process, thus a rate limiting step for release. By the slow process, distribution of the dissolved antacids through the polymer matrix and removal of acid byproducts from the matrix are also delayed, thus resulting in more

protein aggregates and less complete release. Therefore, the critical key parameter to control release of water soluble drugs from the hydrophobic polymer matrix is the loading of osmotically active components.

To increase the loading and the total cumulative release, and to enhance the release kinetics simultaneously, in Chapter 4 a simple coating technique with pure polymer over the core implant was developed. The optimized formulation released bevacizumab for 6 weeks with near zero-order release kinetics and the total cumulative release of 89 %. Stability of the released antibodies was analyzed in various aspects and it was shown that colloidal stability, immunoreactivity, and secondary structures were well-preserved during the release period. Therefore, most desired characteristics of the ideal formulations for sustained delivery of the anti-VEGF antibodies were obtained by the strategy of coated implant, namely: (a) high loading capacity (w/w) and loading efficiency; (b) near zero-order release kinetics with high total cumulative release; and (c) minimal instability of encapsulated and released antibodies. One unmet characteristic is duration of release which was ultimately aimed at 3 months or longer. Assuming complete insulation of the lateral surface of coated implants, duration of release should be controlled by the length of implant, but it was not dependent on the length. It was observed that protein was also released through the lateral surface of coated implants, since the coating was not uniform on all sides and pores were formed on the lateral PLGA coating after release study started. Therefore, future studies are directed toward discovering an appropriate coating material and developing a new coating technique for more complete insulation of the lateral surface. Then, evaluating *in vivo* release behavior

and efficacy in animals is also needed to understand the clinical potential of our new approach.

Current strategies for sustained delivery of anti-VEGF antibodies discussed in Chapter 1 have their own pros and cons as an ideal formulation with the desired characteristics and the incompleteness hinders their clinical development. By addressing the issue encountered in the strategy of coated implant, this approach may have a great potential for clinical development of a sustained anti-VEGF antibody release formulation. In addition, the structural similarity of monoclonal antibodies enables formulating other antibody drugs, which need sustained local delivery, in this delivery platform. Also, with an appropriate stabilizing strategy, this sustained delivery approach can be broadly utilized for any water soluble drugs due to its generalizable nature.

5.1 References

[1] G. Zhu, S.R. Mallery, S.P. Schwendeman, Stabilization of proteins encapsulated in injectable poly (lactide-co-glycolide), Nat. Biotechnol. 18 (2000) 52–57. doi:10.1038/71916.

[2] S.E. Reinhold, K.G.H. Desai, L. Zhang, K.F. Olsen, S.P. Schwendeman, Self-healing microencapsulation of biomacromolecules without organic solvents, Angew. Chemie - Int. Ed. 51 (2012) 10800–10803. doi:10.1002/anie.201206387.

[3] R.B. Shah, S.P. Schwendeman, A biomimetic approach to active self-microencapsulation of proteins in PLGA, J. Control. Release. 196 (2014) 60–70. doi:10.1016/j.jconrel.2014.08.029.

Appendix A: PLGA implants of recombinant adeno-associated virus for gene therapy

A.1 Introduction

Gene therapy has been tremendously researched over the last few decades and will be an important treatment option for several genetic and acquired diseases because it is aimed at treating or eliminating the cause of diseases, whereas most current drugs are designed to treat the symptoms [1,2]. In order to deliver "therapeutic genes" into the target cells, enormous research efforts in the area of gene delivery vectors have been performed worldwide. There are two categories of gene delivery vector for gene therapy: non-viral vectors and viral vectors [3]. Viral vectors have an obvious advantage in gene transfer efficiency over non-viral vectors since viruses have a natural capability of gene transfer to host target cells; however, immunogenicity of viral vectors has been a major safety issue for clinical development [4]. Recombinant adeno-associated virus (AAV) vector is among the various viral vector species, and has several promising properties for gene therapy: non-pathogenicity, capability to transduce both dividing and non-dividing cells, and capability of long-term transgene expression [5]. Although AAV has shown relatively low immunogenicity compared to other viral vector species, a major challenge that prevent the clinical use of AAV in patients is humoral immune responses against the AAV capsid proteins or the transgenic proteins [6]. To overcome this issue, several strategies have been used, including a high dose injection, the use of alternative routes of

administration, the use of alternative serotypes, a transient host immunosuppression, the use of AAV capsid decoys, and modification of capsid proteins/epitopes [7–10]. However, all these strategies have been tested in preclinical models, so limited information is available in patients and many of these approaches will have to be adjusted to each individual due to the variability of the AAV immune response. Considering these complexities, new universal strategies are necessary to exploit AAV for clinical gene therapy.

As a new approach, a controlled release technology might be a probable strategy to overcome the issues for clinical use of AAV. Controlled release systems have been developed to control the temporal and spatial exposure of therapeutics to a defined target as a means to protect the drugs from physiological degradation and unwanted side effects and improve patient compliance [11]. AAV needs to reside only in the target area, however, injections may cause leakage of AAV to systemic circulation, and this may result in more humoral immune response against the administered AAV. In this chapter, potential of poly(lactic-co-glycolic acid) (PLGA) millicylindrical implants was investigated for controlled release of AAV to address the issue. In the previous chapters, PLGA implant has proved its high potential for controlled release of proteins with minimal instability. AAV capsid is also proteinaceous, so it is expected that PLGA implants can be formulated for an optimal controlled release system of AAV.

A.2 Materials and Methods

A.2.1 Materials

Pre-made AAV2 was purchased from Vector BioLabs (Malvern, PA). AAV clone C4 was constructed and kindly provided by Dr. David Schaffer (University of California at Berkeley, CA). PLGA 50:50 (inherent viscosity = 0.64 dL/g and Mw = 54.3 kDa, ester terminated) was purchased from LACTEL Absorbable Polymers (Birmingham, AL). Trehalose dihydrate (trehalose), ethylenediaminetetraacetic acid (EDTA) and bovine serum albumin (BSA) were purchased from Sigma-Aldrich Chemicals (St. Louis, MO). Magnesium carbonate ($MgCO_3$), magnesium hexahydrate ($MgCl_2$), sodium chloride (NaCl), 4-(2-hydroxyethyl)-1-piperazineethanesulfonic acid (HEPES), Tween 80 (10%), acetone, phosphate buffered saline (PBS), silicone rubber tubing, and Coomassie plus reagent assay kit were purchased from Fisher Scientific (Hanover Park, IL). PD SpinTrap G-25 desalting column was purchased from GE Healthcare Life Sciences (Pittsburgh, PA). ONE-Glo™ Luciferase Assay System was purchased from Promega (Madison, WI). HEK-293 cell was a generous gift from Dr. Mark Cohen (University of Michigan at Ann Arbor, MI).

A.2.2 Cation-exchange high-performance liquid chromatography (CEX-HPLC)

A TSKgel SP-NPR (Tosoh Bioscience, Japan) cation-exchange column was used to quantify AAV samples in HPLC. The column was equilibrated at a flow-rate of 1 mL/min on a Waters Agilent HPLC system (Waters, Milford, MA) equipped with a PDA detector. Empower® 3 Software (Waters) was used to integrate peak areas. After sample loading, the column was washed for 1 min with equilibration buffer (100 mM NaCl, 50 mM HEPES, 1 mM EDTA, 5 mM $MgCl_2$, pH 7.5) followed by a linear gradient from 100

to 500 mM NaCl in 50 mM HEPES, 1 mM EDTA, 5 mM $MgCl_2$, pH 7.5. Area under curve (AUC) of the eluted peak was quantitated at 280 nm (Figure SA.1). The column was cleaned after running every sample set with a 0.6-ml injection of 0.5 M NaOH.

A.2.3 Preparation of AAV powder

The buffer (PBS with 0.001 % Tween 20 or PBS with 5 % glycerol) of AAV solution was exchanged into HEPES buffered saline (HBS, 20 mM HEPES, 130 mM NaCl, pH 7.4) with 5 mM $MgCl_2$ and 0.02 % Tween 80 using a PD SpinTrap G-25 desalting column. Then, trehalose and BSA were added at 10 mg/mL and 15 mg/mL, respectively, and the solution was lyophilized. The lyophilized solid was then ground using a spatula to form as fine powder as possible.

A.2.4 Preparation of PLGA implant with AAV powder

The resulting AAV powder was suspended into 50 % (w/w) PLGA solution in acetone with 3% (w/w) $MgCO_3$ in a 2 mL centrifuge tube, then mixed and transferred into a 3 mL syringe. The suspension was extruded into silicone rubber tubing (I.D. = 0.8 mm), then dried at room temperature for 48 h followed by vacuum drying at 40°C and -23 in. Hg vacuum for an additional 48 h. The final dried implants were obtained by removal of silicone tubing and were cut into segments of desired length for future use.

A.2.5 Measurement of AAV and BSA loading in implants

Implants (2-5 mg) were dissolved in 1 mL of acetone for 1 h and centrifuged to precipitate the AAV/BSA powder. PLGA dissolved in supernatant was removed and the protein pellet was washed with acetone and centrifuged three times more to remove residual PLGA. The pellet was then air dried, reconstituted in 0.15 mL of HBS with 5 mM $MgCl_2$ and 0.02 % Tween 80 at 37°C overnight and analyzed by CEX-HPLC for

AAV and Coomassie plus reagent for BSA. Loading efficiency of AAV was calculated by the following equation.

$$\text{Loading efficiency (\%)} = \frac{\text{AUC of AAV in extract}}{\text{AUC of AAV in powder}} \times 100\ \%$$

Extracted loading and loading efficiency of BSA were calculated by the following equations.

$$\text{Extracted loading (\%)} = \frac{\text{Weight of extracted BSA}}{\text{Weight of total implant}} \times 100\ \%$$

$$\text{Loading efficiency (\%)} = \frac{\text{Extracted loading}}{\text{Theoretical loading}} \times 100\ \%$$

A.2.6 *In vitro* release study of AAV and BSA from implants

Implants (~ 5 mg) were added in 1.5 mL centrifuge tubes with 0.12 mL of HBS with 5 mM $MgCl_2$ and 0.02 % Tween 80 and incubated at 37°C. The release medium was replaced with fresh medium at each time point. The amount of released AAV and BSA at each time point was measured by CEX-HPLC and Coomassie plus reagent, and calculated as percentage of the released amount out of the extracted loading of AAV and BSA.

A.2.7 Cell culture

HEK-293 cells were kindly provided by Dr. Mark Cohen (University of Michigan at Ann Arbor, MI) and cultured in Dulbecco's modified Eagle's medium (Thermo Fisher Scientific, Waltham, MA) at 37°C and 5 % CO_2. The medium was supplemented with 10 % fetal bovine serum (Thermo Fisher Scientific) and 1 % penicillin/streptomycin (Thermo Fisher Scientific).

A.2.8 Luciferase assay

Luciferase assay was performed using a ONE-Glo™ Luciferase Assay System according to the manufacturer's manual. HEK-293 cells were seeded in a 96-well clear bottom white plate at a density of 15000 cells in 100 µL of media per well. Phenol red-free medium was used for luciferase assay because phenol red affects luminescence. The next day, 10 µL of the known concentration of AAV as standards and the samples were added into each well in triplicate. The concentration of standards was expressed as genomic multiplicity of infection (MOI) which is the ratio of vector genome of AAV to the number of cells. After 24 h, the equal volume of luciferase assay reagent to the media was added and the plate was read on SpectraMax M3 (Molecular Devices, Sunnyvale, CA). The MOI of samples was calculated in reference to a standard curve (Figure SA.2).

A.3 Results and Discussion

A.3.1 Finding a proper release buffer for AAV stability

AAV is prone to aggregate easily at high concentration in aqueous buffer, so efforts to formulate AAV with stabilizers have been made to prevent aggregation [12–

14]. To test *in vitro* release kinetics of AAV from PLGA implants, a proper release medium is needed to avoid artifacts caused by aggregation of AAV. First, a known concentration of AAV was incubated in PBS at 37°C and run in CEX-HPLC at select time points to compare AUC of AAV to the initial one. The relative AUC of AAV decreased to 20 % after day 14 and 6 % after day 28, and no AAV was detected after day 63 (Figure A.1). Therefore, PBS is not a good release medium for *in vitro* release study of AAV because it will exhibit less AAV release than actually released. There was a report utilizing divalent cations to stabilize AAV in aqueous buffer [15]. Accordingly, 5 mM $MgCl_2$ was tested as a stabilizer in release buffer. Magnesium, however, forms insoluble precipitates when mixed with phosphate, therefore, HBS was used instead of PBS. Also, 0.02 % Tween 80 was co-added with the expectation of its anti-aggregating property for proteins [16–19]. In this release buffer, the relative AUC of AAV was 88 % after day 14, 89 % after day 28, and 64 % after day 63 compared to the initial AUC (Figure A.1). Therefore, this buffer was used for all the experiments in this study (e.g. the solution to lyophilize AAV, and the release medium).

A.3.2 Evaluation of AAV loaded PLGA implants

To prepare PLGA implants, water-soluble drugs to be encapsulated need to be lyophilized into powders, so the powders are suspended in PLGA/organic solvent solution and the implants hardened by evaporating the organic solvent [20]. To achieve controlled release of encapsulated drugs, the volumetric loading of drug powders needs to be above a certain level [21,22]. However, the mass of feasible amount of AAV particles is too small for powder preparation. In order to increase the volumetric loading, BSA was co-lyophilized with AAV as a bulk excipient and 1.5 times as much trehalose as BSA

was also added to stabilize BSA as described in Chapter 3 (Table A.1). Along with the lyophilized powders of AAV, 3 % $MgCO_3$ was also added into PLGA implants (Table A.2) to neutralize PLGA acid byproducts which induce low pH and is deleterious to the encapsulated proteins [23]. The AAV powder was extracted from the implant using acetone and dissolved in the release buffer to measure extracted loading of AAV and BSA. The extracted loading efficiency of AAV was analyzed by CEX-HPLC and was 78 ± 14 % (mean ± SD, n=3) and the extracted w/w loading and loading efficiency of BSA measured by Coomassie protein assay were 3.7 ± 0.3 % and 99 ± 8 % (mean ± SD, n=3) respectively. The implants were incubated in the release buffer (HBS with 5 mM $MgCl_2$ and 0.02 % Tween 80) at 37°C for *in vitro* release study. The implant demonstrated near zero-order release of AAV for 3 weeks and total cumulative release normalized to the extracted loading was 94 % (Figure A.2 A). Release of BSA followed first-order kinetics for 4 weeks and total cumulative release was 105 % (Figure A.2 B). Therefore, PLGA implant can serve as a sustained release formulation of AAV and can be further optimized to extend the duration of release. It is thought that AAV release kinetics should follow the BSA release, but the differences in release kinetics and duration of release need to be further investigated.

A.3.3 Infectivity of AAV loaded in PLGA implants

It was demonstrated that AAV can be released from PLGA implant in a sustained manner, but infectivity of AAV also needs to be maintained in PLGA implant and after release. Therefore, AAV clone C4 encoding a firefly luciferase as a reporter gene provided by Dr. David Schaffer [24] was loaded into PLGA implants. A luciferase assay was performed with the known concentration of AAV standards, and the MOI of

extracted and released AAV from the implants was measured. The resulting infectivity of extracted AAV from the implants was 116 ± 18 % (mean ± SD, n=3), but it was at the basal level for released AAV. Although the infectivity of released AAV was not quantified due to the limit of detection, it was confirmed that infectivity of encapsulated AAV in PLGA implants was well-preserved.

A.4 Conclusion

In conclusion, we have successfully encapsulated AAV into PLGA implants for controlled release while preserving its infectivity. A preliminary experiment was performed to find a proper release buffer for a reliable *in vitro* release determination and it was demonstrated that HBS with 5 mM $MgCl_2$ and 0.02 % Tween 80 provides a proper buffer in which more than 85 % of AAV incubated at 37°C can be detected by CEX-HPLC up to 4 weeks. For sufficient volumetric loading of AAV powder, BSA was co-encapsulated in PLGA implants. Also, trehalose, and $MgCO_3$ were incorporated in the implants to stabalize the encapsulated AAV and BSA. AAV was released continuously with near zero-order release kinetics over 3 weeks from the implants and the total cumulative release normalized to its extracted loading was 94 %. Luciferase assay confirmed that infectivity of AAV encapsulated in the PLGA implants is well-preserved. Further work to measure the infectivity of released AAV from the implants is needed, along with evaluation for efficacy and advantages of the PLGA implant over free AAV injection in animals.

Table A.1: Composition in 1 mL of AAV solution and dry weight percentage of each component in lyophilized AAV powder.

Composition	Weight (mg)	Dry weight percentage (%)
AAV	0[a]	0
BSA	10	25.2
Trehalose dihydrate	15	37.7
HEPES	4.77	12.0
Sodium chloride	8.77	22.1
Magnesium chloride	1.02	2.6
Tween 80	0.20	0.5

[a] 2.2×10^{13} vg of AAV has negligible weight.

Table A.2: Weight percentage of each component in implant.

Composition	Weight percentage (%)
PLGA (50:50)	82.0
$MgCO_3$	3.0
AAV powder	15.0
(BSA)[a]	(3.8)

[a] BSA is a part of AAV powder.

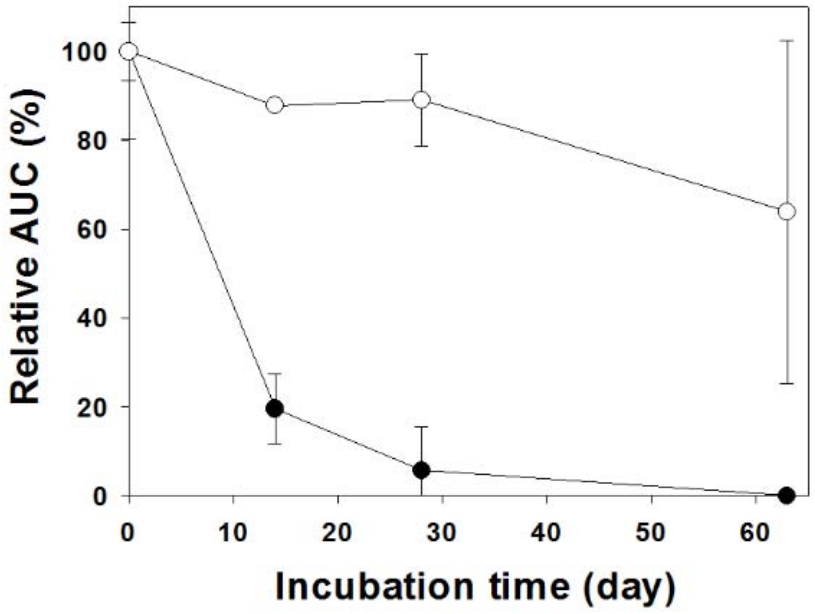

Figure A.1: Relative AAV stability in PBS (●) and HBS with 5 mM $MgCl_2$ and 0.02 % Tween80 (○) at 37 °C. *Data reported as mean ± SD, n=3.*

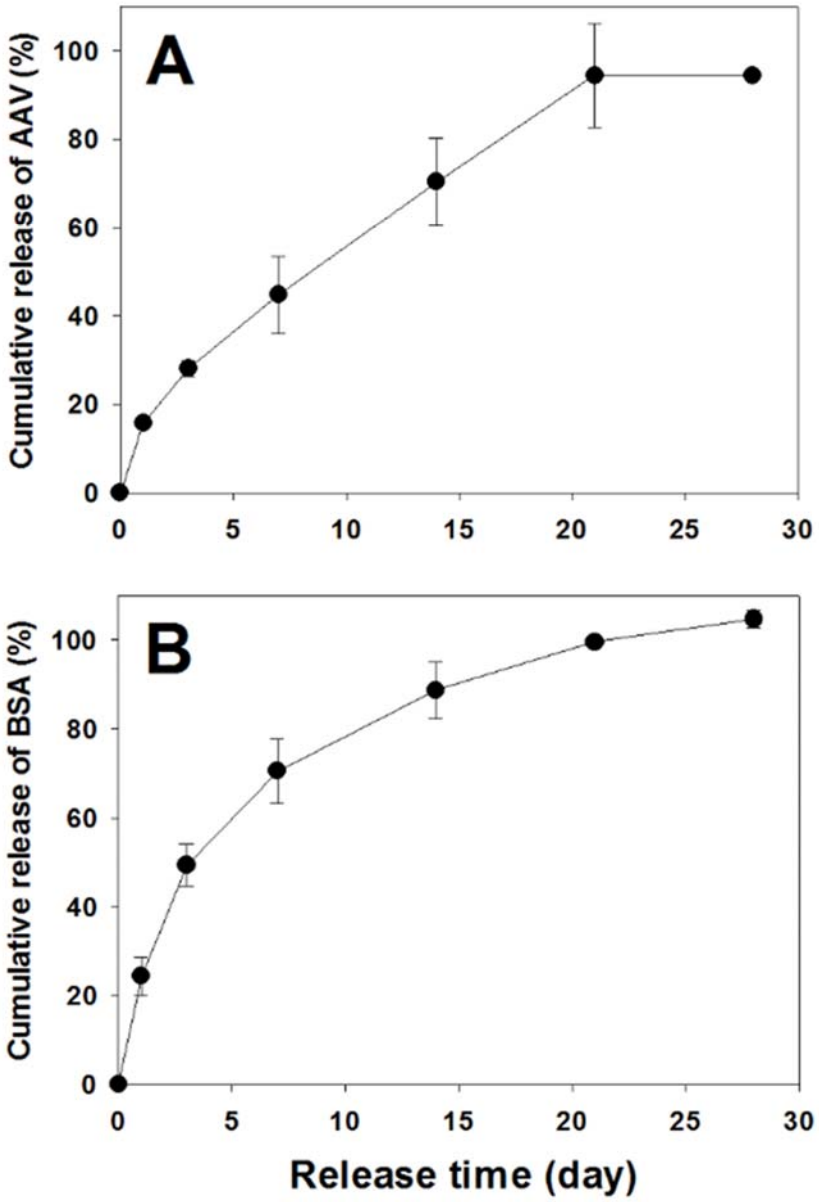

Figure A.2: Release kinetics of AAV (A) and BSA (B) from PLGA implants in HBS with 5 mM $MgCl_2$ and 0.02 % Tween 80. *Data reported as mean ± SD, n=2.*

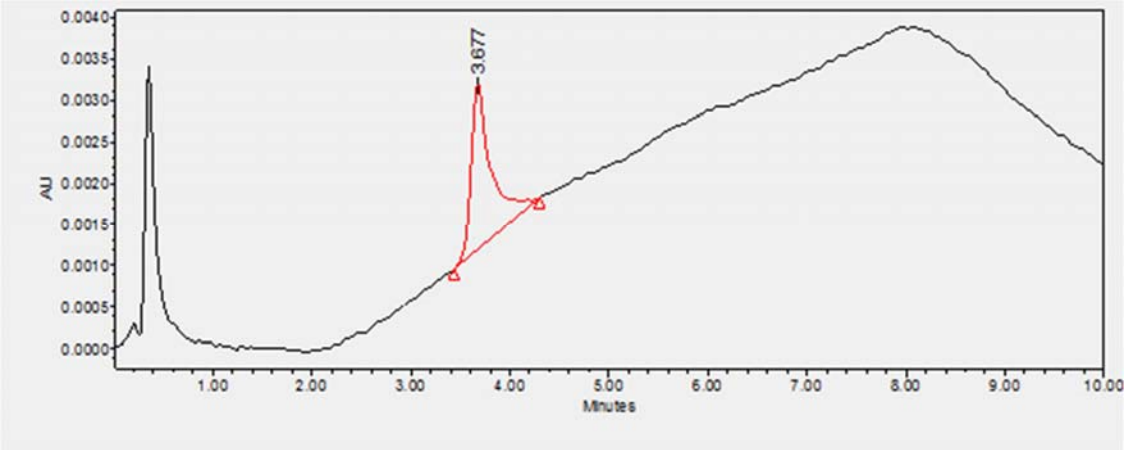

Figure SA.1: Representative chromatogram of AAV in CEX-HPLC. *AAV peak is in red.*

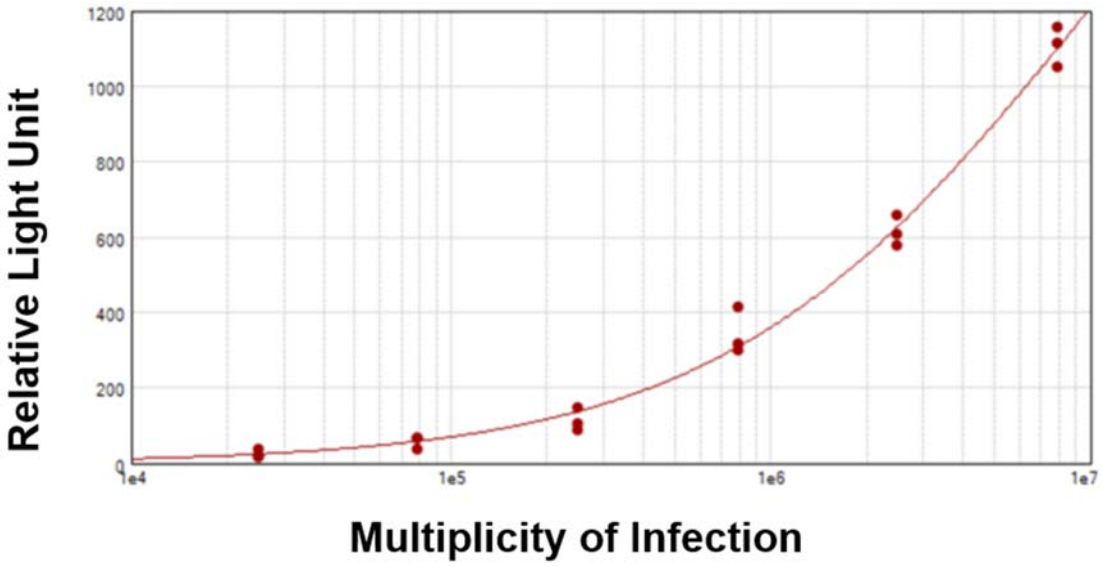

Figure SA.2: Standard curve of luciferase assay.

A.5 References

[1] A. Mountain, Gene therapy: The first decade, Trends Biotechnol. 18 (2000) 119–128. doi:10.1016/S0167-7799(99)01416-X.

[2] C. Sheridan, Gene therapy finds its niche., Nat. Biotechnol. 29 (2011) 121–128. doi:10.1038/nbt0511-459d.

[3] A. El-Aneed, An overview of current delivery systems in cancer gene therapy, J. Control. Release. 94 (2004) 1–14. doi:10.1016/j.jconrel.2003.09.013.

[4] Sushrusha Nayak M S Roland W Herzog, Progress and prospects: immune responses to viral vectors. by S Nayak, R W Herzog, Gene Ther. 17 (2011) 295–304. doi:10.1038/gt.2009.148.Progress.

[5] Y. Lu, Recombinant adeno-associated virus as delivery vector for gene therapy--a review., Stem Cells Dev. 13 (2004) 133–145. doi:10.1089/154732804773099335.

[6] J.Y. Sun, V. Anand-Jawa, S. Chatterjee, K.K. Wong, Immune responses to adeno-associated virus and its recombinant vectors., Gene Ther. 10 (2003) 964–976. doi:10.1038/sj.gt.3302039.

[7] F. Mingozzi, X.M. Anguela, G. Pavani, Y. Chen, R.J. Davidson, D.J. Hui, M. Yazicioglu, L. Elkouby, C.J. Hinderer, A. Faella, C. Howard, A. Tai, G.M. Podsakoff, S. Zhou, E. Basner-Tschakarjan, J.F. Wright, K.A. High, Overcoming preexisting humoral immunity to AAV using capsid decoys, Sci Transl Med. 5 (2013) 194ra92. doi:10.1126/scitranslmed.3005795.

[8] V. Louis Jeune, J.A. Joergensen, R.J. Hajjar, T. Weber, Pre-existing anti-adeno-associated virus antibodies as a challenge in AAV gene therapy., Hum. Gene Ther. Methods. 24 (2013) 59–67. doi:10.1089/hgtb.2012.243.

[9] C.L. Halbert, T.A. Standaert, C.B. Wilson, A.D. Miller, Successful readministration of adeno-associated virus vectors to the mouse lung requires transient immunosuppression during the initial exposure., J. Virol. 72 (1998) 9795–805. http://www.pubmedcentral.nih.gov/articlerender.fcgi?artid=110491&tool=pmcentrez&rendertype=abstract.

[10] E. Basner-Tschakarjan, E. Bijjiga, A.T. Martino, Pre-clinical assessment of immune responses to adeno-associated virus (AAV) vectors, Front. Immunol. 5 (2014) 1–5. doi:10.3389/fimmu.2014.00028.

[11] S. Mitragotri, P.A. Burke, R. Langer, Overcoming the challenges in administering biopharmaceuticals: formulation and delivery strategies., Nat. Rev. Drug Discov. 13 (2014) 655–72. doi:10.1038/nrd4363.

[12] M.A. Croyle, X. Cheng, J.M. Wilson, Development of formulations that enhance physical stability of viral vectors for gene therapy., Gene Ther. 8 (2001) 1281–1290. doi:10.1038/sj.gt.3301527.

[13] Q. Xie, J. Hare, J. Turnigan, M.S. Chapman, Large-scale production, purification and crystallization of wild-type adeno-associated virus-2, J. Virol. Methods. 122 (2004) 17–27. doi:10.1016/j.jviromet.2004.07.007.

[14] J.F. Wright, T. Le, J. Prado, J. Bahr-Davidson, P.H. Smith, Z. Zhen, J.M. Sommer, G.F. Pierce, G. Qu, Identification of factors that contribute to recombinant AAV2 particle aggregation and methods to prevent its occurrence during vector purification and formulation, Mol. Ther. 12 (2005) 171–178. doi:10.1016/j.ymthe.2005.02.021.

[15] a E. Turnbull, a Skulimowski, J. a Smythe, I.E. Alexander, Adeno-associated virus vectors show variable dependence on divalent cations for thermostability: implications for purification and handling., Hum. Gene Ther. 11 (2000) 629–35. doi:10.1089/10430340050015815.

[16] T. Arakawa, Y. Kita, Protection of Bovine Serum Albumin from Aggregation by MATERIALS AND METHODS, J. Pharm. Sci. 89 (2000) 646–651. doi:10.1002/(SICI)1520-6017(200005)89.

[17] O. Joshi, L. Chu, J. McGuire, D.Q. Wang, Adsorption and function of recombinant factor VIII at the air-water interface in the presence of tween 80, J. Pharm. Sci. 98 (2009) 3099–3107. doi:10.1002/jps.21569.

[18] W. Wang, Y.J. Wang, D.Q. Wang, Dual effects of Tween 80 on protein stability, Int. J. Pharm. 347 (2008) 31–38. doi:10.1016/j.ijpharm.2007.06.042.

[19] O. Joshi, J. McGuire, Adsorption behavior of lysozyme and tween 80 at hydrophilic and hydrophobic silica-water interfaces, Appl. Biochem. Biotechnol. 152 (2009) 235–248. doi:10.1007/s12010-008-8246-8.

[20] V. Milacic, S.P. Schwendeman, Lysozyme Release and Polymer Erosion Behavior of Injectable Implants Prepared from PLGA-PEG Block Copolymers and PLGA/PLGA-PEG Blends., Pharm. Res. 31 (2013) 436–448. doi:10.1007/s11095-013-1173-6.

[21] B. Amsden, Review of osmotic pressure driven release of proteins from monolithic devices., J. Pharm. Pharm. Sci. 10 (2007) 129–43. http://www.ncbi.nlm.nih.gov/pubmed/17706172.

[22] B.G. Amsden, Y. Cheng, M.F.A. Goosen, A mechanistic study of the release of osmotic agents from polymeric monoliths, 3659 (1994).

[23] G. Zhu, S.R. Mallery, S.P. Schwendeman, Stabilization of proteins encapsulated in injectable poly (lactide-co-glycolide), Nat. Biotechnol. 18 (2000) 52–57. doi:10.1038/71916.

[24] J. Santiago-Ortiz, D.S. Ojala, O. Westesson, J.R. Weinstein, S.Y. Wong, A. Steinsapir, S. Kumar, I. Holmes, D. V Schaffer, AAV ancestral reconstruction library enables selection of broadly infectious viral variants, Gene Ther. 22 (2015) 1–13. doi:10.1038/gt.2015.74.